



A survey, review, and future trends of skin lesion segmentation and classification

Md. Kamrul Hasan ^{a,b,*}, Md. Asif Ahamad ^b, Choon Hwai Yap ^{a,1}, Guang Yang ^{c,d,1}

^a Department of Bioengineering, Imperial College London, UK

^b Department of Electrical and Electronic Engineering (EEE), Khulna University of Engineering & Technology (KUET), Khulna 9203, Bangladesh

^c National Heart and Lung Institute, Imperial College London, UK

^d Cardiovascular Research Centre, Royal Brompton Hospital, UK



ARTICLE INFO

Keywords:

Computer-aided diagnosis
Deep learning
Machine learning
Skin lesion segmentation and classification
Skin lesion datasets

ABSTRACT

The Computer-aided Diagnosis or Detection (CAD) approach for skin lesion analysis is an emerging field of research that has the potential to alleviate the burden and cost of skin cancer screening. Researchers have recently indicated increasing interest in developing such CAD systems, with the intention of providing a user-friendly tool to dermatologists to reduce the challenges encountered or associated with manual inspection. This article aims to provide a comprehensive literature survey and review of a total of 594 publications (356 for skin lesion segmentation and 238 for skin lesion classification) published between 2011 and 2022. These articles are analyzed and summarized in a number of different ways to contribute vital information regarding the methods for the development of CAD systems. These ways include: relevant and essential definitions and theories, input data (dataset utilization, preprocessing, augmentations, and fixing imbalance problems), method configuration (techniques, architectures, module frameworks, and losses), training tactics (hyperparameter settings), and evaluation criteria. We intend to investigate a variety of performance-enhancing approaches, including ensemble and post-processing. We also discuss these dimensions to reveal their current trends based on utilization frequencies. In addition, we highlight the primary difficulties associated with evaluating skin lesion segmentation and classification systems using minimal datasets, as well as the potential solutions to these difficulties. Findings, recommendations, and trends are disclosed to inform future research on developing an automated and robust CAD system for skin lesion analysis.

1. Introduction

Malignant melanoma is the deadliest skin cancer [1], yet early diagnosis can cure it. Doctors and radiologists utilize gold-standard dermatoscopy to diagnose pigmented skin lesions using hand-held instruments and computer vision algorithms. Medical image processing has recently grown with more effective techniques to help dermatologists recognize and classify skin lesions [2]. Therefore, a Computer-aided Diagnosis (CAD) is an inescapable tool for physicians and/or dermatologists in decision-making, especially when dealing with a large number of patients in a short time [3–5]. CAD computational techniques comprise image acquisition, preprocessing, segmentation, feature extraction, and classification [6]. It is noteworthy that some academics consider segmentation a preprocessing step for feature extraction and classification. Segmented lesion masks and classification

results can be used for contemporaneous lesion detection and recognition [3,7] (see example on YouTube²). From 2011 to 2022, various studies were conducted on Skin Lesion Analysis (SLA) (see Fig. 1), especially lesion segmentation and classification, applying different techniques: computer vision algorithms, manual feature engineering, and automated Artificial Intelligence (AI).

Fig. 1 remarks that SLA is a fast-growing study area, and the publication numbers have increased yearly for both tasks, especially after 2016. Henceforth, the extensive number of articles necessitates a systematic survey and in-depth discussions of datasets, preprocessing methodologies, segmentation strategies, manual feature engineering procedures, classification techniques, and evaluation benchmarks for automated SLA procedure(s) to help researchers strategize future research.

* Corresponding author at: Department of Bioengineering, Imperial College London, UK.

E-mail addresses: k.hasan22@imperial.ac.uk (Md.K. Hasan), asif.fx@live.com (Md.A. Ahamad), c.yap@imperial.ac.uk (C.H. Yap), g.yang@imperial.ac.uk (G. Yang).

¹ Co-senior last author.

² https://youtu.be/nlfr_NCPy4U [Access date: 12-Mar-2022]

| Nomenclature | | PRISMA | Preferred Reporting Items for Systematic Reviews and Meta-Analyses |
|----------------|--|--------|--|
| Acronym | Full Form | PSNR | Peak to Signal Ratio |
| ACC | Accuracy | QDA | Quadratic Discriminant Analysis |
| AdB | AdaBoost | RF | Random Forest |
| AI | Artificial Intelligence | SCC | Squamous Cell Carcinoma |
| AK | Actinic Keratosis | SE | Segmentation Error |
| ANN | Artificial Neural Network | SEN | Sensitivity |
| AUC | Area Under Curve | SENet | Squeeze-and-Excitation Networks |
| BACC | Balanced Accuracy | SGD | Stochastic Gradient Descent |
| BCC | Basal Cell Carcinoma | SHAP | Shapley Additive Explanations |
| BEMD | Bi-dimensional Empirical Mode Decomposition | SIFT | Scale-Invariant Feature Transform |
| CAD | Computer-aided Diagnosis | SK | Seborrheic Keratosis |
| CAM | Class Activation Map | SLA | Skin Lesion Analysis |
| CC | Correlation Coefficient | SLC | Skin Lesion Classification |
| DF | Dermatofibroma | SLS | Skin Lesion Segmentation |
| DL | Deep Learning | SPE | Specificity |
| DSC | Dice Similarity Coefficient | SSIM | Structural Similarity Indices |
| DT | Decision Tree | SVM | Support Vector Machine |
| EBC | Ensemble Binary Classifier | TDS | Total Dermatoscopy Score |
| ENN | Elman Neural Network | VL | Vascular Lesion |
| F1S | F1-score | XAI | Explainable Artificial Intelligence |
| FFBPNN | Feed Forward Back Propagation Neural Network | | |
| FNR | False Negative Rate | | |
| FOM | Figure of Merit | | |
| FPR | False Positive Rate | | |
| FCN | Fully Convolutional Network | | |
| GAN | Generative Adversarial Network | | |
| GLCM | Gray Level Co-occurrence Matrix | | |
| GLDM | Gray Level Difference Method | | |
| HcCNN | Hyper-Connected CNN | | |
| HD | Hausdorff Distance | | |
| HMD | Hammoude Distance | | |
| IAD | Interactive Atlas of Dermoscopy | | |
| IRMA | Image Retrieval in Medical Applications | | |
| ISIC | International Skin Imaging Collaboration | | |
| JI | Jaccard Index | | |
| KMC | K-Means Clustering | | |
| KNN | K-Nearest Neighbors | | |
| LBP | Local Binary Patterns | | |
| LDA | Linear Discriminant Analysis | | |
| LIME | Local Interpretable Model-agnostic Explanation | | |
| LR | Learning Rate | | |
| MCC | Matthew Correlation Coefficient | | |
| Mel | Melanoma | | |
| ML | Machine Learning | | |
| MPNN | Multilayer Perceptron Neural Network | | |
| MSM-CNN | Multi-Scale Multi-CNN | | |
| NB | Naive Bayes | | |
| Nev | Nevus | | |
| NPV | Negative Predictive Value | | |
| PNN | Probabilistic Neural Network | | |
| PRE | Precision | | |

This article provides a systematic survey, assessment, and analysis of SLA approaches from 2011 through 2022, focusing on Skin Lesion Segmentation (SLS) and Skin Lesion Classification (SLC). SLS schemes

employ image analysis (and/or computer vision) algorithms [6,8] or end-to-end Deep Learning (DL) methodologies [9], while SLC uses Machine Learning (ML) [10] or end-to-end DL algorithms [10,11]. It is noteworthy that the employment of ML-based SLC requires comprehensive feature engineering [6]. Therefore, we discuss SLA's feature extraction steps in the SLC task. This article summarizes input data (dataset utilization, preprocessing, augmentations, and solving imbalance problems), method configuration (techniques, architectures, module frameworks, and losses), training tactics (hyperparameter settings), and evaluation criteria (metrics) from past publications. It systematically presents their simple technological fundamentals and usage trends with recommendations to help researchers. It can make contributions in the following contexts:

- Provide essential knowledge regarding SLA tasks by compiling articles published over the past twelve years (2011–2022), covering SLS and SLC mechanisms with a variety of integral strategies and insightful back-and-forth exchanges.
- Investigate the insight scenario of a variety of datasets with potential future trends and their existing requirements in the field of survey analysis that is being addressed.
- Analyze the many different preprocessing and augmentation procedures that are used in SLA in order to reveal their effectiveness, trends, and necessity to construct a robust supervised SLA model and mitigate class imbalance issues.
- Summarize the many SLS and SLC strategies, such as automated DL algorithms, manual feature engineering, ML models, ensemble models, and SLS post-processing, employed over the past twelve years.
- Examine the trends in employment over a range of training conditions, as well as the hyperparameters such as batch size, learning rate, loss function, optimizer, and epoch.
- Review a variety of assessment benchmarks along with adequate explanation details to disclose the tendencies in the SLS and/or SLC tasks.
- In the end, categorize all the necessary SLA actions according to the number of times they have been employed in the past 594 articles. These categories are **High-frequency** (mostly applied), **Medium-frequency** (moderately applied), and **Low-frequency**

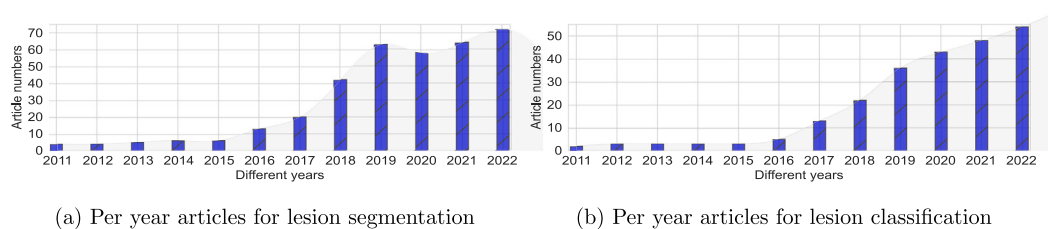


Fig. 1. The number of publications (in blue bars) in the past from 2011 to 2022 on lesion segmentation (left) and lesion classification (right), collected from Google Scholar (see details in Section 2) by searching for “skin lesion segmentation” and “skin lesion classification”. The publication numbers in 2020 (left figure) have probably decreased due to the COVID-19 pandemic. This figure shows the growing interest in this field and the complexity of the science involved due to the increasing number of contributions, requiring that these two factors necessitate a review such as ours to help readers navigate the complexity.

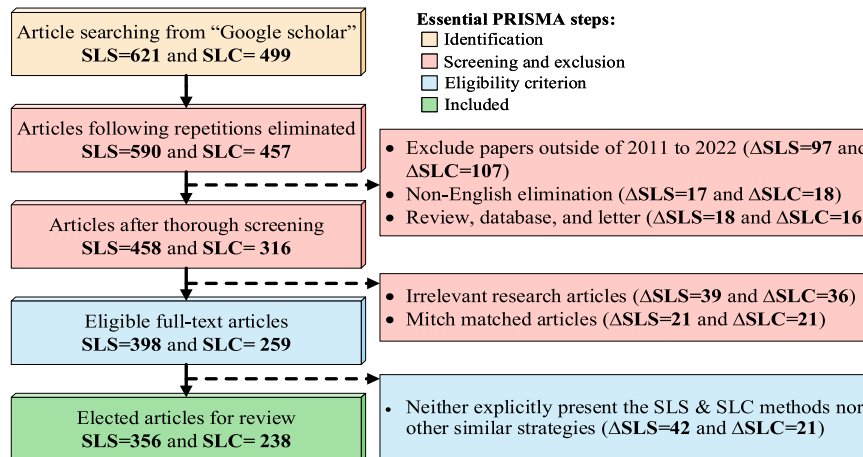


Fig. 2. The employed PRISMA process for articles exploring approach, where we describe the evidence for the article's inclusion and exclusion standards.

(less applied). Additionally, uncover the prospective essentials in the SLA tasks that will be an open challenge for researchers interested in this field.

This paper is organized as follows: Section 2 clarifies the inclusion and exclusion criteria for SLA article selection. Section 3 describes various available skin lesion datasets and scrutinizes their utilization trends. The employment of various preprocessing and augmentations for the automated SLA task is explored in Section 4 with the class imbalance problem solution analysis. Section 5 reports different SLS techniques along with past trends. This section also highlights different post-processing schemes in the SLS task. Various SLC elements, like lesion features and ML- and DL-based classifiers, are investigated in Section 6. The training schemes with different hyperparameter settings and evaluation benchmarks are described in Section 7, while Section 8 explores different explainability schemes in the SLA techniques. Lastly, Section 9 provides informative observations, recommendations, and trends for future research directions in related fields of interest, with the article's conclusion in Section 10.

2. Article selection

This review's article-searching approach adopts the Preferred Reporting Items for Systematic Reviews and Meta-Analyses (PRISMA) strategy [12] (see Fig. 2), along with inclusion and exclusion benchmarks [13] for paper selection.

A google scholar search yields 621 SLS and 499 SLC publications with the keywords “skin lesion segmentation” and “skin lesion classification”, respectively. After removing duplicates, there are 590 SLS and 457 SLC articles. Then, in the first screening round (first-level exclusion), non-English articles ($\Delta SLS = 17$ and $\Delta SLC = 18$) and review, database, or letter-type articles ($\Delta SLS = 18$ and $\Delta SLC =$

16) are discarded. Only publications from 2011–2022 are kept in this cycle, returning 458 SLS and 316 SLC articles (see Fig. 2). 39 SLS and 36 SLC articles with research objectives that are not relevant to the current review, and 21 SLS and 21 SLC articles with schemes that are not suitable to the current review are excluded. This second exclusion produces 398 SLS and 259 SLC articles (see Fig. 2). Again, $\Delta SLS = 42$ and $\Delta SLC = 21$ articles are deleted since they do not explicitly illustrate the SLS and SLC systems or other similar strategies. Finally, 356 SLS and 238 SLC articles are included in this review. Fig. 1 depicts the per-year distribution of those included papers from 2011 to 2022 on the SLS and SLC, revealing that publications have substantially increased, especially after 2016.

3. Image acquisition

A computerized SLA system acquires images using non-invasive techniques such as dermoscopy, photography, confocal scanning laser microscopy, optical coherence tomography, ultrasound imaging, magnetic resonance imaging, and spectroscopic imaging. However, macroscopic and dermoscopic images are widely utilized for SLA [6]. Accumulating acquired images in a dataset is key to any automated SLS and/or SLC in the SLA system. Long-used public datasets for SLA are International Skin Imaging Collaboration (ISIC) [14–19], PH2 [20], Interactive Atlas of Dermoscopy (IAD) [21], Image Retrieval in Medical Applications (IRMA) [22], Dermaquest [23], etc. The ISIC datasets include five distinct open versions with various image numbers and classes for five consecutive years: ISIC-16 [14], ISIC-17 [15], ISIC-18 [16,17], ISIC-19 [18], and ISIC-20 [19] respectively for the years from 2016 to 2020. The next Section 3.1 briefly summarizes those datasets.

Table 1

Publicly available SLS and SLC datasets with variable amounts of classes and image samples.

| Datasets | Number of images for various tasks and classes | | | | | | | | | |
|------------|--|-------|--------------------------------|-------|------|------|-----|-----|-----|------|
| | SLS task | | Class-wise images for SLC task | | | | | | | |
| | Images | Masks | Nev | SK | BCC | AK | DF | VL | Mel | SCC |
| ISIC-16 | Training | 900 | 900 | 727 | – | – | – | – | 173 | – |
| | Testing | 379 | 379 | 304 | – | – | – | – | 75 | – |
| ISIC-17 | Training | 2000 | 2000 | 1372 | 254 | – | – | – | 374 | – |
| | Validation | 150 | 150 | 78 | 42 | – | – | – | 30 | – |
| | Testing | 600 | 600 | 393 | 90 | – | – | – | 117 | – |
| ISIC-18 | Training | 12500 | 12500 | 6705 | 1099 | 514 | 327 | 115 | 142 | 1113 |
| ISIC-19 | Training | – | – | 12875 | 2624 | 3323 | 867 | 239 | 253 | 4522 |
| ISIC-20 | Training | – | – | 32542 | – | – | – | – | 548 | – |
| PH2 | – | 200 | 200 | 160 | – | – | – | – | 40 | – |
| IAD | – | 100 | 100 | 70 | – | – | – | – | 30 | – |
| Dermaquest | – | 137 | 137 | 61 | – | – | – | – | 76 | – |
| IRMA | – | – | – | 560 | – | – | – | – | 187 | – |

3.1. Datasets

The **ISIC-16**³ is a dataset for binary SLS and SLC containing 900 training and 379 testing images but no validation images (see Table 1). It distinguishes Nevus (Nev) from Melanoma (Mel) using images with resolutions of 556 × 679 to 2848 × 4828 pixels. The **ISIC-17**⁴ is a binary SLS and multi-class SLC challenge. The latter SLC has Nev, Seborrheic Keratosis (SK), and Mel (see Table 1) classes. This dataset comprises 2750 images for training, validation, and testing with resolutions ranging from 453 × 679 to 4499 × 6748 pixels. The **ISIC-18**⁵ images are derived from the HAM10000 dataset [17], including 10015 images for multi-class SLC and 12500 images for binary SLS. This dataset does not publish validation or test images, and all images have resolutions of 450 × 600 pixels. It comprises seven classes: Nev, SK, Basal Cell Carcinoma (BCC), Actinic Keratosis (AK), Dermatofibroma (DF), Vascular Lesion (VL), and Mel (see Table 1). The **ISIC-19**⁶ has an extension of one more class, i.e., Squamous Cell Carcinoma (SCC), in ISIC-18 with almost double sample images. It has 25331 images from multiple sites (HAM10000, BCN20000 [18], and MSK) applying different preprocessing methods. The images of ISIC-19 have resolutions of 600 × 450 to 1024 × 1024 pixels, without explicit validation and test images like ISIC-18 (see Table 1). The **ISIC-20**⁷ contains 33126 dermoscopic images with the resolutions of 1024 × 1024 pixels (see Table 1). Similar to ISIC-16, this dataset also contains binary SLC images from over 2000 patients, aiming to be classified as Nev and Mel.

The **PH2**⁸ is a database acquired at the Dermatology Service of Hospital Pedro Hispano, Portugal. This dataset contains 200 images of melanocytic lesions, including 160 in the Nev class and 40 in the Mel class, with a 768 × 560 pixel resolution. The **IAD**⁹ dataset has 700 × 447 RGB pixels of images but does not have segmentation masks. However, the authors in [24] provide ground truth masks to continue

the research study. The **Dermaquest** dataset has 137 images for the binary SLS. The SLC is a binary classification task with 76 samples in the Mel class and 61 in the Nev class. The **IRMA** dataset is unlisted but available under special request to the authors and was created by the Department of Medical Informatics, RWTH Aachen University. It comprises 747 dermoscopic images with a resolution of 512 × 512 pixels, of which 187 images are in the Mel class, and 560 are in the Nev class.

An overview of these datasets with their sample distributions for SLS and SLC tasks in Table 1 reveals that the SLC class ranges from binary to eight classes, with most binary tasks. Per-class sample figures indicate a vast disparity, especially for ISIC-19 and ISIC-20. Such an uneven class distribution causes a supervised SLC system to favor the overrepresented class if this is not considered during training [3]. It is very challenging for automated SLS and SLC systems to be generic while training with fewer samples. Section 4.2 explores different ways in the past literature, ranging from 2011 to 2022, to mitigate these challenges. The following Section 3.2 looks at the frequency of dataset usage in SLA literature from 2011 to 2022.

3.2. Datasets' utilization and trends

Table 2 illustrates the usage of different datasets in 356 SLS articles. Some articles are assigned to multiple columns of datasets because the authors used multiple datasets in their papers. It can be observed that researchers employed publicly available IAD and other private datasets (in the last column) to validate image analysis (and/or computer vision)-based SLS methods between 2011 and 2015, when automated DL models were still not popular for the SLS task. Recalling Fig. 1, the publication numbers after 2016 have significantly increased; one of the underlying reasons is the release of ISIC datasets, as reflected in Table 2 (most of the articles are in the first four columns after 2016). A similar pattern of the usage frequency of various SLC datasets in the 238 SLC articles is noticed in Table 3.

In Fig. 3, a summary of various dataset utilization in the specified 594 articles is presented, showing the frequencies of dataset applications. As illustrated in both images, the earlier articles applied relatively small and non-public datasets to their SLA system, limiting the research community's ability to reproduce their findings.

As obtaining annotated medical images is extremely expensive [7, 505], few researchers were interested in working on the SLA until 2015. However, this obstacle was overcome to some extent after introducing the ISIC datasets in 2016, as reflected in Fig. 3(a) and (b). Despite being introduced after the PH2, IAD, Dermaquest, and other earlier private datasets, the ISICs datasets were extensively used in numerous articles, as seen in Fig. 3 and the last rows of Tables 2 and 3.

³ <https://challenge.isic-archive.com/landing/2016> [Access date: 21-Jun-2022]

⁴ <https://challenge.isic-archive.com/landing/2017> [Access date: 21-Jun-2022]

⁵ <https://challenge.isic-archive.com/landing/2018> [Access date: 21-Jun-2022]

⁶ <https://challenge.isic-archive.com/landing/2019> [Access date: 21-Jun-2022]

⁷ <https://www.kaggle.com/c/siim-isic-melanoma-classification/overview> [Access date: 21-Jun-2022]

⁸ <https://www.fc.up.pt/addi/ph2%20database.html> [Access date: 21-Jun-2022]

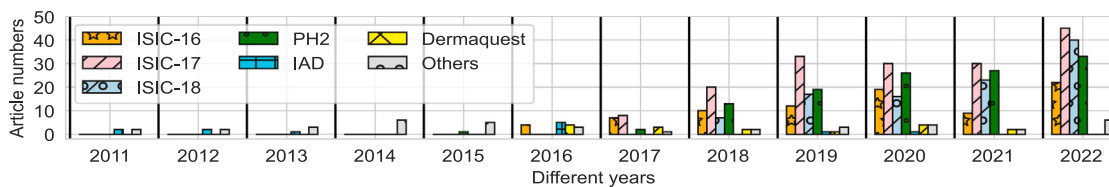
⁹ <https://espace.library.uq.edu.au/view/UQ:229410> [Access date: 21-Jun-2022]

Table 2The number of SLS articles each year on various publicly available datasets in [Table 1](#).

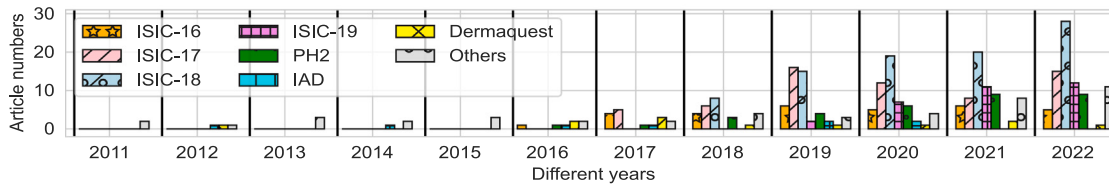
| Year | ISIC-16 | ISIC-17 | ISIC-18 | PH2 | IAD | Dermaquest | Others |
|-------|---------------|---------------------------------------|---|---|---------------|---------------|------------|
| 2022 | [25–46] | [25–28,30–38,40,41,43–73] | [27,29,30,32–35,37,40–46,48,50–52,55,58,61–63,65,68–70,73–87] | [26,28,30–33,36,37,40,42–48,51–53,55,60,62–64,66,69,70,78,82,84,85,87,88] | | | [50,88–92] |
| 2021 | [93–101] | [93–95,97,99–124] | [93,96,98,100–102,109,111,112,114,116,123,125–135] | [93,96,98,99,102–108,110,113,114,117,119,121,125,128,130,131,136–141] | | [117,119] | [142,143] |
| 2020 | [3,7,144–160] | [3,7,145,149,152,154,155,157,159–180] | [7,149,151,152,154,157,164,172,174,180–186] | [2,144,147,149,151,152,154,158,160,162,165,166,169,170,173–177,179,183,187–191] | [2] | [188,192–194] | [195–198] |
| 2019 | [199–210] | [200,203,204,207–236] | [203,207,213,219,226,229,234,237–246] | [177,200,201,209,210,213,214,218,221,232–234,238,247–252] | [253] | [254] | [255–257] |
| 2018 | [258–267] | [260,264–282] | [283–289] | [258,262–264,266,268,274,278,279,281,290–292] | | [293,294] | [295,296] |
| 2017 | [273,297–302] | [273,300,303–308] | | [273,309] | | [310–313] | [314] |
| 2016 | [315–318] | | | | [315,319–322] | [9,321,323] | [324–326] |
| 2015 | | | | [327] | | | [328–332] |
| 2014 | | | | | | | [333–338] |
| 2013 | | | | | [339] | | [340–342] |
| 2012 | | | | | | [343,344] | [345,346] |
| 2011 | | | | | | [347,348] | [349,350] |
| Total | 83 (15.4%) | 166 (30.7%) | 103 (19.0%) | 121 (22.4%) | 12 (2.2%) | 16 (3.0%) | 39 (7.3%) |

Table 3The number of SLC articles each year on various publicly available datasets in [Table 1](#).

| Year | ISIC-16 | ISIC-17 | ISIC-18 | ISIC-19 | PH2 | IAD | Dermaquest | Others |
|-------|---------------------|---------------------------------------|-------------------------------------|----------------------------------|--------------------------------------|-----------|-------------------------------|---------------|
| 2022 | [33,34,351–353] | [33,34,48,60,351,353–362] | [33,34,48,351,352,356–358,360–379] | [82,354,358,363,365,378,380–385] | [33,48,60,351–353,362,378,386] | [351] | [351,378,387–395] | |
| 2021 | [93,396–400] | [93,396,399–404] | [93,125,128,371,405–420] | [401,409,414,421–428] | [93,128,140,399,408,410,421,429,430] | [408,412] | [142,408,410,412,424,431–433] | |
| 2020 | [182,434–438] | [164,177,178,178,182,434,436,439–443] | [164,182,436,439,444–459] | [164,460–465] | [177,437,441,442,449,466] | [467,468] | [470–473] | |
| 2019 | [1,201,207,474–476] | [1,207,216,219,234,235,476–487] | [1,207,219,234,243,476,483,488–495] | [496,497] | [1,201,247,491] | [1,253] | [491] | [491,498,499] |
| 2018 | [264,500–502] | [264,276,503–507] | [289,504,508–513] | | [292,503,514] | [515] | [516–519] | |
| 2017 | [297,520–522] | [523–527] | | | [521] | [521] | [522,528,529] | [530,531] |
| 2016 | [532] | | | | [533] | [534] | [534,535] | [534,536] |
| 2015 | | | | | | | | [537–539] |
| 2014 | | | | | | [540] | | [541,542] |
| 2013 | | | | | | | | [543–545] |
| 2012 | | | | | | [546] | [547] | [548] |
| 2011 | | | | | | | | [549,550] |
| Total | 31 (9.7%) | 62 (19.5%) | 90 (28.3%) | 32 (10.0%) | 33 (10.4%) | 13 (4.1%) | 12 (3.8%) | 45 (14.2%) |



(a) Per year SLS articles using a specific dataset



(b) Per year SLC articles using a specific dataset

Fig. 3. The summary of the dataset's utilization from 2011 to 2022 for the SLS (top) and SLC (bottom) on different publicly available datasets, demonstrating the most valuable datasets in the past years.

Although the ISIC-18 has more samples than other SLS datasets, it was not used like as ISIC-17 dataset. This trend has been noticed in the last six years (2017–2022) (see [Fig. 3\(a\)](#)). Since ISIC-18 lacks independent test and validation sets, it necessitates time-consuming cross-validation to describe the results. A robustly trained SLS model may only sometimes be produced by random validation and test set selection. On the other hand, the ISIC-16 for SLS also has fewer training examples and no validation images. Significantly few articles [110, 137,139,393] used the ISIC-19 SLS dataset in the past. Therefore,

the choice of ISIC-17 to build a robust SLS model is preferred by researchers, as this trend is reflected in the last twelve years' scenario. Again, [Table 3](#) and [Fig. 3\(b\)](#) demonstrate that the authors have favored datasets with more class numbers for constructing an SLC model, which led to an increased usage of the ISIC-18 dataset. The SLC models are challenged by the increased class number and unbalanced class sample distribution, and researchers have attempted to create trustworthy SLC models that are free from specific class bias [3,7].

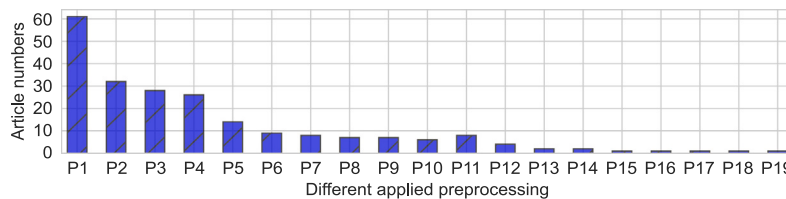


Fig. 4. The number of articles employing different preprocessing, where the preprocessing P1 to P19, respectively, indicate Hair removal, Contrast enhancement, Normalization, Color space transformation, Median filter, Automatic color equalization, Remove light reflections, Standardization, Dark region removal, Mean filter, Gaussian filter, Elimination of shading, Histogram equalization, Gamma correction, Sharpening filter, Wiener filter, Gabor filter, Bias field correction, Contrast Limited Adaptive Histogram Equalization.

It is also noticed from Fig. 3 that the PH2, Dermaquest, IAD, and other private datasets were also used in some articles even after 2016, although they have fewer sample images. The discernible reason is that some authors trained and evaluated their models on ISIC [173,551], where they further evaluated their SLS and SLC models on those datasets to uncover guaranteed robustness, as they were neither utilized during the training nor validation phases. However, among PH2, Dermaquest, IAD, and other private datasets, PH2 was most commonly applied in the past literature. Thus, our review confirms that PH2 has been commonly employed as an external dataset in the last twelve years to validate the results obtained from the ISIC training.

4. Preprocessing and augmentations

Preprocessing seeks to improve image data quality, suppress distortions, or enhance additional processing features, while augmentation creates new training examples from the existing data distribution. Identifying those optimal procedures requires a basic understanding of the problem, data collection, and system environment. This is a complex task because procedures work satisfactorily in some circumstances but not in others. Therefore, this article summarizes the applied preprocessing (in Section 4.1) and augmentation (in Section 4.2) techniques. The approaches to mitigating the class bias problem (addressed in Section 3.1) are also surveyed in Section 4.2.

4.1. Preprocessing

Image preprocessing eliminates noise and enhances the quality of the original image by removing uncorrelated information and surplus background portions for further processing. An appropriate selection of preprocessing approaches can considerably increase the accuracy of the intended system [3,7,87,552]. Examining selected articles reveals that skin lesion images contain many types of noise and artifacts: markers, body hairs & veins, body fibers, air bubbles, reflections, non-uniform lighting, rolling lines, shadows, non-uniform vignetting, artificial landmarks, and patient-specific effects like lesion textures, colors, diverse shape & size of lesion area [173]. Table 4 highlights all the preprocessing methods employed for SLA in the past twelve years with their short descriptions and corresponding articles.

Describing the detailed theories of all preprocessing techniques is not the objective of this paper; instead, we focus on their efficacy in the SLA domain. However, citations for such theories are given in Table 4. Fig. 4 displays the utilization frequencies of various preprocessing techniques used in 594 SLA articles from 2011 to 2022, revealing that hair removal, contrast enhancement, normalization, color space transformation, and median filtering are massively acknowledged top-5 preprocessing methods used throughout 27.9%, 14.6%, 12.8%, 11.9%, and 6.4% SLA articles, respectively.

Due to their high usage, these five preprocessing techniques are likely to be highly effective for SLA and can be grouped as **High-frequency** techniques. They can thus be the benchmark for SLA preprocessing for future research. Other preprocessing methods like automatic color equalization, removal of light reflections, standardization, dark region removal, mean filter, and Gaussian filtering are employed in the

same number of SLA articles, approximately 2.7% ~ 4.1% of articles. They could be categorized as **Medium-frequency** preprocessing strategies for SLA. The remaining elimination of shading, histogram equalization, gamma correction, sharpening filter, wiener filter, Gabor filter, bias field correction, and contrast limited adaptive histogram equalization could be organized as **Low-frequency** preprocessing schemes due to their less common usage in the last twelve years. With the help of Fig. 4, this finding would assist researchers in choosing a preprocessing strategy for lesion analysis. In addition, numerous authors utilized grayscale images instead of the provided RGB images. Such a conversion can be obtained in many ways, for instance, by averaging RGB channels and taking a single channel from different color spaces. Eq. (1) demonstrates the most frequent grayscale conversion technique.

$$Y = 0.299 \times R + 0.587 \times G + 0.114 \times B, \quad (1)$$

where R, G, and B are the weighted summations of red, green, and blue pixels, respectively, and Y is the grayscale luminance value.

4.2. Augmentation and imbalance problem

Data augmentation raises training data samples to minimize model overfitting. Affine transformations and color alteration are the basic augmentation techniques, while texture transformation preserves contours, shading, lines, strokes, and areas of information [556]. Recently, Generative Adversarial Network (GAN) [556] is a new technology for unsupervised image creation utilizing the min–max strategy and is beneficial for text-to-image synthesis, superresolution, image-to-image translation, blending, and inpainting. However, the survey of the selected 594 articles returns the following augmentations in the past from 2011 to 2022 for the SLA task: Rotation [1,26,28,29,31,36–43,47,49,56,58,64,69,72,74,77,79,81–84,86,91,95,101,102,104,106,107,109,111,114–118,120,126,127,129,131,132,136,139,148,152,154,158,160,164,164,166,170,172,173,177–180,183,186,198,202,210,213,216,217,222,230,235,236,238,241,243,244,250,260,267,269,270,272,273,275,276,280,284,285,288,299,307,310,353,356–358,360–362,366–369,371,374,379,383,384,386–388,390,392,395,400–403,406,406,407,412–414,416,418,419,421–423,426,430,437–439,443,445,453,456,457,460,462,464,466,471,475,481,482,484,485,488,494,498,500,505,510,511,522,523,525,526], Horizontal flipping [28,67,93,148,152,154,159,160,166,169,170,172,173,177–180,183,185,186,198,202,204,209,210,213,216,217,222,224,226,227,230,235,236,238,243,244,250,267,269,270,272,273,275,276,279,280,284,288,298,302,303,307,310,371,396,398,400,401,418,419,437,438,440,445,453,456,457,460,462,463,466,471,475,481,482,488,494,498,500,505,510,511,522,523,525], Vertical flipping [28,50,67,152,154,159,160,166,169,170,172,173,177–180,185,186,198,202,204,209,210,213,216,222,224,226,227,230,235,236,238,243,244,250,267,269,270,272,273,275,276,279,280,284,288,298,302,303,307,310,371,396,398,400,401,418,419,437,440,445,453,456,457,460,462,463,466,471,475,481,482,488,494,498,500,505,510,511,522,523,525], Scaling [26,28,29,36,38,40–42,65,69,72,74,78,79,81,86,91,94,95,98,106,111,115,117,118,129,131,132,139,152,158,170,172,177–179,186,198,204,241,243,267,269,270,272,273,276,284,285,299,356,357,361,366,367,369,372,374,378,382,

Table 4

Commonly employed preprocessing in the last twelve years, scrutinizing a total of 594 articles: 356 for SLS and 238 for SLC.

| Methods | Remarks | Employed articles |
|------------------------------|--|---|
| Hair removal | The lesion's boundary and texture information are often occluded due to the presence of hair, leading to over-segmentation and weak pattern analysis [553]. Therefore, an automatic hair removal method [553] is necessitated, preserving all the lesion features. | [1,9,30,38,48,53,70,76,103,121,125,134,136,140,145,147,175,182,189,195,212,233,245,249,252,255,258,262–264,274,278,280,292,297,304,306,316,317,319,322,323,334,335,344,414,429,447,459,467,502,506,510,520,525,531,536,538,545,554] |
| Normalization | Subtraction of mean RGB values computed over each image or whole training dataset to exclude poor contrast issues, which also deals with the various lighting conditions in the skin images [452,482]. | [1,175,216,218,230,273,274,278,304,323,329,344,347,443,452,458,465,467,481,482,494,496–498,518,522,526,535] |
| Standardization | Applies the mean and standard deviation of RGB values to scale all images to the same range to decrease biasing from different sources [458]. | [1,175,198,244,458,482,494] |
| Median filter | Filtering an image by placing the median value in the input window at the center of that window to lessen impulsive, salt-and-pepper, or sudden random noise. | [145,147,266,328,333,334,336,342,458,467,470,525,531,538] |
| Remove light reflections | Devices' light reflections are eliminated by applying morphological closing and erosion. A non-linear median filter is also helpful for removing light reflection and other tiny dots in the background outside the lesion area [334]. | [9,245,304,322,323,334,342,531] |
| Sharpening filter | The sharpening spatial filter removes blurring, improving the definition of fine detail and sharpening edges that are not clearly defined in the original given image. | [536] |
| Wiener filter | It is a low pass linear filter, usually applied in the frequency domain, for images degraded by additive noise, blurring, and constant power additive noise. | [538] |
| Gabor filter | A Gabor filter is a bandpass filter and can be defined as a sinusoidal plane of particular frequency and orientation, modulated by a Gaussian envelope. | [538] |
| Histogram equalization | It improves the contrast of an image by utilizing its histogram, spreading out the most frequent pixel intensity values, or stretching out the image's intensity range. | [322,538] |
| Elimination of shading | It is induced by imaging non-flat skin surface and light-intensity falloff towards the edges of the skin image, causing color degradation and poor segmentation results [344]. | [218,344,465,545] |
| Mean filter | It is a smoothing method to overcome the noise effect by reducing the intensity variation between neighboring pixels, a circular or square neighbor. | [255,311,313,327,344,544] |
| Automatic color equalization | This method enhances both color information and contrast by applying two main stages, including chromatic or spatial adjustment and dynamic tone reproduction scaling [347]. | [178,304,344,347,443,470,496,497,544] |
| Contrast enhancement | It adjusts the relative brightness and darkness of lesions to improve their visibility. The contrast or tone of the skin image can be modified by mapping the gray levels in the image to new values through a gray-level transform. | [2,38,45,53,76,178,195,201,201,207,245,255,262,264,264,274,278,280,291,292,292,313,317,319,327,331,333,347,441,455,459,476,506] |
| Dark region removal | The black corners having nearly the same lesion's intensity due to a round circular lens can be excluded by applying binary masks of the dark corners obtained from the OTSU's thresholding [319]. | [212,249,252,264,319,342,488] |
| Gamma correction | It controls the overall brightness that is not adequately corrected, seeming either bleached out or too dark. | [323,486] |
| Color space transformation | It is the translation of the representation of a color from one basis to another. In general, CIE L*a*b*, CIE L*u*v*, YCrCb (Y color component has most of the image details), and HSV are remarkably practiced in literature [317]. | [2,40,62,63,91,124,147,169,176,230,262,273,288,295,308,309,313,317,323,327,329,337,443,459,476,555] |
| Bias field correction | It adjusts the bias field signal before the next processing, reducing intensity heterogeneity. | [327] |
| Gaussian filter | A Gaussian filter blurs an image using a Gaussian function to decrease noise and detail, similar to a mean filter. | [2,33,142,293,317,327,455,459] |
| CLAHE [†] | CLAHE is a variant of adaptive histogram equalization and applied to enhance foggy skin images' perceptibility level. | [306] |

[†]CLAHE: Contrast Limited Adaptive Histogram Equalization

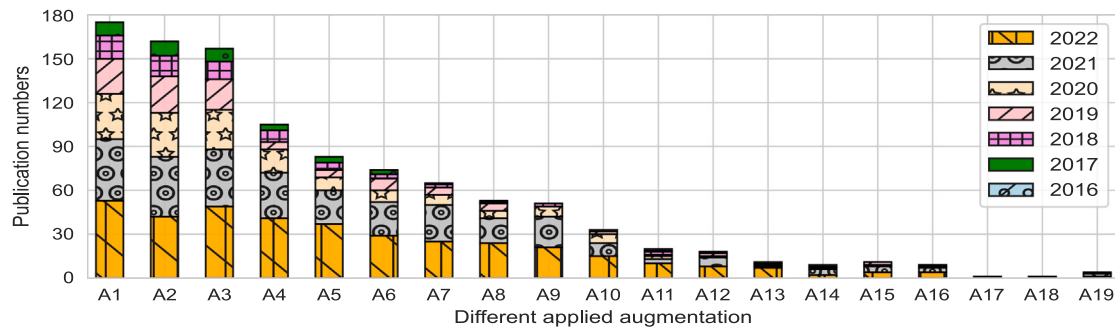


Fig. 5. The number of SLS and SLC articles using augmentations A1 to A19 (defined in Table 5) in the past literature.

388, 392, 412, 414, 418, 423, 430, 439, 449, 453, 457, 466, 468, 471, 482, 488, 522], Region cropping [37, 79, 91, 94, 101, 102, 113, 120, 126, 131, 172, 177, 180, 183, 209, 213, 227, 267, 276, 288, 298, 302, 307, 357, 358, 360, 361, 377, 384, 390, 396, 402, 406, 421, 422, 445, 449, 452, 456, 468, 490, 498, 511, 513, 525], Shifting [1, 42, 72, 78, 115, 122, 173, 177, 186, 210, 222, 238, 241, 243, 244, 270, 272, 273, 285, 366, 367, 369, 378, 391, 392, 412, 418, 423, 438, 439, 457, 462, 471, 498, 522, 526], Contrast adjustment [29, 43, 82, 102, 131, 157, 158, 172, 178, 198, 213, 222, 224, 236, 284, 294, 303, 378, 437, 466, 488], Shearing [42, 102, 106, 126, 136, 139, 152, 177, 186, 213, 241, 288, 371, 388, 406, 413, 414, 430, 453, 475, 482, 488, 523], Horizontal and vertical or both flipping [26, 28, 29, 31, 36, 37, 39, 42, 43, 47, 49, 58, 64, 65, 67, 69, 74, 77–79, 82, 82–84, 86, 91, 93–95, 98, 99, 101, 104, 107, 109, 111, 113, 115–118, 120, 122, 126, 129, 131–133, 136, 139, 158, 169, 173, 186, 226, 267, 276, 353, 357, 358, 360, 361, 367–369, 371, 374, 377–380, 382–384, 387, 390–392, 395, 402, 403, 406, 412–414, 416, 421, 422, 426, 430, 460, 464, 468], Adaptive histogram equalization [82, 102, 131, 158, 172, 178, 213, 226, 242, 358, 372, 374, 377, 378, 380, 382, 388, 407, 412, 421, 430, 439, 449, 535], Gaussian noises [28, 82, 106, 133, 157, 158, 273, 276, 279, 378, 421, 490, 535], RGB to HSV transformation [31, 131, 169, 222, 236, 303, 358, 358, 378, 378, 380, 382, 388, 412, 421], Elastic distortion [79, 86, 127, 158, 210, 289, 535], Adding noises (salt or pepper noises) [172, 490, 535], Color jittering [227, 236, 440], Gamma correction [226, 437], GAN [454, 490], Whitening [177], and Dihedral transformation [284]. These typically applied augmentations are briefly discussed and explained in Table 5.

Fig. 5 indicates the frequency of these augmentations in the past twelve years' articles. It illustrates that rotation, horizontal flipping, vertical flipping, scaling, region of interest cropping, and shifting are the top-6 SLA augmentations, used throughout respectively in 29.5%, 27.3%, 26.4%, 17.7%, 14.0%, and 12.5% of the total of 594 articles.

Notably, these six most common augmentations (**High-frequency**) were more frequently operated in 2022, and their deployments have dropped from 2022 to 2016. Again, contrast adjustment, shearing, both axis flipping, histogram equalization, and adding Gaussian noise can be classified as the **Medium-frequency** augmentation methods due to their medium utilization frequency. The remaining augmentation techniques were less commonly applied in the past twelve years and could be termed as **Low-frequency**.

Furthermore, a close inspection of Fig. 5 demonstrates that none of the augmentations were applied before 2016. It is also remarkable that the number of articles with augmentation applications has significantly increased trends from 2016 to 2022. Recalling Fig. 1 shows that the number of SLA articles published after 2016 has enormously increased after DL's engagement, especially using CNN methods. Such an advancement in CNN models for SLA tasks promotes the need for diverse augmentations, as CNNs rely on a large amount of data to be robust and effective. Besides, Fig. 5 in conjunction with Table 5 and Fig. 1 demonstrates that geometric augmentations, i.e., spatial information transformation, are more common in CNN-based learning systems. In contrast, color or texture augmentations are more common in manual feature-based ML and computer vision algorithms. Although the usage

of GAN [557] is a recent trend in other domains, it has yet to be widely employed in SLA in the last twelve years (see Fig. 5). The generator and discriminator need to be in sync with each other, and the learning process of GANs may miss underlying anatomical structures and attributes. It could be mitigated by incorporating anatomical constraints for making realistic images.

The big picture of the class sample distributions of all datasets in Table 1 reveals that class sample images are imbalanced, which could bias the classifier towards the class with more samples [3]. This is especially true in skin lesion datasets with few manually annotated training examples. However, SLA researchers attempted numerous methods to reduce class bias. The authors in [178, 363, 363, 379, 379, 380, 383, 404, 409, 432, 452, 462, 464–466, 473, 482, 486, 488, 494, 500] rewarded more extra consideration to the class with minority samples, estimating the class weight using a portion of $W_n = N_n/N$, where W_n , N , and N_n separately indicate the n th-class weight, the total number of samples, and the sample in the n th-class. Some authors acquired more photographs and integrated them with the minority class to balance it with the majority class [234, 495, 526]. The augmentations in Table 5 are sometimes applied to the minority class to increase its representative sample, as in [1, 140, 164, 234, 267, 443, 449, 454, 457, 471, 483, 484, 494, 496]. A SMOTE oversampling technique was applied in [459], demonstrating an improvement in the differentiation of melanoma and benign lesion images. To handle imbalanced classes, an ensemble method using three classifiers with a linear plurality voting was employed in [461], where the other two models can overcome the bias from any candidate model. Lastly, the authors in [453, 460, 463, 467, 491, 510, 519, 522, 523, 533] employed random oversampling and undersampling. The first technique randomly adds minority class samples to the training dataset. In contrast, the latter undersampling chooses examples from the majority class and deletes them from the training dataset. To sum up, class weighting, minority class augmentations, oversampling, and undersampling are the most frequent strategies for overcoming class imbalance in SLA tasks. These strategies can help researchers construct a generic SLA framework.

5. Segmentation techniques

In recent years, segmentation algorithms for SLA have been improved [10] using different approaches. These approaches are categorized into four groups to contrast them: **edge-based SLS**, **region-based SLS**, **threshold-based SLS**, **AI-based SLS**, and **other SLS**. The following five paragraphs briefly introduce those clusters of SLS techniques. Then, we provide our insightful discussions regarding them from the 356 SLS papers in the rest of the paragraphs.

Edge-based SLS. Edge-based SLS methods look for edge pixels and link them to produce image contours, which can be manual or automatic. The manual application utilizes the trackpad to delineate lesion boundaries. In contrast, the automatic method employs edge detection algorithms like the watershed algorithm [293], active contours [124,

Table 5

Typically engaged augmentations in the past, surveying a total of 594 articles: 356 for SLS and 238 for SLC.

| Method | Details descriptions |
|-------------------------------|---|
| Rotation (A1) | Rotate the image coordinates of (x_1, y_1) by an angle of θ around (x_0, y_0) , resulting the coordinates of (x_2, y_2) where $x_2 = \cos(\theta) \times (x_1 - x_0) + \sin(\theta) \times (y_1 - y_0)$ and $y_2 = -\sin(\theta) \times (x_1 - x_0) + \cos(\theta) \times (y_1 - y_0)$. |
| Horizontal flipping (A2) | Change the image by a mirror-reversal of an original across a vertical axis, where the left side switches to the right side and vice versa. |
| Vertical flipping (A3) | Modify an image with a mirror-reversal of the original across a horizontal axis, where the top side switches to the bottom side and vice versa. |
| Scaling (A4) | Enlarge or reduces the image's physical size by changing the number of pixels it contains, changing the size of the contents of the image and resizing the canvas accordingly. |
| Region cropping (A5) | A data augmentation technique that picks a random subset of the original image containing more salient information about the region of interest. |
| Shifting (A6) | Translation of an image in up, down, left, or right, along with any combination of the above direction, where every point of the object must be moved in the same direction and for the same distance. |
| Contrast adjustment (A7) | Remap image intensity values to the full display range of the data type, sharpening differences between black and white. It can either make an image more vivid or mute the tones for a more subdued feel. |
| Shearing (A8) | Shift one part of an image, a layer, a selection, or a path to a direction and the other part to the opposite direction; for example, a horizontal shearing will shift the upper part to the right and the lower part to the left, resulting in a diamond from a given rectangle. |
| Both flipping (A9) | Modify an image with a mirror-reversal of the original across both the vertical and horizontal axes, where the top side switches to the bottom side and then the left side switches to the right side and vice versa. |
| Histogram Equalization (A10) | Adjust the contrast of an image by using its histogram, spreading out the most frequent pixel intensity values, or stretching out the image's intensity range. It allows the image's areas with lower contrast to gain a higher contrast. |
| Gaussian noises (A11) | A type of mean spatial filtering that produces a new image by altering the structural details of an input image. |
| HSV (A12) | Provide a numerical readout of the image corresponding to the color names contained therein, abstracting the color (hue) by separating it from saturation and pseudo-illumination. |
| Elastic distortion (A13) | Generate a coarse displacement grid with a random displacement for each grid point that is then interpolated to compute a displacement for each pixel. Finally, the input image is then deformed using displacement vectors and spline interpolation. |
| Adding noises (A14) | An impulse noise caused by sharp and sudden disturbances in the image signal that presents as sparsely occurring white and black pixels. |
| Color jittering (A15) | A type of image data augmentation that randomly changes the brightness, contrast, and saturation of the image. It also adds random noise to the image. |
| Gamma correction (A16) | A nonlinear operation that encodes and decodes luminance or tristimulus values in video or still image as $V_{in} = A \times V_{out}^{\gamma}$, where γ and A are the raised power and multiplied factors, respectively. |
| Whitening (A17) | A whitening transformation converts a vector of random variables with a known covariance matrix into a set of new variables whose covariance is the identity matrix, which has widely been adopted to remove redundancy by making adjacent pixels less correlated. |
| Dihedral transformation (A18) | A linear transformation that includes rotations and reflections of the images in the eight possible directions or angles of a dihedron. |
| GAN (A19) | Produce new data samples from a given random noise from a latent space and deliver unique images that mimic the feature distribution of the original dataset. |

[258,292,337,345,545,558], canny edge detector [328,331], and multi-direction gradient vector flow snake model [545]. In this segmentation, an edge filter is applied to the image, pixels are classified as edge or non-edge based on the filter output, and pixels not separated by an edge are assigned to the same class. Active contours are the most common edge-based SLS method out of the 356 papers written in the last twelve years.

Region-based SLS. In these systems, images are divided into regions or groups of comparable pixels based on their attributes, assuming neighboring pixels should have the same value. Each pixel in a region is compared to its neighbors and clustered based on specific conditions. This form of SLS covers iterative region-based [136,290,347], iterative stochastic region-merging [349], mean shift-based gradient vector flow [348], K-means & fuzzy C-means clustering [87,121,124,128,139, 274,282,297,304,306,308,312–314,325,330,336,338,340,343,346,559], and Eikonal-based region growing clustering [335]. Lastly, this article suggests that K-means & fuzzy C-means clustering are the most common

region-based SLS methods, which would be viewed as a representation of the region-based SLS approach.

Threshold-based SLS. Threshold-based SLS can be classified as point-based or pixel-based segmentation, depending on the threshold estimation approaches, and commonly suffers from difficulty in estimating effective thresholds due to dermoscopic artifacts [173]. OTSU [87,124, 161,166,167,192,193,195,214,252,255,295,309,317,320,323,341,344, 545,555], histogram estimation [306,312,329], morphological operations [263,295,342], optimal color channel-based empirical threshold estimation [333], and mean pixel intensity level-based threshold estimation [334] are examples of this cluster of techniques. Notably, the OTSU thresholding technique is the most common threshold-based SLS strategy in the selected 356 SLS papers, setting it to stand apart from other techniques. This technique's automatic and faster threshold estimate could be the reason for its popularity.

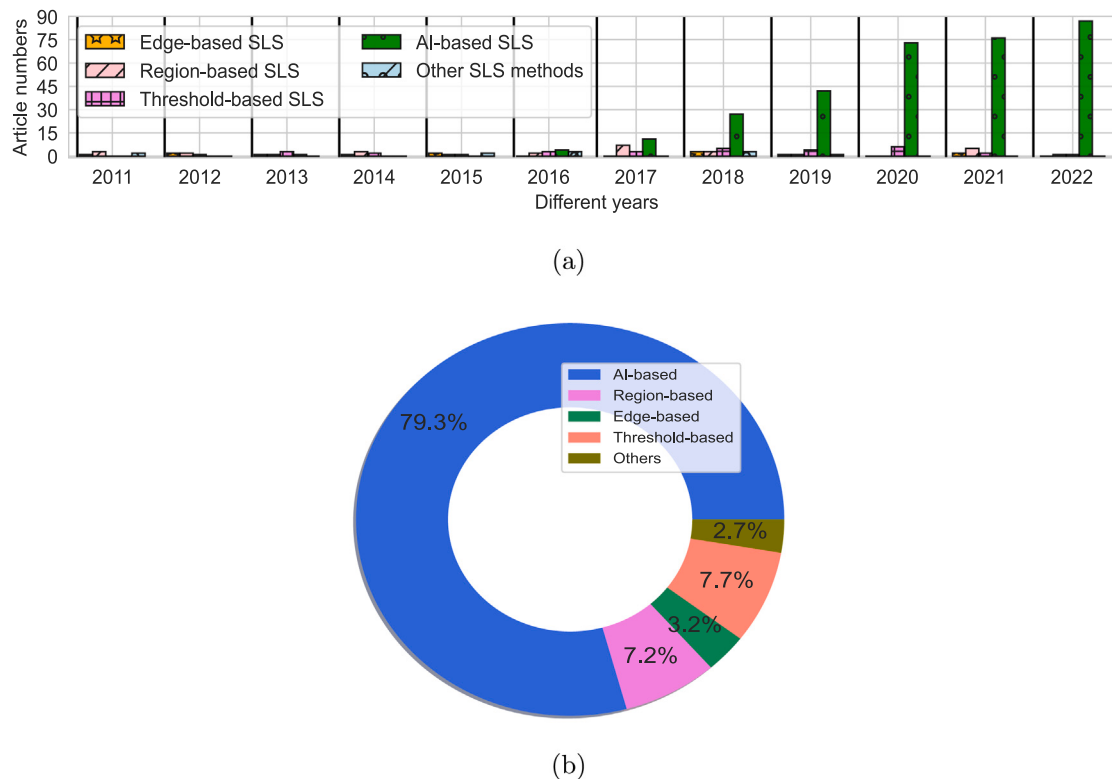


Fig. 6. (a) The number of articles employed different SLS methods, consulting the commonly applied techniques and (b) the percentage donut chart of the SLS articles for the five SLS categories.

AI-based SLS. AI models, especially CNNs, make it possible to build an end-to-end supervised model without having to manually extract features [560,561], and they have been very successful in many areas of medical imaging: arrhythmia detection [562–564], skin lesion segmentation and classification [3,7,173,565,566], breast cancer detection [567–569], brain disease classification [570], pneumonia detection from CXR images [571], fundus image segmentation [572,573], minimally invasive surgery [574], lung segmentation [575], etc. This category of methods applies computational intelligence techniques to the segmentation process, including genetic algorithms [190,339], fully convolutional neural networks [9, 25–27, 29, 31, 35–41, 43, 46, 47, 49–52, 54, 59, 61–66, 68–75, 77, 80–82, 88, 89, 93–103, 105, 106, 108–116, 118–120, 122, 124, 125, 127, 129–133, 135, 137, 138, 140–142, 202, 203, 210, 217, 221, 230, 240, 244, 257, 259–261, 265, 268, 269, 271–273, 275–280, 283–289, 294, 298–301, 303, 305, 307, 308, 310, 393, 406, 501, 558, 576], expectation–maximization [316], rule-based algorithms [315], Co-operative neural network [347], and artificial bee colony [266]. Individual scrutiny of the specified 356 SLS reveals that fully convolutional neural networks are the most frequently employed in the SLS challenge, establishing them as the characteristic AI-based SLS methods.

Other SLS methods. Other approaches include probabilistic maximum-a-posteriori [264,350], Markov random field [296,327,332], Delaunay Triangulation [322], Grap-cut [274], Cellular Automata [321], Wavelet transform [291,319], and optimized color feature [207,262]. They are grouped as other SLS task approaches from 2011 to 2022, like four other segmentation groups.

Fig. 6(a) demonstrates year-wise SLS article numbers in the past, bestowing the frequency of various SLS techniques covered in the previous five paragraphs.

AI-based SLS methods have been most extensively employed over the last twelve years, notably after 2016. Again, the application frequencies of the five SLS categories are shown in Fig. 6(b), highlighting that 79.3% of publications used AI-based SLS. Figs. 1 and 6 (a & b)

collectively demonstrate that the employment of AI-based SLS models has become crucial to the SLS task as the number of AI-based SLS articles has been expanding tremendously since 2016. Even in the last few years, the application of remaining SLS methods, except AI-based methods, has significantly reduced. This AI-based SLS category would be considered a **High-frequency** SLS method. Thus, this SLS approach will likely continue its dominance in the future. Threshold-and region-based SLS can be designated **Medium-frequency** SLS techniques, while the remaining SLS methods can be considered as **Low-frequency** SLS approaches (see Fig. 6(b)). Discussions on the details of SLS techniques are not the focus of this article. For such discussions, the reader is referred to a previous review article of [10]. However, our analysis reveals that 87.2% of AI-based SLS articles employed DL methods, in particular, deep CNNs. We thus review the details of this particular CNN technique in the following paragraph.

In order to build an end-to-end CNN-based SLS system, a model consists of two essential components: the encoder and the decoder [173]. The former component, the encoder, comprises convolutional and subsampling layers and is responsible for automatic feature extraction. The convolutional layers are applied to construct the feature maps, whereas the subsampling layers are employed to achieve spatial invariance by decreasing the maps' resolution. This reduction in resolution leads to an extension of the field of view of the feature map, which in turn makes extracting more salient features easier and minimizes the computational cost [574]. This is notably observed from the chosen 356 SLS article that many authors have employed different variants of pre-trained (on ImageNet, PASCAL-VOC, MS-COCO, etc.) CNN models in the encoders like AlexNet [61,207,298], Xception [174, 210], VGG [108,155,198,205,207,208,217,240,244,259,276,303,305, 406], ResNet [31,39,61,70,89,129,146,164,168,175,182,185,187,198, 216,217,224,234,235,260,284,294], LeNet [182], Inception [89,125, 165,218,242], InceptionResNet [155], MobileNet [114,141], and DenseNet [95,129,165,173,179,180,236,269,275]. Remarkably, it is revealed that 37.3%, 23.7%, and 15.3% of the articles used ResNet,

VGG, and DenseNet, respectively, for transfer learning (backbone in the encoder). Again, the latter component in the CNN-based SLS system, the decoder, semantically projects the distinctive lower-resolution features learned by the encoder onto the pixel space of higher resolution to achieve a dense pixel-wise classification. The semantic segmentation networks have similar encoder designs, but they vary mainly in their decoder mechanisms concerning how the discriminating features are projected onto the pixel space. However, the significantly decreased feature maps due to subsampling often undergo spatial resolution loss, which introduces coarseness, less edge information, checkerboard artifacts, and over-segmentation in semantically segmented masks [173]. To resolve these problems, skip connections in a U-Net were proposed in [577], which allowed the decoder to recover the relevant features learned at each stage of the dropped encoder due to pooling. Similarly, the features at various coarseness levels of the encoder in a Fully Convolutional Network (FCN) were fused in [578] to refine the segmentation. However, when the deconvolution kernel size is not divisible by the up-scaling factor, a deconvolution overlap occurs as the number of low-resolution features that contribute to a single high-resolution feature is not consistent across the high-resolution feature map [579]. Due to this deconvolution overlap, checkerboard artifacts may appear in the segmented mask. Therefore, a full-resolution convolution network was designed in [551], excluding subsampling layers in the encoder to conserve the spatial information of the feature maps. However, the subsampling of feature maps is exceptionally desirable to be employed on CNN due to the several positive perspectives, as previously mentioned. A complete survey and review on those decoder mechanisms and skip (shortcut) connection can be found in [580].

Many authors in [26,29,36,40,41,46,61–63,68,70,74,77,80–82,88,93,94,96,97,102,103,106,109–116,119,130–133,135,137,140,141,393,558,576] have customized CNN networks by exploiting different segmentations architectures like U-Net, FCN, and SegNet [38]. It is notable that many recent works applied different attention mechanisms (channel, spatial, and/or atrous attention) in the CNN-based SLS methods [25,47,49,50,52,54,59,64,66,67,69,72,73,86,99,100,105,112,114,119,122,132,133,581,582]. Some authors also proposed semi-supervised CNN-based SLS techniques [51,65,71,127]. Recently, transformer models were also applied for automated lesion segmentation [27,35,43,75,98]. Often, the authors ensembled multiple SLS models or outputs to produce a refined lesion segmentation [31,37,101,120,129,142,164,165,170,180,184,218,230,246,273,276,284,287–289,304,406]. For example, a bagging-type ensemble approach was executed in [273] to combine the outputs of various FCNs while improving the image segmentation performance on the testing images, multi-scale ensembles [31,37,120], and adaptive ensembles [101]. Again, the authors in [230,276,288] ensembled different outputs at the post-processing stage to increase the segmentation results. Firstly, they segmented an input image by augmenting it to generate various outputs. Then reverse operations were performed on the results that were finally averaged to get a lesion mask. DeeplabV3 [118,406] and Mask R-CNN [77,118] were employed in [218] to propose three ensemble model variants. Ensemble-ADD combines the results from both models, Ensemble-Comparison-Large picks the larger segmented area by comparing the number of pixels in the output of both methods, and Ensemble-Comparison-Small picks the smaller area from the output. Lastly, a pixel-wise majority voting ensemble for lesion segmentation was proposed and implemented in [170]. Also, the authors in many articles have incorporated different post-processing methods to refine the segmented lesion masks, as explained in Table 6.

The above table reveals that morphological operations, such as dilation, erosion, closing, and opening, have been the workhorse and are massively employed for post-processing segmented lesion masks [87,159,190,191,200,212,218,233,244,252,273,277,291,304,311,333,336,555]. Small holes and disconnected island regions in the segmented lesion masks were resolved in various ways in the 356 SLS articles. For example, hole-filling algorithms can be used to fill tiny holes [9,

124,210,289,304,307,308,312], and island regions can be removed by preserving the target region(s) using the region property techniques [9,184,205,307,312,347]. In some articles [170,209,222,235,242,294], the authors have employed Conditional random field techniques to refine the segmented masks from the coarse output masks.

6. Classification techniques

Computational SLC methods related to the lesion features are founded on the ABCD(E) rule [140,410,415,581], pattern analysis, the seven-point checklist, and Menzies' method. Those methods are illustrations of clinical techniques used for the prognosis and diagnosis of image-based skin cancer [6], color, diameter (or differential structures in the case of dermoscopic images), and evolution (or elevation) features, according to the standards delivered in [6]. The other traditional methods of the SLC have been reviewed in detail in [6]. However, those SLC methods require a dermatologist for the naked-eye assessment, which may incur subjectivity associated with human evaluations and human errors. Dermatologists' manual examination is usually monotonous, time-consuming, and subjective. The accuracy of manual assessment can also depend on the reviewer's experience and workload. Hence, CAD systems have been developed to avoid the above-mentioned limitations. This article focuses on reviewing automated CAD systems. There has been a significant advancement in developing automated lesion classification algorithms and approaches for SLA in the recent past [10]. Some methods were based on manual feature engineering with ML models, but DL-based automatic feature learning schemes are becoming more popular [10]. These two main approaches are surveyed and reviewed below.

6.1. ML-based SLC

As noted previously, ML-based SLC strategies depend on successfully engineering the manual lesion features that are first described and reviewed in Section 6.1.1. Then, the employed classifiers are inspected in Section 6.1.2.

6.1.1. Lesion features

Lesion attributes (or features) can be extracted either globally or locally to acquire category information. Most works explore the global features of the lesion, for instance, extracting features from all segmented regions [178,206,264,292,520,530,533]. Some examinations have employed local characteristics, allowing the characterization of a diverse lesion region. Lesion features can generally be organized into different categories: shape, color variation, texture analysis, and other miscellaneous. These lesion features are summarized in Table 7.

Shape features consider the lesion's asymmetry or border's irregularity, dividing the lesion region into two sub-regions by an axis of symmetry to analyze the area's similarity by overlapping the two sub-regions of the lesion along the axis. Then, the asymmetry index is estimated by the difference between the two sub-regions of the lesion, for example, with the XOR operation between them [6]. Sometimes, geometrical measurements from the segmented lesion area are computed to assess the lesion's asymmetry and border irregularity, which include the area of the lesion, aspect ratio, compactness, perimeter, greatest diameter, shortest diameter, equivalent convex hull, eccentricity, solidity, rectangularity, entropy measures, circularity index, and irregularity index (see details in Table 7) [1,439,470,533]. Out of the 238 SLC articles, 33 articles (13.9%) employed lesion shape features in the last twelve years for the SLC task.

The RGB color space is commonly employed to represent the colors of skin lesions. Other color spaces have also been applied in order to acquire more specific information about a lesion's colors, such as normalized RGB, HSV, HVC, CMY, YUV, I1/2/3, Opp, iIN, JCh, L*C*H, CIEXYZ, CIELAB, and CIELUV (see details in [6]). Several statistical measures such as minimum, maximum, average, standard deviation,

Table 6

Commonly employed post-processing for SLS from 2011 to 2022, scrutinizing a total of 356 for lesion segmentation.

| Details post-processing method | Articles |
|--|--|
| Conditional random fields, as a statistical modeling method for structured prediction, considering neighboring pixels' information in the new pixel prediction. | [170,209,222,235,242,294] |
| The binary lesion masks are followed by morphological dilation operations. The region closer to the image center is picked, followed by unwanted components like corner effect removal and filling of the small holes. | [159] |
| The best cluster from all the predicted clusters is determined by calculating the mean value for each cluster and selecting the maximum mean value. Then morphology operations, for example, opening, closing, and filling holes are applied to enhance the segmented lesion masks. | [190] |
| Subtraction of smaller or misclassified areas and sharp fragments from the mask's borders. | [145,278] |
| Iterative self-organizing data analysis technique was employed to threshold the output probability map from the sigmoid activator of their DSNet to retrieve the lesion mask. | [173] |
| Simply morphological smoothing and extracting the largest connected component from the predicted binary lesion mask. | [9,184,205,307,312,347] |
| Watershed-based postprocessing feeds high-confidence pixel classifications as seeds into the watershed algorithm. | [198] |
| Several consecutive morphological filtering, such as dilation, erosion, closing, and opening, for enhancing the predicted lesion boundary. | [87,191,200,212,218,233,244,252,273,277,304,311,333,336,555] |
| A convex hull operation follows the morphological opening process of the predicted binary mask for lesion shape approximation. | [157] |
| Region merging and morphological operations are applied to obtain the final lesion mask. | [153] |
| Fill in the small holes in the predicted binary lesion mask. | [9,124,210,289,304,307,308,312] |
| The output probability map is subjected to three consecutive post-processing actions constructing the final mask: thresholding the probability map at 0.5, choosing the largest connected component, and finally, filling the small holes. | [240,258] |
| k-means clustering and flood-fill techniques are combined to get the final lesion mask. Then, holes are sealed using a hole-filling algorithm. | [274] |
| The central lesion location is identified, then hole filling and morphological closing are applied to fill tiny holes and islands. For the final segmented mask, a Gaussian mask looks at how closely connected regions are to the image's center. | [291] |
| A dual-threshold method to generate a binary mask, where a relatively high threshold (= 0.8) is devoted to determining the lesion center, and a lower threshold (= 0.5) is applied to the output map. After filling small holes with morphological dilation, the final lesion mask is decided. | [273,285] |
| The largest connected binary objects are kept and joined. Then, morphological operations are performed to patch gaps and remove excess skin. Finally, lesion masks are smoothed using a convolution filter. | [38,319] |
| A graph-cut algorithm is applied to the output score maps to fine-tune the predicted masks. | [299] |

skewness, and variance are widely applied to feature extraction from skin lesion images, computing each color channel of the lesion region using one or several color models [206,264,292,297,439,443,459,467,502,521,536,545,548,550,589]. Furthermore, these measures may also be applied to other regions associated with the lesion's border to identify a sharp transition, indicating malignancy. Skin lesion features based on relative colors have been proposed to assess color features in different regions associated with the lesion. The relative color consists of comparing each pixel value of the lesion to the average color value of the surrounding skin. Likewise, the use of this feature may present advantages such as compensating for the variability in the image's color caused by uneven illumination and varying equalization in skin color across individuals. The occurrence of possible primary colors present in skin lesions has also been analyzed through the quantification of the number or percentage of pixels within the segmented area for each of

the primary colors [590]. Out of the 238 SLC articles, 34 SLC articles (14.3%) employed lesion color features in the past SLC task.

Texture analysis is generally used to discriminate between benign and malignant lesions by estimating their structure's roughness, encompassing descriptors like statistical-, model-, and filter-based methods [6]. Among the various statistical-based texture descriptors applied in the literature, the Gray Level Co-occurrence Matrix (GLCM) has been one of the most commonly utilized [1,253,459,467,499,506,516,527,530,536,586]. GLCM is a statistical measure that computes the joint probability of occurrence of gray levels considering two pixels spatially separated by a fixed vector. Several measures may be computed based on the GLCM, such as mean, correlation, homogeneity, contrast, energy, dissimilarity, kurtosis, variance, entropy, maximum probability, inverse difference, angular second moment, and standard deviation [1,253,459,467,499,506,516,527,530,536,586]. Model-based texture descriptors

Table 7

Different pigmented skin lesion features from macroscopic and dermoscopic images in the past from 2011 to 2022.

| Different lesion attributes | Articles |
|---|---|
| Shape-based lesion attributes | |
| Convex hull to estimate notched and ragged edges | [550] |
| Circularity Index ($(4\pi A)/P^2$) for border's irregularity, where A and P are the lesion contour's area and perimeter, respectively. | [459,545,550] |
| Hull/Contour Ratio to measure the raggedness or spikiness of the lesion border | [545,550] |
| The lesion boundary comes from a snake-based edge detection technique, segmenting the image into skin area A_s and lesion area A_l . The average skin pattern isotropies in the skin (m_s) and lesion (m_l) areas are calculated as $m_s = \frac{1}{N_s} \sum_{(i,j) \in A_s} I(i,j)$ and $m_l = \frac{1}{N_l} \sum_{(i,j) \in A_l} I(i,j)$, where N_s and N_l are the number of sub-images in the skin and lesion areas. | [543,549] |
| Clinical border irregularity features, delineating a skin lesion into eight segments. | [547] |
| Morphologically fine irregularities feature from the image I, as $f^B = \frac{I_o - I_c}{I_l} + \frac{I_c - I_o}{I_l}$, where I_l , I_c , and I_o respectively denote the original lesion area, ROI's closing, and ROI's opening. | [547] |
| Coarse irregularities from the perimeters of the low-frequency border and the original border as $f^B = \frac{ P_{lesion} - P_{low} }{P_{lesion}}$, where P_{lesion} and P_{low} are the lengths of the perimeter of the original and low-frequency border (details in [547]). | [547] |
| Structural irregularities from the Fourier descriptors as $f^B = \sum_{u=0}^{N-1} (C(u) - C(\bar{u}))^2$, where C is the Fourier coefficient (details in [547]). | [410,547] |
| Asymmetry features were extracted by a shrinking active contour model to find major and minor axes, vertical and horizontal dash lines, of the lesion boundary. | [140,394,546] |
| The asymmetry feature by computing the principal and secondary axes of inertia, where the axes of the image were aligned with the axes of inertia, allowing a better assessment of the lesion symmetry in terms of geometry and internal structures. | [544] |
| The border feature for finding the abrupt ending of pigment pattern in two peripheral regions: inside and outside the lesion, using the Euclidian Distance Transform. | [544] |
| The asymmetry characterization features such as the ratio between the lesion area and its bounding box area, equivalent diameter ($4A/(L_1\pi)$), the ratio between the principal axes (L_2/L_1), the ratio between sides of the lesion bounding box, the ratio between the lesion perimeter (p) and its area (A), $(B_1 - B_2)/A$ [B_1 and B_2 are the areas in each side of axis L_1 or L_2], and B_1/B_2 ratios concerning the axis L_1 or L_2 . | [297,459,498,502,536,545] |
| Boundary Irregularity description features like average and variance gradient magnitudes of the pixels in the extended lesion rim in each of the three channels ($i = 1, 2, 3$); average and variance of the $R (= 1, 2, \dots, 8) \mu_{R,i}$ values in each of the three channels. $\mu_{R,i}$ is the mean of 8 different symmetric regions, obtained by rotating orthogonal axes by 45 degrees. | [297,410,545] |
| Ulnar variance measures the relative length of articular surfaces of some particular radius and image asymmetry. | [536] |
| Solidity, asymmetry index, extent, diameter, circularity, eccentricity, aspect ratio, structural similarity, and the ratio of the major to the minor axis as structural features. | [1,439,470,533] |
| 2D and 3D shape features (details in [521]). | [521] |
| Color-based lesion attributes | |
| R, G, B colors means ($\mu = (\mu_R, \mu_G, \mu_B)$) and their covariance matrices (Σ) (details in [548]). | [142,410,548,550] |
| Six color features from two-stage detection algorithms: color clustering using a mean-shift algorithm and color supervised classification based on a dataset of reference RGB codes. | [544] |
| Maximum, minimum, mean, and variance of the intensities of the pixels inside the lesion segment in the color variation channel and each of the three original channels; ratios between the mean values of the original three channels, for example, μ_R/μ_G , assuming only pixels inside the lesion segment. | [206,264,292,297,443,459,467,502,521,545] |
| The variance, skewness, and entropy as color-related features. | [206,264,439,443,459,536] |
| Boundary color value differences for each channel as $f = \frac{1}{N} \sum_{i=1}^N (V_i - V_m)^2$, where V_i , V_m , and N are the value of i th boundary pixel, the mean value of the boundary pixel, and the number of boundary pixels. | [528] |
| Boundary color clustering features, clustering a lesion with different k groupings (details in [528]). | [528] |
| Color features of six different colors like white, red, light brown, dark brown, blue-gray, and black (estimation details in [506]). | [253,506] |
| Histogram-based features (color distribution) | [142,371,397,426,429,583–585] |
| Color asymmetry | [585] |
| Kullback–Leibler divergence of the color distribution (each channel separately) from the two halves along each axis. | [533] |

(continued on next page)

Table 7 (continued).

| Different lesion attributes | Articles |
|---|---------------------------------------|
| Texture-based lesion attributes | |
| Twelve generalized cooccurrence matrices features like energy, contrast, correlation, entropy, homogeneity, inverse difference moment, cluster shade, cluster prominence, max probability, autocorrelation, dissimilarity and variance. | [371,397,426,548] |
| Five differential structures based on texture relevant for the detection of melanoma: homogeneous areas, streaks, dots, globules, and pigment network. | [544] |
| Textural variation in the channel as maximum, minimum, mean, and variance of the intensities of the pixels inside the lesion segment. | [297,545] |
| Texture-base Gray Level Co-occurrence Matrix (GLCM) features that include mean, correlation, [1,142,253,370,387,397,459,467,499,506,516,527,530,536,586] homogeneity, contrast, energy, dissimilarity, kurtosis, variance, entropy, maximum probability, inverse difference, angular second moment, and standard deviation. | |
| Haralick texture features using gray-tone spatial-dependence matrices (details in [521]). | [371,426,521] |
| SFTA features (details in [292]). | [292] |
| SURF, SIFT, and ORB features | [443] |
| Texture-based RSurf features | [532] |
| Bi-dimensional Empirical Mode Decomposition (BEMD), BEMD-Riesz, Gray-level Difference Method (GLDM), and combined BEMD-Riesz with GLDM. | [410,520] |
| Fractal dimensions and GLDM features (details in [502]). | [1,410,429,502] |
| Histogram of oriented gradients features (details in [292]). | [206,253,264,292] |
| Gabor wavelets features (details in [253]). | [206,253,360,397] |
| Fractal-based regional texture analysis-based texture features (details in [1]). | [1] |
| Edge and local edge Histogram features (details in [206]). | [206] |
| Texture feature-based on fractional Poisson to estimate the structure of regions in an image (details in [531]). | [531] |
| Coarseness features that measure of different angle of texture representation. | [536] |
| Other (miscellaneous) lesion attributes | |
| Local Binary Patterns (LBP) features | [206,253,370,397,426,443,469,499,532] |
| Manual information | [587] |
| Model-based features. | [6,588] |

have also been proposed to assess the skin lesion's texture, such as fractal dimensional [1,502], auto-regression, and Markov random fields. Among these, fractal dimension has been applied with the box-counting method, one of the most commonly used methods since it is simple and effective [1,502]. Wavelet, Fourier, and Gabor transform [206,253], and the Scale-invariant Feature Transform (SIFT) [292,443], which are filter-based texture descriptors, have also been proposed for feature extraction of skin lesion images. Such descriptors allow the decomposition of the input image into parts in order to extract features from the structures of interest. Sobel, Hessian, Gaussian, and difference of Gaussian features have also been extracted based on the bank of Gaussian filters [206,253,264,292]. 46 articles (19.3%) of 238 SLC articles utilized lesion texture characteristics in the past twelve years for the SLC task.

Some authors combined the color and texture features in some articles [499,548,587,591] to construct a distance measure between a test image and a database image, using color covariance-based features and the Bhattacharyya distance metric [548]. Although texture-based lesion features are slightly more commonly exploited, most articles apply all three types of features to represent the feature vector with all categories of lesion characteristics, as various feature types expose various properties of the skin lesion. Fig. 7 displays the most generally applied (at least in two articles) lesion characteristics from Table 7 in the past from 2011 to 2022 for the SLC task. A close observation in Fig. 7 indicates a wide range of attributes from each type of feature category, revealing that Asymmetry characterization (F4), Maximum, minimum, mean, and variance of the intensities (F8), Gray level co-occurrence matrix (F13), and Local binary patterns (F17) are the most common shape, color, texture, and other types of lesion

attributes, respectively. These lesion features can be considered to be the representative lesion characteristics of those attribute categories (**High-frequency**) used in SLC, and their popularity likely indicates more substantial effectiveness. Again, structural features, skewness, and entropy as color-related features and histograms of oriented gradients are the next most commonly used (**Medium-frequency**) lesion characteristics of shape-, color-, and texture-based lesion attributes, whereas the other remaining attributes in Fig. 7 are applied in a few articles (**Low-frequency**) in the past.

6.1.2. Lesion classifiers

After feature extraction, a feature selection step is crucial [592], and has been employed for the SLC task to determine the most relevant features and reduce the dimensionality of the feature space [1,356,376,410,443,467,469,502,593]. Moreover, such features may influence the performance of the classification process, i.e., render it slower. Several benefits are associated with the application of feature selection schemes [6] such as reducing the feature extraction time, decreasing the classification complexity, improving the classification accuracy rate, lowering training–testing time, simplifying the understanding, and visualizing the data. The feature selection process has the following steps: feature subset selection, feature subset evaluation, stopping criterion, and validation procedure [6], which is then headed by lesion classification step(s).

The classification phase consists of recognizing and interpreting the information about the skin lesions based on extracted and selected lesion features. The classification process is generally accomplished by randomly dividing (or K-folding) the available image samples into training and testing sets. The training step consists of developing a

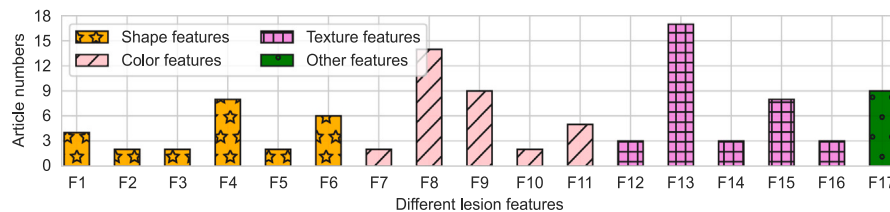


Fig. 7. The frequency of utilization of various skin lesion attributes with their complementary number of employed articles for the SLC task. F1↔ Circularity index, F2↔ Contour ratio, F3↔ Average skin pattern isotropies, F4↔ Asymmetry characterization, F5↔ Boundary irregularity description, F6↔ Structural features, F7↔ RGB colors means and covariances, F8↔ Maximum, minimum, mean, and variance of the intensities, F9↔ Variance, skewness, and entropy as color-related features, F10↔ White, red, light brown, dark brown, blue-gray, and black color features, F11↔ Color histogram-based features, F12↔ Textural variation in the channels, F13↔ Gray level co-occurrence matrix, F14↔ Fractal dimension, F15↔ Histogram of oriented gradients, F16↔ Gabor wavelets features, and F17↔ Local binary patterns.

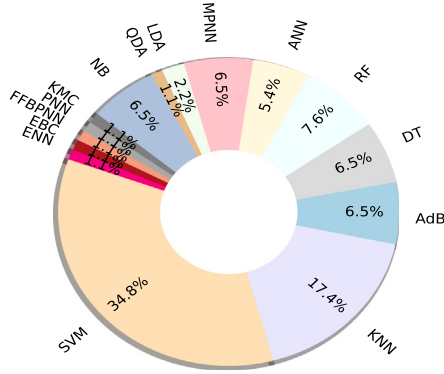


Fig. 8. The pie chart of the percentage of SLC articles employing various ML models on manual lesion features in the past from 2011 to 2022.

classification model to be employed by one or more classifiers based on the samples of the training set. Each sample comprises features extracted from a provided image and its corresponding class value, which are applied as input data to the classifier for the learning process. The testing step measures the model's accuracy learned by the training step over the test set. From 2011 to 2022, the commonly used SLC models were Support Vector Machine (SVM) [1,48,200,201, 253,264,292,297,356,371,375,376,410,430,455,467,502,516,520,521, 527,530,531,533,536,539,546,547,586,594–596], K-nearest Neighbors (KNN) [297,356,364,371,429,441,467,498,531,533,537,545,548,550, 594,595], AdaBoost (Adb) [140,426,447,521,531,533], Decision Tree (DT) [371,375,376,439,533,595], Random Forest (RF) [140,356,371, 426,439,447,544], Artificial Neural Network (ANN) [370,375,429,536, 595], Multilayer Perceptron Neural Network (MPNN) [82,356,376,380, 387,467], Linear Discriminant Analysis (LDA) [201,371], Quadratic Discriminant Analysis (QDA) [201], Naive Bayes (NB) [140,352,364, 371,376,533], K-means Clustering (KMC) [540], Probabilistic Neural Network (PNN) [597], Feed Forward Back Propagation Neural Network (FFBPNN) [594], Ensemble Binary Classifiers (EBC) [542], and Elman Neural Network (ENN) [467].

Fig. 8 demonstrates the percentage of publications from 2011 to 2022 that use ML models, revealing that the top ML models are SVM and KNN, which account for 34.8% and 17.4% of publications, respectively. These two ML models were applied in 52.2% of articles; therefore, they can be regarded as the representative ML classification models (**High-frequency**) for SLC. This is followed by Adb, DT, RF, ANN, MPNN, and NB classifiers, which were the next most popular models (**Medium-frequency**) and accounted for 39.0% of SLC articles. The other ML models, such as LDA, QDA, KMC, PNN, FFBPNN, EBC, and ENN, were less significant (**Low-frequency**), accounting for 8.8% of SLC articles. Quick calculation time, a simple algorithm to interpret, versatile usefulness for regression and classification, and evolution with new data are potential reasons for the high frequency of usage for SVM and KNN models.

6.2. DL-based SLC

As discussed in the earlier section, ML-based SLC requires extensive feature engineering with comprehensive parameter tuning to achieve better and more robust performance, which is often challenging due to the appearance of various intrinsic and extrinsic noises in dermoscopic images (see details in [3,173]). On the other hand, the CNN-based DL-SLC approaches provide excellent SLC results and boost diagnostic procedure rates while being end-to-end systems. Nowadays, CNN-based segmentation networks have been widely applied to medical images, outperforming traditional image processing methods relying on manual features [573]. However, our review of the 238 SLC articles demonstrates that most authors employed pre-trained (on ImageNet, PASCAL-VOC, MS-COCO, etc.) CNN models and fine-tuned them with the skin lesion datasets. The most commonly employed pre-trained CNN models found in the SLC literature from 2011 to 2022 are: MobileNet [356,366,382,388,389,392,392,411,412,416,437,449, 451,459,497,514], variants of EfficientNet [178,355,372,376–378,383, 385,387–389,401,421,422,451,452,460,466,488], DenseNet [93,267, 356,357,362,363,363,366,369,385,389,400,401,403,407,412,414,422, 430,437,442,445,446,453,457–459,461,488,490,497,510], SeReNeXt-50 [353,357,361,363,452], variants of VGGNet [357,389] like VGG16 [60,182,207,276,289,356,376,386,387,412,413,418,422,437,438,449, 455,458,459,464,465,471,472,481,482,497,505,522,525,598,599] and VGG19 [356,386,398,401,411,413,422,438,472,514], LeNet-5 [182, 486,512], GoogleNet [366,386,388,416,436,456,465,472,505], PNASNet-5-Large [460,489], Squeeze-and-Excitation Networks (SENet) [386,460,466,489,511], AlexNet [60,207,276,366,386,436,465,481, 482,505,532,534], Xception [356,366,377,383,392,401,411,412,414, 418,437,453,459,460,462], different versions of Inception model like Inception-V2 [366,369,374,377,383,401,411,422], Inception-V3 [356, 377,383,387,401,411,412,437,456,459,460,472,483,488,497,524,526], and Inception-V4 [383,460,489,503], variants of ResNet like ResNet18 [363,384,386,388,400], ResNet101 [93,164,366,377,386,403,407, 419,437,445,453,458,460,472,473,476,479,482,492], ResNet152 [360, 360,383,383,401,422,422,460], ResNet50 [182,216,234,235, 267,276,352,353,356,357,361,366,369,376,379,382,385,386, 389,400,407,411,412,418,419,423,432,436,454,458,459,463– 465,476,481,482,484,488,490,491,498,500,504,505,513–515, 517,529,600], ResNeXt with webly supervised learning [414,466, 488,519], and SE-ResNeXt101 [385,414,460,488], NASNet [364,383, 388,392,401,437,460,462], and a mixture of Inception and ResNet (InceptionResNet-V2 [366,369,374,377,383,401,411,422,437,442,455, 460,462,489]).

Moreover, some authors in [367,386] experimented on various CNN models by changing different activation functions. In the past, different attention-based modules were also integrated with CNN models for the SLC task [358,361,377,390,396]. [424] presented federated learning for SLC to train decentralized models in a privacy-preserved fashion relying on labeled data on the client side. The patient-specific metadata also has been incorporated with CNN models for the SLC task [389, 421,601]. Furthermore, a few authors have proposed new networks, a

modification of the current models, or hybrid methods dedicated to the SLC task, for example, in [3,7,80,128,142,351,367,379,391–393,399, 402,405,408,417,420,428,433,434,448,452,468,602]. Some of them are briefly illustrated in the next paragraph.

An end-to-end hybrid-CNN classifier with a two-level ensembling was presented and designed in [7]. A channel-wise concatenated 2D feature map was proposed to enhance the first-level ensembling's depth information. In contrast, the authors also proposed aggregating the various outputs from different fully connected layers in the second-level ensemble, learning more discriminating features with limited training samples. The authors in [434] proposed a densely connected convolutional network with an Attention and Residual learning method for the SLC task, where each ARDT block consists of dense blocks, transition blocks, and attention and residual modules. Compared to a residual network with the same number of convolutional layers, the size of the parameters of the densely connected network proposed was reduced by half. The improved densely connected network added an attention mechanism and residual learning after each dense and transition block without additional parameters. The authors of [468] presented a hyper-connected CNN (HcCNN) to classify skin lesions, having an additional hyper-branch that hierarchically integrates intermediary image features, unlike existing multi-modality CNNs. The hyper-branch enabled the network to learn more complex combinations between the images at early and late stages. They also coupled the HcCNN with a multi-scale attention block to prioritize semantically meaningful and subtle regions in the two modalities across various image scales. A CNN-based framework for simultaneous detection and recognition of skin lesions was proposed in [3], named Dermo-DOCTOR, consisting of two encoders. The feature maps from the two encoders were fused channel-wise, called the fused feature map. This fused feature map was utilized for decoding in the detection sub-network, concatenating each stage of two encoders' outputs with corresponding decoder layers to retrieve the lost spatial information due to pooling in the encoders. For the recognition sub-network, the outputs of three fully connected layers, utilizing feature maps of two encoders and fused feature maps, were aggregated to obtain a final SLC class. The authors in [452] developed a three-level fusion scheme named multi-scale multi-CNN (MSM-CNN). They trained CNN models with cropped images at a fixed size at level one. At level two, they also fused the results from the individual networks trained on the six different image sizes (i.e., 224 × 224, 240 × 240, 260 × 260, 300 × 300, 380 × 380, and 450 × 450). At the third and final fusion level, the authors fused the predicted probability vectors of the various architectures to yield the final classification result. The final MSM-CNN classification was thus derived from 90 (5 × 6 × 3) sub-models. Lastly, the authors in [448] constructed a CNN-based SLC model that is loosely based on a baseline vanilla CNN network. The basic structure was two convolutional layers followed by a max-pooling layer containing fewer filters to reduce the training time. Additionally, their network included more dropout layers and fewer fully connected neurons to combat the overfitting present when replicating the original network.

This review reveals that some authors, such as in [48,82,93,206, 207,243,267,352,356,371,375,376,387,388,397,406,430,437,440,443, 445,455,459,461,464,476,483,492,501,532], combined the CNN's automated lesion features and manual features (described in Table 7) for the SLC task to enhance the classification results in the past. They either extracted CNN attributes and merged them with manual features and then categorized them using typical ML model(s) (as mentioned in 6.1.2) or manually extracted lesion features and stacked them in a particular CNN layer and then classified them using a Fully-connected layer. Furthermore, single CNN models are often indirectly limited when trained with highly variable and distinctive image datasets with limited samples. The authors of many SLC articles [60,178,365,366, 369,385,387,400,406,412,414,416,422,452,453,456,462,465,481,482, 489,505] mitigated this difficulty by applying the ensemble techniques. There are many analyses on the design of these ensemble techniques; for instance, whether the individual ensemble's candidate model should

be trained first and then aggregation should be performed, such as in [218,452,466,505,510,603–605]? Despite their approaches' satisfactory results, such an ensemble is tedious and time-consuming, requiring excessive time and resources for training and testing, as each model is independently trained and tested. Therefore, an end-to-end ensemble strategy that mitigated those weaknesses in [218,407,452,466,505, 510,603–605] without compromising the state-of-the-art SLC results as demonstrated in [7].

The frequency of usage of various DL models in the last twelve years from the specified 238 SLC articles is shown in Fig. 9. It can be observed in Fig. 9 that ResNet, VGG, DenseNet, InceptionNet, and EfficientNet are the top-5 most SLC methods in those 238 SLC articles, which account for 36.1%, 17.2%, 13.9%, 12.2%, and 8.0% of the total SLC article, respectively. These techniques are thus the most significant CNN-based SLC approaches (**High-frequency**) in the past 238 SLC articles. The other architectures are employed in 1.3% ~ 6.7% of the SLC articles, where the MobileNet, InceptionResNet, Xception, AlexNet, and GoogleNet are separately used in 3.8% ~ 6.7% articles and would be thought of as the **Medium-frequency** CNN models for SLC. Other CNN models in Fig. 9 are assumed to be **Low-frequency** CNN-based SLC models in the past.

Further analysis reveals that out of the 36.1% using ResNet models, the ResNet-50 and ResNet-101 are applied to 21.4% and 8.0% of SLC articles, respectively. Out of the 17.2% using VGG architectures, the VGG-16 and VGG-19 are applied in the 12.2% and 4.2% articles. Again, the Inception-V3 is more commonly employed than the Inception-V4 in 7.1% (out of 12.2%) SLC articles. Similar patterns are also visible in all other networks; that is, the smaller network of each type of architecture is most commonly employed, for example, EfficientNetB0 than other EfficientNets, DenseNet121 than other DenseNets, and MobileNet-V2 than other MobileNets. This is summarized in Fig. 10. This figure also illustrates different CNN architectures with their corresponding numbers of learning parameters. With larger parameter numbers, an increasing number of samples are needed in the training set, as DL requires large datasets to be effective. Both Figs. 9 and 10 can demonstrate that smaller networks with fewer parameters have often been used for SLC in the last twelve years. Although this is likely a result of challenges in obtaining large sample sizes in medical imaging [3,7,173,505], it is also likely preferred due to reduced computational costs. Further, several authors [178,452,453,456,462,465,481,482,489,505] could show that such smaller networks could be combined for ensemble design that performed very well even with fewer training samples.

7. Training and evaluation

This section surveys and explores the model training and evaluation protocols used for SLA tasks from 2011 to 2022. We investigate hyperparameter settings and training environments in Section 7.1 and 7.2, respectively, and analyze the evaluation strategies for SLA in Section 7.3. These issues are often explicitly addressed in these articles, which informed our review here.

7.1. Hyperparameter settings

The identification of a good set of hyperparameters is essential for the robust performance of the CNN model [592]. However, hyperparameters cannot be directly learned from regular training processes and must be tuned separately. Our review of the 594 SLA articles reveals several explicitly mentioned hyperparameters, which are summarized below. We also analyze the frequency of hyperparameter choices in past studies so as to inform future investigations.

Batch size is the number of images utilized to train a single forward and backward pass and is one of the essential hyperparameters. Larger or smaller batch size does not usually guarantee a better outcome, as there is a tradeoff between achieved results and computational resource availability [606]. The authors in [606] experimented on different

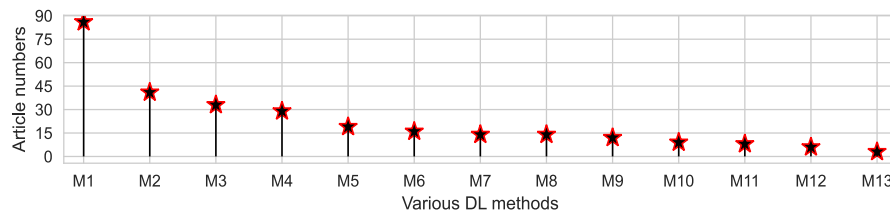


Fig. 9. A discrete usage frequency plot of various DL models for SLC, where M1 to M13 denotes ResNet, VGG, DenseNet, InceptionNet, EfficientNet, MobileNet, InceptionResNet, Xception, AlexNet, GoogleNet, NASNet, SENet, and LeNet-5, respectively.

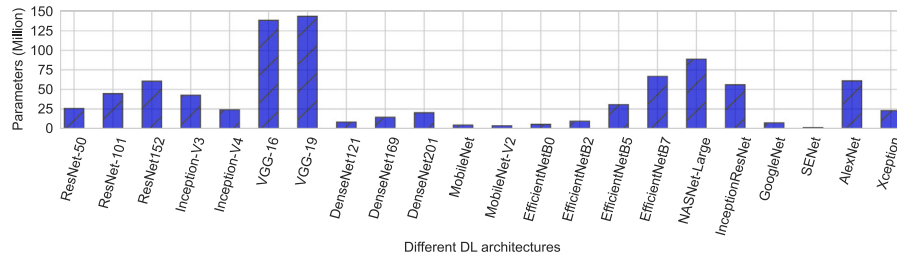


Fig. 10. The bar plot of diverse CNN architectures with their complementary number of learning parameters employed for the SLC task in the past from 2011 to 2022.

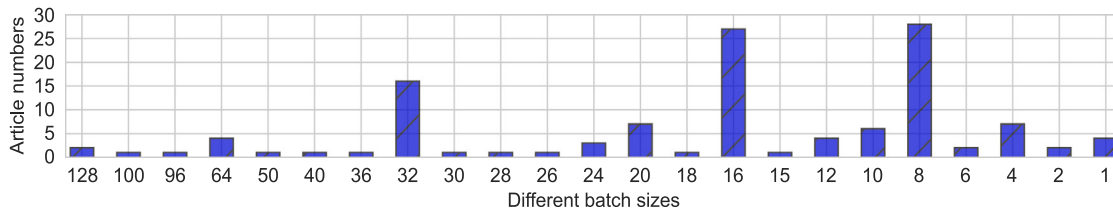


Fig. 11. The number of articles that utilized various batch sizes in the past SLA articles.

batch sizes with fixed data and CNN architecture and revealed that it significantly impacted the network's performance. However, this review of 594 articles showed that the utilized batch sizes were 128 [374, 409], 100 [456], 96 [518], 64 [119, 233, 367, 451], 50 [351], 40 [84], 36 [168], 32 [26, 115, 139, 144, 362, 371, 383, 384, 414, 418, 423, 440, 460, 491, 495, 508], 30 [408], 28 [93], 26 [607], 24 [55, 98, 445], 20 [208, 260, 265, 267, 473, 515, 529], 18 [165], 16 [32, 65, 68, 69, 105, 109, 116, 127, 133, 150, 154, 164, 172, 184, 230, 240, 276, 278, 289, 380, 398, 401, 405, 414, 416, 421, 427], 15 [403], 12 [35, 100, 185, 483], 10 [49, 269, 416, 418, 420, 434], 8 [33, 58, 59, 82, 83, 95, 99, 101, 102, 107, 113, 117, 118, 120, 130, 160, 176, 198, 222, 242, 283, 285, 288, 366, 396, 401, 426, 608], 6 [29, 305], 4 [51, 53, 110, 152, 186, 351, 428], 2 [119, 203], and 1 [138, 171, 205, 227]. Fig. 11 indicates that the most commonly employed (78.7%) batch sizes lie between 8 and 32, where the topmost batch sizes of 8, 16, and 32 are applied to the 23.0%, 22.1%, and 13.1% of the total articles, respectively. Those three topmost batch sizes follow the power of two (2^n) patterns, which is usually maintained for batch size selection. It is also observed that the larger batch sizes, like 64 and above, are used in merely 6.6% of the articles, likely because they are associated with high computational resources. On the other hand, smaller batch sizes take a longer time to reach convergence during the training of the models. This likely explains why small batch sizes of 6 and below were applied to only 12.3% of SLA articles.

Learning Rate (LR) (η) is a hyperparameter that controls how much the network's weights (W) are adjusted ($W_{new} = W_{old} - \eta \times \nabla$) concerning the loss gradient (∇). Too small of an LR functions a slowly converging training, while too large of an LR creates the training model diverge [7]. Our review reveals that the employed LRs were 0.1 [105, 169, 173, 241], 0.01 [130, 132, 183, 185, 187, 215, 269, 399, 462, 512, 526, 527, 595], 0.001 [32, 53, 58, 68, 81, 84, 93, 98, 117, 118, 129, 138, 139, 144, 152, 159, 160, 164, 165, 175, 197, 250, 268, 272, 275, 288, 294, 303, 305, 367, 371, 384, 401, 405, 407, 426,

440, 448, 451, 454, 457, 460, 463, 508, 510, 513, 515, 516, 529, 608], 0.0001 [26, 29, 35, 51, 52, 65, 94, 100, 120, 127, 134, 149, 150, 154, 162, 171, 177, 184, 186, 202, 208, 209, 221, 222, 230, 234, 235, 242, 246, 270, 280, 283, 285, 298, 307, 310, 359, 362, 374, 383, 396, 416, 420, 421, 434, 445, 452, 456, 473, 479, 483, 489–491, 494–496, 518, 523], 0.00001 [49, 55, 59, 82, 83, 97, 107, 115, 119, 133, 213, 260, 265, 267, 276, 278, 351, 366, 369, 371, 380, 408, 414, 500], 0.000001 [69, 113, 259, 607], 0.0000000001 [299], 0.0002 [72, 99, 102, 168, 172, 203, 224, 227, 232, 236, 308, 576], 0.03 [108], 0.003 [157], 0.0003 [96, 116], 0.00003 [95, 109, 179, 378, 391], 0.005 [101, 110, 176, 438], 0.0005 [468], 0.00005 [240, 427], and 0.007 [180, 239]. Fig. 12 displays that the LRs of scales between e-2 and e-5 were employed in 95.1% of the total articles while the remaining 4.9% articles applied other LRs of e-1, e-6, and e-10 scales. Specifically, the LRs of 0.001, 0.0001, and 0.00001 were the most popular in past SLA articles. This likely implied that most investigators found this range of LRs to be the most effective for developing the supervised SLA model. These results may imply that LRs that are too large or too small are not recommended.

Loss function, also known as the cost function or error function, is an objective function or criterion for minimizing during the supervised DL model's training. The scrutiny of the selected articles reveals that the most commonly employed loss function is cross-entropy for both the SLS and SLC tasks that are employed in [37, 65, 82, 94, 97, 99, 113, 118, 120, 127, 129, 148, 160, 163, 169, 175, 177, 179, 182, 208–210, 213, 217, 221, 230, 234, 246, 259, 267, 269, 273, 276, 280, 283, 284, 287, 294, 303, 308, 353, 363, 368, 371, 380, 384, 391, 396–398, 403, 405, 421, 423, 433, 438, 440, 456–458, 465, 466, 468, 488, 500, 503, 514, 523, 524]. Other loss functions in the past were Softmax [105, 241, 299, 305, 529, 534, 609], Square error [179, 530], Logistic loss function [445], Tversky loss [47, 62, 133] and Focal loss [96, 109, 115–117, 133, 409, 421, 609, 610]. Although binary or categorical cross-entropy functions are widely employed as loss functions in SLS, they

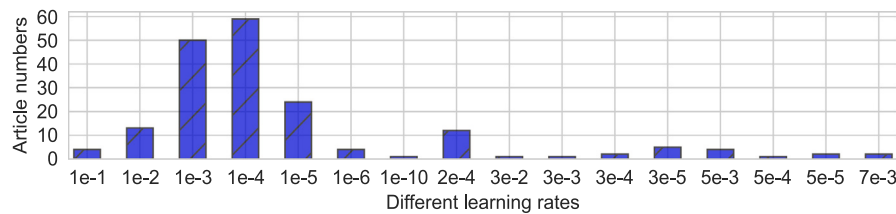


Fig. 12. The number of articles that employed various LRs in the past 594-SLA papers.

may lead to bias effects as the size of a lesion is drastically smaller than the size of the background [574]. Therefore, some authors employed Dice Similarity Coefficient (DSC) (as in Eq. (2)) or Jaccard Index (JI) (as in Eq. (3)), which are applied in [2, 37, 61, 68, 72, 95, 96, 98, 100, 102, 106, 107, 109, 110, 114, 116, 118, 133, 134, 151, 158, 166, 168, 179, 183, 202–204, 218, 226, 228, 232, 240, 242, 257, 260, 261, 268, 270, 273, 288, 295, 310, 504].

$$L_{DSC}(y, \hat{y}) = -1 + \frac{2 \times \sum_{i=1}^N y_i \times \hat{y}_i}{\sum_{i=1}^N y_i + \sum_{i=1}^N \hat{y}_i}, \quad (2)$$

$$L_{JI}(y, \hat{y}) = -1 + \frac{\sum_{i=1}^N y_i \times \hat{y}_i}{\sum_{i=1}^N y_i + \sum_{i=1}^N \hat{y}_i - \sum_{i=1}^N y_i \times \hat{y}_i}, \quad (3)$$

where y , \hat{y} , and N are the true label, predicted label, and the total number of pixels, respectively. In those two equations, the product of y and \hat{y} is the measure of similarity (intersection) between true and predicted masks. Again, some authors in [35, 43, 49, 53, 58, 66, 72, 77, 82, 83, 89, 90, 113, 131, 150, 152, 157, 172, 173, 177–179, 184, 185, 198, 222, 226, 235, 236, 272, 289] combined BCC and Eq. (2) or Eq. (3) for further enhancing the lesion segmentation results, as mentioned in Eq. (4).

$$L_{SLS}(y, \hat{y}) = 1 - \frac{\sum_{i=1}^N y_i \times \hat{y}_i}{\sum_{i=1}^N y_i + \sum_{i=1}^N \hat{y}_i - \sum_{i=1}^N y_i \times \hat{y}_i} - \frac{1}{N} \sum_{i=1}^N [y_i \log \hat{y}_i + (1 - y_i) \log(1 - \hat{y}_i)], \quad (4)$$

where $\log \hat{y}_i$ and $\log(1 - \hat{y}_i)$ are the measure of the log-likelihood of the pixel being lesion or not, respectively. In summary, our review of loss function usage demonstrates that the BCC was widely applied for the SLC and SLS tasks, whereas Eq. (2) or Eq. (3) or Eq. (4) were commonly applied for the SLS task in the past 594 articles.

Optimizer calculates the value of the model's parameters (weights), minimizing the error (cost function as described in the previous paragraph) and maximizing the predefined metric (see Table 10) when mapping inputs to outputs. It widely affects the CNN models' accuracy and training speed [7]. In the past (2011–2022), the most commonly applied optimizers (with their corresponding articles) for the SLA models are Adam, also known as an adaptive optimizer, [29, 33, 35, 49, 53, 55, 58, 59, 61, 66, 69, 83, 84, 95, 97, 97, 100, 107–110, 113, 115, 116, 120, 127, 129, 132, 134, 150, 152, 154, 157, 159, 160, 163, 168, 172, 175, 177, 177, 179, 180, 186, 187, 202, 203, 209, 213, 217, 221, 222, 230, 232, 234–236, 240, 242, 246, 265, 268, 270, 272, 273, 278, 280, 285, 288, 289, 294, 303, 308, 310, 369, 371, 391, 412, 414, 420, 427, 445, 448, 452, 458, 463, 466, 482, 483, 489, 491, 494, 496, 518, 526], Stochastic Gradient Descent (SGD) [32, 101, 102, 105, 119, 138, 144, 149, 159, 165, 169, 176, 185, 205, 208, 217, 220, 224, 239, 250, 259, 260, 267, 269, 271, 273, 275, 276, 283, 289, 298–300, 305, 307, 351, 383, 384, 396, 403, 407, 409, 421, 434, 440, 440, 460, 479, 482, 508, 510, 512, 515,

519, 529, 607, 611], Adadelta [173], RMSprop [398, 409, 414], and Nadam [198, 409]. Indeed, 96.6% of the articles applied Adam (60.5%) and SGD (35.7%) optimizers. However, it has also appeared from the current review that the authors had fine-tuned optimizers' control parameters like the momentum in SGD, the decay rate in Adadelta, and the exponential decay rate for the first and second moments (β_1 and β_2) in Adam and Nadam. The variations of these parameters in the 594 SLA articles are summarized in Table 8.

Momentum increases the rate of convergence in gradient descent in the appropriate direction and dampens oscillations, while the decay rate continuously changes the LR values to construct an adaptive optimizer. On the other hand, β_1 and β_2 are the initial decay rates utilized when estimating the first and second moments of the gradient, which are multiplied by themselves (exponentially) at the end of each training step (batch). However, it is noteworthy from the table that the most commonly applied momentum, decay rate, β_1 , and β_2 in the past SLA articles were 0.90, 0.0001, 0.90, and 0.999, respectively.

Epoch refers to one forward and one backward pass over the entire dataset. The initial weights of models will be subjected to transformations during the next cycle of the same training dataset. Epoch optimization mainly faces two significant problems: underfitting and overfitting. Using a few epochs will lead to an underfitting of the data during the network's training, which indicates that the network cannot capture the underlying tendency of the data. Increasing the epoch numbers will enable a more optimal solution with better accuracy. However, beyond the optimal number of the epoch, further increases in epoch numbers will lead to overfitting of data, which means that the network is now less accurate as it is capturing noise in the data. Unfortunately, there is no simple solution for choosing the best epoch. Here, we reviewed the 594 selected SLA articles to investigate the choice of epoch numbers in the past twelve years' studies. We find that the epoch numbers are 1000 [397, 428], 500 [98, 162, 177, 179, 427, 508, 576], 400 [65], 300 [26, 32, 164, 265, 267, 300], 360 [215], 250 [109, 132, 172, 307, 369, 391], 200 [29, 35, 72, 82, 99, 100, 115, 133, 168, 169, 218, 227, 240, 278, 438], 192 [518], 165 [198], 150 [28, 59, 81, 224, 371, 396], 120 [127], 110 [102], 100 [51, 52, 55, 117, 144, 152, 157, 165, 175, 289, 359, 362, 366, 374, 392, 399, 403, 408, 420, 426, 434, 440, 445, 448, 466, 468, 486, 510], 90 [107, 213], 80 [183, 222, 276], 75 [69], 70 [409], 60 [33, 53, 421, 495, 607], 50 [58, 96, 105, 118, 130, 138, 235, 401, 405, 451, 454], 40 [49, 383, 483], 35 [176, 398], 30 [120, 408, 414, 612], 24 [490], 20 [84, 93, 116, 365, 367], 15 [246, 378], 13 [184], 10 [139], and 3 [230]. Those epoch values and their appliance frequencies demonstrate that the fewer epochs (< 50) are applied to a smaller number of articles, approximately in 16.1% of the total articles, whereas the high number of epochs (> 200) are also employed in fewer articles (19.5%). On the other hand, the epochs between 50 and 200 were most commonly employed in 64.4% of the articles that confirm the epoch numbers to train the SLA models.

7.2. Training environments

In order to train different ML and DL algorithms and architectures, there are numerous frameworks and libraries that provide a convenient training protocol. These frameworks assemble complex mathematical functions, training algorithms, and statistical modeling tools, allowing

Table 8

The variations of different parameters in optimizer(s) like momentum, decay rates, β_1 , and β_2 in the selected 594 articles.

| Parameters | Values | Corresponding articles |
|-------------|----------|---|
| Momentum | 0.25 | [527] |
| | 0.90 | [32, 51, 53, 102, 105, 130, 149, 165, 169, 171, 176, 180, 185, 208, 220, 233, 234, 239, 259, 260, 267, 269, 275, 289, 298–300, 305, 351, 362, 365, 383, 384, 434, 440, 460, 468, 510, 512, 519, 523, 529, 595, 607] |
| | 0.95 | [146] |
| | 0.99 | [119, 138, 159, 205, 271] |
| Decay rates | 0.001 | [233, 260, 491] |
| | 0.0001 | [96, 146, 185, 220, 267, 300, 305, 362, 405, 434, 479, 495, 515, 529] |
| | 0.00001 | [82, 146, 351, 463] |
| | 0.000001 | [97, 171] |
| | 0.00158 | [198] |
| | 0.5 | [236] |
| | 0.005 | [53, 160, 275, 407, 512] |
| | 0.0005 | [32, 130, 159, 165, 205, 271, 298] |
| β_1 | 0.00005 | [105, 127, 468] |
| | 0.50 | [72, 163, 168, 203, 234, 236] |
| | 0.60 | [494] |
| β_2 | 0.90 | [96, 99, 127, 159, 234, 265, 374, 414, 420, 482, 518] |
| | 0.990 | [127, 234, 482, 518] |
| | 0.995 | [494] |
| | 0.999 | [72, 96, 99, 159, 163, 168, 203, 236, 265, 374, 414, 420] |

Table 9

Widespread ML and/or DL frameworks in SLA tasks with their common attributes.

| Framework (Year) | Written in | Popularity ^a | Corresponding SLA articles |
|-------------------|-------------------|-------------------------|---|
| Caffe (2015) | C++ | 33K | [159, 205, 298, 299, 310] |
| Keras (2015) | Python | 56.6K | [59, 68, 69, 95, 114, 129, 138, 141, 150, 173, 177, 179, 182, 184, 198, 202, 217, 230, 237, 245, 250, 257, 259, 261, 269, 272, 278, 285, 307, 369, 392, 398, 401, 413, 426, 607] |
| TensorFlow (2015) | C++, Python, CUDA | 169K | [68, 97, 182, 184, 198, 202, 209, 218, 222, 224, 230, 257, 275, 277, 280, 283, 285, 286, 294, 303, 307, 369, 397] |
| Theano (2008) | Python | 9.6K | [273] |
| PyTorch (2016) | Lua | 60.1K | [26, 35, 43, 49, 51–53, 55, 64–66, 81–84, 99, 101, 105, 107, 110, 113, 115, 116, 120, 127, 130, 149, 157, 160, 162, 163, 168, 169, 172, 203, 215, 218–221, 224, 232, 235, 236, 240, 271, 288, 289, 359, 362, 379, 380, 383, 391, 396, 405, 407, 409, 421, 428, 576] |

^aThese values are the number of stars, taken from their official GitHub accounts [Access date: 07-Nov-2022].

their convenient usage without the need to program from scratch. **Table 9** shows the commonly used DL and/or ML frameworks in the SLA articles that explicitly specified the training protocol(s).

It can be observed from **Table 9** that Keras, TensorFlow, and PyTorch with Python and/or MATLAB programming languages (most commonly Python) have been most popularly applied to train automated SLA models. Remarkably, most recent articles preferred PyTorch with Python as an SLA development tool. Moreover, those three frameworks are also most popular in other domains according to their popularity. However, applying those DL frameworks depends on many factors, for example, the level of API, computational speed, architecture, and debugging facilities.

7.3. Model evaluation

Once the SLS and SLC are accomplished, the next step is the assessment of those two methods. The successes of SLS and SLC are typically reported in a confusion matrix that includes statistics about actual and predicted pixels or classes [13]. However, the employed metrics for the SLS and SLC evaluations in the past from 594 selected articles are Accuracy (ACC), Sensitivity (SEN), Precision (PRE), Specificity (SPE), Figure of Merit (FOM), Segmentation Error (SE), False Positive Rate (FPR), F1-score (F1S), Negative Predictive Value (NPV), DSC, Hausdorff Distance (HD), Area Under Curve (AUC), JI, False Negative Rate (FNR), XOR [580], Correlation Coefficient (CC), Hammoude Distance (HMD),

Matthew Correlation Coefficient (MCC), Peak to Signal Ratio (PSNR), Structural Similarity Indices (SSIM), and Balanced Accuracy (BACC). These metrics are summarized in **Table 10**, along with the articles using them.

Qualitative evaluations are also reported in many articles in addition to the quantitative SLS evaluation [3, 7, 9, 144, 150, 153, 154, 160, 161, 163, 169, 173, 178, 180, 181, 184, 190, 193, 197, 202–204, 209, 213, 229, 254, 256, 262, 271, 275, 279, 283, 284, 294, 299, 301, 305, 307, 310, 314, 319, 322, 332, 343, 346, 618, 624]. Overlaying the segmented masks onto the ground truth masks is one such way to perform a qualitative evaluation. The intersected region(s) indicates true positive results, while non-overlapping regions correspond to false-positive and false-negative results. However, in some cases, the multi-class evaluation metrics are required for the SLS and SLC tasks, which are the expansions of the binary metrics in **Table 10**. These metrics are averaged to achieve a multi-class metric across all the classes in two possible ways: micro and macro. The former averaging method (micro) considers class imbalance, calculating the metrics globally by counting the number of times each class was correctly and incorrectly predicted. In contrast, the latter approach (macro) does not assume class imbalance, measuring each class's metrics independently and attaining their unweighted mean. Sometimes, investigators employ k-fold cross-validation to verify the robustness of the trained model. In such a case, the obtained metrics from each fold are expressed as an average value with a standard deviation [569], which can be expressed as Eq. (5). If the standard

Table 10

A list of SLS and SLC evaluation metrics with their corresponding articles applied in the past (2011 to 2022), examining a total of 594 articles (356 for segmentation and 238 for classification).

| Metrics | SLS articles | SLC articles |
|---------|--|--|
| ACC | [9,26–28,30,33–35,37,38,43,47,51–53,55,56,58–61,64–66,68,69,72,81–83,89,93–95,97,99–103,105–110,113–118,120,121,124–133,141,142,145,147–151,154–156,158–166,168–172,174,176–183,185,187,189,191,193–195,198,200–204,206–208,210,213,214,216–220,222,224,225,230,232–234,236–239,245–247,250,251,253,254,257,259–276,278,279,281,282,287,292–295,297,298,300,302,303,305,307,310,311,314,321–323,325,327,328,330,333,334,336,340,342,406,501,545,555,576,596,607,608,613–619] | [1,33,48,60,125,128,142,164,177,182,199–201,206,207,216,234,247,253,264,276,292,297,351,354,356,358–365,367,370,371,377,379,380,382,384–386,390,392,397,398,402–405,410–414,418,427–431,433,434,436–443,446,447,449,450,452–456,459,461,462,464,467–470,472–476,480,482,486,492,494–496,498,500–504,506,510,512,516,517,519,520,522–524,526–528,532–537,539–543,545,547,550,586,594,595,611,620] |
| SEN | [2,9,26–28,30,33,35,37,38,43,47,51–53,55,56,58–60,64–66,69,72,77,81,82,84,97,99–101,103,105,106,109,110,113–116,116–118,120,121,125–130,132,133,139,141,142,145–147,149,150,152,155,160–164,166,168,169,172–174,176,177,179–181,183,184,191,193–195,200–203,205–208,210,213,216–218,222,224–226,230,233,234,236–240,247,250,253,254,257,259,261–266,268–275,278,279,281,287,290–295,297,298,302,303,305,307,310,314,317,319,321,322,325,327,328,333,334,336,340–344,346,348–350,406,501,545,555,558,576,596,596,607,608,613–619,621] | [1,33,48,60,82,125,128,142,164,177,200,206,207,216,234,247,253,264,267,292,297,351,354–356,358,359,365,367,370–372,374,377,379,380,383,385,386,390,391,395–397,397,398,402–404,407,410–414,418,420,421,427,429–434,437,439,441–443,446,450,453,454,454,456–462,464,466–474,476,480,486,488,490,494–496,501–504,506,520–522,528,530–533,535,540,542,543,545,547,550,586,595,620] |
| PRE | [28,33–35,37,66,81,82,84,99,100,128,139,141,146,164,181,183,195,200,201,205–207,250,259,262–264,290,291,315,317,328,340,344,555,558,596] | [33,48,82,128,164,200,206,207,247,264,267,351,354,356,358,361,364,365,367,369,371,372,374,377,382,384,386,390–392,397,398,407,411,412,414,418,420,427,429,430,432,437,442,450,453,454,454,456–459,461,462,468,471,473,475,476,480,490,495,496,500,503,515,517,522,523,528,529,532,533,542,550,595] |
| SPE | [9,26,27,30,33–35,38,43,47,51–53,55,56,58,60,64–66,69,72,77,81,99–101,103,105,106,109,110,113–116,116–118,120,121,125,126,128–130,132,133,141,142,147,149,150,152,155,160,161,163,166,168,169,172–174,176,177,179–181,183,184,191,193–195,200,202,203,205,207,208,210,213,216–218,222,224–226,230,233,234,236–240,247,250,253,254,257,261,263,266,268–275,278,279,281,287,292–294,297,298,302,303,305,307,310,311,314,317,321,322,325,327,328,333,334,336,340–344,346,348,350,406,501,545,576,596,607,608,613–616,618,619] | [1,33,48,60,125,128,142,177,200,207,216,234,247,253,264,292,297,351,354,355,358,359,365,370,379,380,383,385,386,390,391,395,402–404,410,413,421,430,431,433,434,439,441,443,446,453,454,456,459–461,464,466–474,476,480,486,488,494,495,501–504,506,520,521,528,530–533,535,540,542,543,545,547,586,595,620] |
| FOM | [350] | |
| SE | [2,187,221,310,311,319,338,349,558,596,621] | |
| FPR | [2,34,128,195,201,207,263,264,319,325,349,621,622] | [128,207,264,397,405,418,441,442,476,542] |
| F1S | [28,32,52,82,99,108,128,134,141,143,164,174,182,195,205,206,221,279,281,292,322,344,617] | [48,82,128,164,182,206,267,292,354,356,361,363,365,367,369,371,372,374,377,384,386,392,396,407,411,412,414,418,420,427,437,449,450,453,457–459,464,472,488,490,496,502,504,520,533,542,595] |
| NPV | [128,195,263,328,340] | [247,433,471,495] |

(continued on next page)

Table 10 (continued).

| Metrics | SLS articles | SLC articles |
|---------|--|--|
| DSC | [26–30,33,35,38,43,47,51–53,55,56,58–60,64–66,68,69,72,77,81–85,90,94,95,97,100–107,109,110,113–116,116–118,120,121,124,127,129–131,133,138,139,145,147–155,158,160–163,166–172,175–177,179–181,183–185,189–191,193,194,202–204,208–211,213,215–220,222,224–228,230–233,235–242,248,250,251,255,257,258,260–262,265–268,270–276,278,282,287,290,291,297–302,305,307,308,310,313,338,555,558,576,608,615] | [1,216,235,297,398,410,429,536] |
| HD | [2,84,325] | |
| AUC | [34,82,103,139,143,173,178,200,207,259,315,607] | [5,82,177,178,200,207,355,358–360,362,363,369,372,377,382,390,391,400,402,403,405,409,414,421,429,434,438,440,441,443,445,446,449,451,453,456,459,465,466,468,473,475,476,480–482,484–486,500,502–504,508,517,523,525,526,533] |
| JI | [2,26–29,35,37,38,43,47,52–54,56,58–61,64–66,68,69,72,77,81–85,89,94,95,97,99–105,107–110,113–116,116–118,120,122,124,127,129–134,138,148–152,154–156,158,160–163,165–172,172–177,179–181,183–185,189–191,193,194,198,202–204,208–213,215–220,222,224–228,230–233,235–242,244,251,257,260,261,265,266,268–272,274–277,280,282–284,284,286–288,296,297,299,301,313,315,316,338,576,608,615,623] | [1,201,216,235,276,297,536] |
| FNR | [128,195,200,201,263,264,295,319] | [128,200,201,264,441,442] |
| XOR | [143,205,248,252,258,291,317,318,333,346,347,350] | |
| CC | [190,312,313] | |
| HMD | [248,258,291] | |
| MCC | [105,110,128,169,181,195] | [48,128,396,414,418,459,472] |
| PSNR | [190] | |
| SSIM | [190] | |
| BACC | [126,321,406] | [354,355,368,369,378,382,409,431,432,453,454,459,511,514,542,595] |

deviation has a higher value, it symbolizes higher inter-fold variation, consequently poor robustness, and vice-versa.

$$M = \frac{1}{K} \times \sum_{i=1}^K M_i \pm \sqrt{\frac{\sum_{i=1}^K (M_i - \mu)^2}{K}}, \quad (5)$$

where $M_i \in \mathbb{R}$, $i \forall K$, denotes an estimated metric with a mean value of μ and K is the fold numbers. Additionally, the authors in [157,349,459] exploit the statistical validation test, i.e., Analysis of Variance (ANOVA), to evaluate the SLS and SLC techniques for revealing the significance of the experimentations with a suitable p -value. Moreover, Total Computation Time (TCT) is occasionally employed to judge the SLS and SLC methods for determining the time the algorithms need. Short computation times allow SLS and SLC methods to become real-time applications in CAD systems. However, among the reviewed articles, a few papers used TCT in their evaluation strategy, which are: [198,207,220,260,263,264,312,313,322,345] for SLS; and [93,200,207,264,364,441,442] for SLC.

Fig. 13 summarizes the frequency with that various metrics are used in the 594 SLA articles we reviewed. Accuracy, sensitivity, specificity, dice similarity coefficient, and Jaccard index are observed to be the 5 most frequently used metrics, being employed in 54.2%, 44.7%, 39.0%, 41.9%, and 39.6% of the total articles. Therefore, they can be treated as the **High-frequency** SLS evaluation metrics. In contrast,

accuracy, sensitivity, precision, specificity, and AUC are the most-5 regularly applied metrics for the SLC evaluation respectively practiced in 58.0%, 47.5%, 30.7%, 32.8%, and 25.6% articles, leading to the **High-frequency** SLC evaluation metrics. The other metrics are much less frequently used than the top 5 in both SLS and SLC tasks. Thus, we have considered them as the **Low-frequency** metrics rather than **Medium-frequency**. Again, although the dice similarity coefficient and Jaccard index are frequently used in SLS evaluation, they are only sometimes employed for SLC evaluation. Some metrics like accuracy, sensitivity, specificity, precision, F1-score, balance accuracy, and false-positive and false-negative rates are employed for the SLS and SLC evaluations in approximately the same number of articles. Moreover, although many articles applied accuracy as measured by the SLS and SLC metrics, they need to consider the class imbalance measurement. If there are many more samples in one particular class than others, the trained models tend to learn that class more accurately at the expense of accuracy for other classes, leading to a general increase in false positive or false-negative rates. If there is no penalty for class imbalance, conventional metrics like accuracy can still have high values despite a poorly performing model. Some metrics, such as ROC and AUC estimation [3,7,173,551], however, address this imbalance. Nevertheless, the barely 3.4% for SLS and 25.6% for SLC articles acknowledged this issue by determining the AUC values for their assessments.

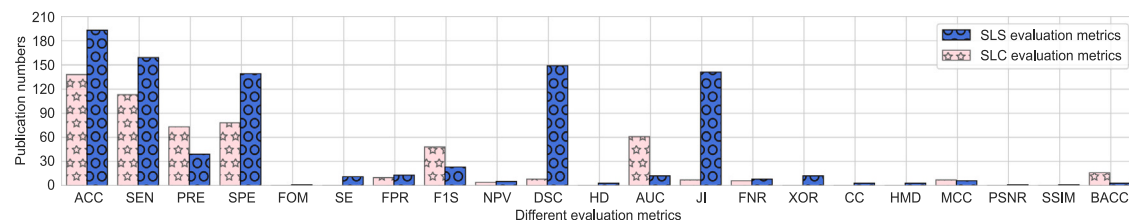


Fig. 13. The number of articles employing different evaluation metrics, conferring the commonly applied metrics.

8. Explainability and clinical impact of SLA methods

Explainable Artificial Intelligence (XAI) aims to unbox how AI systems make decisions, investigate the criteria and models that go into making decisions, and look for ways to describe such criteria and models in more detail [625,626]. [582] used visual attention mechanisms to direct the model to the most discriminative regions and attributes of the lesion at each decision level. They presented a heatmap as a mode of SLA explanation. A Local Interpretable Model-agnostic Explanation (LIME), a post hoc method, was used in [384] that generated a few cues like the mole's size, bleeding, and shape to help the dermatologist make a final decision. Class Activation Map (CAM) was applied in some articles [177,581,600–602,610], where the explanation was presented using a heatmap and/or histogram. A modification of CAM called Gradient CAM (GradCAM) [627], which weights the feature maps based on gradients, was also used in some SLA articles [444,557,598,609,612]. GradCAM used a heatmap and/or histogram for the SLA explanation. The other XAI methods in the past SLA literature are t-SNE [487,599], content-based image retrieval [478,507,599], Shapley Additive Explanations (SHAP) [609,612], Kernel-SHAP [612], and feature activation maps [435].

In terms of clinical applications of SLA CAD, this is not reviewed here as our focus is on the SLA techniques, but a detailed review can be found in [628]. However, it is noteworthy that there is evidence of CNN's ability to outperform human experts. [629] evaluated CNN's SLA task performance and compared it to a systematic evaluation by clinical human experts. The performance of an AI-based SLA algorithm trained exclusively by open-source images was compared to that of a large number of dermatologists covering all levels within the clinical hierarchy by [630]. The authors demonstrated that AI-based SLA outperformed 136 of 157 dermatologists for the melanoma image classification task. [5] demonstrated that the performance of AI-based SLA is better than human raters for the skin cancer detection task. A case study on skin cancer diagnosis in the UK's General Practitioners (GPs) was carried out by [631], and the author showed that AI is accurate; there is a positive effect on GPs' performance and confidence, indicating the possibility of reducing referrals for benign lesions.

Currently, several AI-based SLA technologies are approved by regulatory bodies for use clinically; for example, MelaFind and Nevisense were approved by the US FDA, and an AI-powered digital tool for diagnosing skin cancers (Skin Analytics) was approved by the UK MHRA as a Class IIA medical device.

9. Observations and recommendations

This section highlights our key findings from a critical inspection of the selected 594 articles (356 for segmentation and 238 for classification). Here, we provide suggestions for future SLA tasks, including input data (dataset utilization, preprocessing, augmentation, and imbalance problem solving), approach configuration (techniques, architectures, module frameworks, and loss functions), training protocol (hyperparameter settings), and evaluation criteria (metrics). These suggestions are intended to inform future SLA work.

- Currently, ISIC datasets have been most commonly applied to the SLS and SLC tasks after 2016, turning them into a representative dataset for SLA (see Fig. 3). Our review also reveals that there is a necessity for larger, more diverse, and more representative skin lesion datasets (with more inter-class diversity) to train DL models to make them more accurate and robust. The most popular ISIC Archive contains over 69,900 publicly available skin lesion images, but many cases lack proper ground truth. One way to improve this is to crowdsource annotations from investigators who are experts in this field and then run an ensemble based on the annotations that come up most often.
- Our review suggests that there need to be specific clarifications to the questions: is preprocessing essential, and which preprocessing approach is best for SLA tasks? To answer the first question, two considerations have been uncovered in the past SLA articles: If manual feature engineering with ML models or other computer vision-based models is employed, preprocessing is strongly suggested; conversely, if DL-based automated models are applied, preprocessing is ill-advised. To answer the second question, the proper selection of the preprocessing method depends on the algorithm types. The utilization frequency history provided in this review can help future investigators in their preprocessing design (see details in Section 4.1, especially in Fig. 4).
- The applications of the augmentations need to be recommended only for the DL-based computerized SLA techniques, as they were seldom involved in the other ML (or computer vision)-based SLA techniques in the past (see Fig. 5). The typical baseline augmentation strategies can be found in Section 4.2, leading to help for augmentation preference for SLA. Although augmentations are involved in the minority class to increase its sample numbers, the class weighting has been most commonly suggested to resolve the class imbalance problem (see details in Section 4.2).
- The insight overlooked in the past SLS articles reveals that DL-based procedures, especially CNN models to learn a lesion's spatial information, are the recent trends, especially after 2016 (see Fig. 1, Fig. 6(a) and (b)). Therefore, CNN-based encoder-decoder networks are the most prioritized procedures for the SLS task. Again, the investigation of the encoder structure reveals that the ResNet, VGG, and DenseNet family networks are the most widely applied encoder architectures and are the most popular trends for the SLSs. In contrast, U-Net-like structures are the preferred decoder mechanism in the CNN-based SLS job. Additionally, segmented lesion masks are generally improved by employing several post-processing techniques (see Table 6), where the various morphological operations are the most applied methods in the last twelve years (see back-and-forth in Section 5, particularly in Table 6).
- Although this survey article discloses the most commonly employed lesion's attributes (see Fig. 7) and ML-based classifiers (see Fig. 8) for the manual feature-based SLC strategies, the DL-based automated approaches have been the last few years' trends (see Fig. 9). Further investigation reveals the most frequent CNN architectures like ResNet, VGG, DenseNet, InceptionNet, and AlexNet for lesion's attribute learning, which are discussed in Section 6.2. Using lightweight pre-trained architectures that

are appropriate for the smaller training set is also observed and recommended, as they have been widely applied in the last twelve years with fewer training examples. According to previous research, engaging in ensemble learning and/or combining manual and automated CNN's lesion features is advantageous for capturing the discernment lesion characteristics, thereby improving the SLC outcome(s).

- The 594 SLA literature also enabled researchers to determine the best experimental settings that are most typically used for both SLS and SLC tasks. Although it is challenging to decide the values of the proper hyperparameters, recent history could support resolving it. For illustration, Figs. 11 and 12 would aid in understanding the last twelve years' history of batch size and LR employment, respectively, revealing that their low and/or very high values are rarely used. Cross-entropy (binary or multi-class) is the most suggested loss function for the SLS and SLC tasks. However, many authors have enforced extra care in the SLS's loss function, considering the DSC (or JI) function as in Eqs. (2) and (3) (see details reflection in Eq. (4)). This review would help to determine good optimizers and epoch numbers; for example, adaptive and SGD optimizers and mid-range epoch numbers like 100 to 200 have been most commonly employed in the past. The suitable values of the optimizers' parameters could be chosen by overlooking Table 8. Lastly, the trends of ML and/or DL frameworks for developing the SLA pipeline can be seen in Section 7.2.
- There is no universally appropriate evaluation criterion [580], as different benchmarks grasp different characteristics of an SLS and/or SLC algorithm's performance on a provided dataset. Our analysis in Fig. 13 informs future investigators on which metrics have been most commonly used in the recent past to help investigators decide the best metrics to use. A direct quantitative assessment system using the metrics (see Table 10), qualitative evaluation, and reflection of TCT are the three most standard approaches to estimating the SLA method(s). In order to explain the performance of the SLA technique(s), all three of these evaluation techniques could be involved, as in [198,207,220,260,263,264, 312,313,322,345] for SLS and [93,200,207,264,364,441,442] for SLC. Unfortunately, it has been infrequently used in the past. This is one of the shortcomings of the current practice observed in the SLA articles, and the researchers would consider it in future experimentation.
- Although an enormous number of SLA articles have been published in the past, only a few studies have developed prototype applications, and none of the 594 SLA articles has considered developing user-friendly clinical applications in practical settings. Our review could not find the answer in the 594 articles to how the technologies have been integrated into clinical settings. The researchers should concentrate on real-time clinical applications in conjunction with SLA technique improvement, providing a case study of AI methods' successes.
- Despite some papers studying XAI strategies to unlock the black box of the decision-making SLA pipeline, only a few of these studies [4,487,507] have examined the influence on diagnosis accuracy and dermatologist acceptance. This human factor would be considered in future SLA research. Optimizing the reasoning method for best human usage and improving interpretability beyond visualization approaches are issues that demand more study in this SLA area. Future research should demonstrate how to include XAI in a comprehensive optimization process in order to increase the model's efficacy while reducing its complexity. In addition, defining a model to be explainable based on its capacity to instill confidence may not satisfy the condition of model explainability [626]. Trustworthiness is the assurance that a model will respond as intended when presented with a given problem; nonetheless, this must be added to future SLA literature [632].

10. Conclusion

This survey summarizes the 594 SLA articles published over the course of the past year, with an emphasis on dataset utilization, pre-processing, augmentations, solving imbalance problems, SLS & SLC techniques, training tactics (frameworks and hyperparameter settings), and evaluation benchmarks (metrics). The survey analysis conducted on SLA reveals that ISIC is the most commonly applied dataset that best exemplifies this area. When using ML models with manual feature engineering, preprocessing was typically used; however, when using automatically generated DL models, it had yet to be generally applied in the past twelve years. DL-based computational SLA techniques are becoming the usual trend in the skin lesion arena. This is due to the fact that they perform better than the other SLA methods, require less parameter adjusting, and are end-to-end. In order to evaluate SLA methods, this survey suggests that in addition to qualitative and quantitative evaluations, SLA's TCT would be applied to assess the method(s) from diverse aspects. Our review may be helpful to future investigators in designing their SLA approach. Potential researchers should translate suitable SLA methodologies into real-time applications considering clinical settings, as there is room for such translation.

Declaration of competing interest

The authors declare that they have no known competing financial interests or personal relationships that could have appeared to influence the work reported in this paper.

Acknowledgments

Guang Yang was supported in part by the BHF, UK (TG/18/5/34111, PG/16/78/32402), the ERC IMI (101005122), the H2020 (952172), the MRC (MC/PC/21013), the Royal Society, UK (IEC/NS-FC/211235), the NVIDIA Academic Hardware Grant Program, the SABER project supported by Boehringer Ingelheim Ltd, NIHR Imperial Biomedical Research Centre (RDA01), and the UKRI Future Leaders Fellowship (MR/V023799/1).

References

- [1] S. Chatterjee, D. Dey, S. Munshi, Integration of morphological preprocessing and fractal based feature extraction with recursive feature elimination for skin lesion types classification, *Comput. Methods Programs Biomed.* 178 (2019) 201–218.
- [2] P.M. Pereira, R. Fonseca-Pinto, R.P. Paiva, P.A. Assuncao, L.M. Tavora, L.A. Thomaz, S.M. Faria, Dermoscopic skin lesion image segmentation based on local binary pattern clustering: comparative study, *Biomed. Signal Process. Control* 59 (2020) 101924.
- [3] M.K. Hasan, S. Roy, C. Mondal, M.A. Alam, M.T.E. Elahi, A. Dutta, S.T.U. Raju, M.T. Jawad, M. Ahmad, Dermo-DOKTOR: A framework for concurrent skin lesion detection and recognition using a deep convolutional neural network with end-to-end dual encoders, *Biomed. Signal Process. Control* 68 (2021) 102661.
- [4] P. Tschandl, C. Rinner, Z. Apalla, G. Argenziano, N. Codella, A. Halpern, M. Janda, A. Lallas, C. Longo, J. Malvehy, et al., Human-computer collaboration for skin cancer recognition, *Nat. Med.* 26 (8) (2020) 1229–1234.
- [5] P. Tschandl, C. Rosendahl, B.N. Akay, G. Argenziano, A. Blum, R.P. Braun, H. Cabo, J.-Y. Gourhant, J. Kreusch, A. Lallas, et al., Expert-level diagnosis of nonpigmented skin cancer by combined convolutional neural networks, *JAMA Dermatol.* 155 (1) (2019) 58–65.
- [6] R.B. Oliveira, J.P. Papa, A.S. Pereira, J.M.R. Tavares, Computational methods for pigmented skin lesion classification in images: review and future trends, *Neural Comput. Appl.* 29 (3) (2018) 613–636.
- [7] M.K. Hasan, M.T.E. Elahi, M.A. Alam, M.T. Jawad, R. Martí, DermoExpert: Skin lesion classification using a hybrid convolutional neural network through segmentation, transfer learning, and augmentation, *Inform. Med. Unlocked* (2022) 100819.
- [8] K. Korotkov, R. Garcia, Computerized analysis of pigmented skin lesions: a review, *Artif. Intell. Med.* 56 (2) (2012) 69–90.
- [9] M.H. Jafari, N. Karimi, E. Nasr-Esfahani, S. Samavi, S.M.R. Soroushmehr, K. Ward, K. Najarian, Skin lesion segmentation in clinical images using deep learning, in: 2016 23rd International Conference on Pattern Recognition, ICPR, IEEE, 2016, pp. 337–342.

- [10] M.A. Kassem, K.M. Hosny, R. Damaševičius, M.M. Eltoukhy, Machine learning and deep learning methods for skin lesion classification and diagnosis: A systematic review, *Diagnostics* 11 (8) (2021) 1390.
- [11] M. Dildar, S. Akram, M. Irfan, H.U. Khan, M. Ramzan, A.R. Mahmood, S.A. Alsaiari, A.H.M. Saeed, M.O. Alraddadi, M.H. Mahnashi, Skin cancer detection: a review using deep learning techniques, *Int. J. Environ. Res. Public Health* 18 (10) (2021) 5479.
- [12] M.R. Islam, M.A. Moni, M.M. Islam, M. Rashed-Al-Mahfuz, M.S. Islam, M.K. Hasan, M.S. Hossain, M. Ahmad, S. Uddin, A. Azad, et al., Emotion recognition from EEG signal focusing on deep learning and shallow learning techniques, *IEEE Access* 9 (2021) 94601–94624.
- [13] M.K. Hasan, M.A. Alam, S. Roy, A. Dutta, M.T. Jawad, S. Das, Missing value imputation affects the performance of machine learning: A review and analysis of the literature (2010–2021), *Inform. Med. Unlocked* 27 (2021) 100799.
- [14] D. Gutman, N.C. Codella, E. Celebi, B. Helba, M. Marchetti, N. Mishra, A. Halpern, Skin lesion analysis toward melanoma detection: A challenge at the international symposium on biomedical imaging (ISBI) 2016, hosted by the international skin imaging collaboration (ISIC), 2016, [arXiv:1605.01397](#).
- [15] N.C. Codella, D. Gutman, M.E. Celebi, B. Helba, M.A. Marchetti, S.W. Dusza, A. Kalloo, K. Liopyris, N. Mishra, H. Kittler, et al., Skin lesion analysis toward melanoma detection: A challenge at the 2017 international symposium on biomedical imaging (isbi), hosted by the international skin imaging collaboration (isic), in: 2018 IEEE 15th International Symposium on Biomedical Imaging, ISBI 2018, IEEE, 2018, pp. 168–172.
- [16] N. Codella, V. Rotemberg, P. Tschandl, M.E. Celebi, S. Dusza, D. Gutman, B. Helba, A. Kalloo, K. Liopyris, M. Marchetti, et al., Skin lesion analysis toward melanoma detection 2018: A challenge hosted by the international skin imaging collaboration (isic), 2019, [arXiv:1902.03368](#).
- [17] P. Tschandl, C. Rosendahl, H. Kittler, The HAM10000 dataset, a large collection of multi-source dermatoscopic images of common pigmented skin lesions, *Sci. Data* 5 (1) (2018) 1–9.
- [18] M. Combalia, N.C. Codella, V. Rotemberg, B. Helba, V. Vilaplana, O. Reiter, C. Carrera, A. Barreiro, A.C. Halpern, S. Puig, et al., BCN20000: Dermoscopic lesions in the wild, 2019, [arXiv:1908.02288](#).
- [19] V. Rotemberg, N. Kurtansky, B. Betz-Stablein, L. Caffery, E. Chousakos, N. Codella, M. Combalia, S. Dusza, P. Guitera, D. Gutman, et al., A patient-centric dataset of images and metadata for identifying melanomas using clinical context, *Sci. Data* 8 (1) (2021) 1–8.
- [20] T. Mendonça, P.M. Ferreira, J.S. Marques, A.R. Marcal, J. Rozeira, PH 2-A dermoscopic image database for research and benchmarking, in: 2013 35th Annual International Conference of the IEEE Engineering in Medicine and Biology Society, EMBC, IEEE, 2013, pp. 5437–5440.
- [21] G. Argenziano, H. Soyer, V. De Giorgi, D. Piccolo, P. Carli, M. Delfino, et al., Dermoscopy: a tutorial, *EDRA Med. Publ. New Media* 16 (2002).
- [22] N. Codella, J. Cai, M. Abedini, R. Garnavi, A. Halpern, J.R. Smith, Deep learning, sparse coding, and SVM for melanoma recognition in dermoscopy images, in: International Workshop on Machine Learning in Medical Imaging, Springer, 2015, pp. 118–126.
- [23] R. Amelard, J. Glaister, A. Wong, D.A. Clausi, High-level intuitive features (HLIFs) for intuitive skin lesion description, *IEEE Trans. Biomed. Eng.* 62 (3) (2014) 820–831.
- [24] M.E. Celebi, S. Hwang, H. Iyatomi, G. Schaefer, Robust border detection in dermoscopy images using threshold fusion, in: 2010 IEEE International Conference on Image Processing, IEEE, 2010, pp. 2541–2544.
- [25] J. Sun, W. Xi, G. Bai, X. Liu, F. Yu, C. Zhang, ACFNet: An adaptive context fusion network for skin lesion segmentation, in: 2022 International Joint Conference on Neural Networks, IJCNN, IEEE, 2022, pp. 01–08.
- [26] R. Gu, L. Wang, L. Zhang, DE-Net: A deep edge network with boundary information for automatic skin lesion segmentation, *Neurocomputing* 468 (2022) 71–84.
- [27] K. Feng, L. Ren, G. Wang, H. Wang, Y. Li, SLT-Net: A codec network for skin lesion segmentation, *Comput. Biol. Med.* 148 (2022) 105942.
- [28] P.T. Le, C.-C. Chang, Y.-H. Li, Y.-C. Hsu, J.-C. Wang, Antialiasing attention spatial convolution model for skin lesion segmentation with applications in the medical IoT, *Wirel. Commun. Mob. Comput.* 2022 (2022).
- [29] R. Feng, L. Zhuo, X. Li, H. Yin, Z. Wang, BLA-Net: Boundary learning assisted network for skin lesion segmentation, *Comput. Methods Programs Biomed.* 226 (2022) 107190.
- [30] L. Singh, R.R. Janghel, S.P. Sahu, An empirical review on evaluating the impact of image segmentation on the classification performance for skin lesion detection, *IETE Tech. Rev.* (2022) 1–12.
- [31] Z. Song, W. Luo, Q. Shi, Res-CDD-net: A network with multi-scale attention and optimized decoding path for skin lesion segmentation, *Electronics* 11 (17) (2022) 2672.
- [32] P. Shamsolmoali, M. Zarepoor, J. Yang, E. Granger, H. Zhou, Salient skin lesion segmentation via dilated scale-wise feature fusion network, in: 2022 26th International Conference on Pattern Recognition, ICPR, IEEE, 2022, pp. 4219–4225.
- [33] S. Khouloud, M. Ahlem, T. Fadel, S. Amel, W-net and inception residual network for skin lesion segmentation and classification, *Appl. Intell.* 52 (4) (2022) 3976–3994.
- [34] M.A. Khan, M.I. Sharif, M. Raza, A. Anjum, T. Saba, S.A. Shad, Skin lesion segmentation and classification: A unified framework of deep neural network features fusion and selection, *Expert Syst.* 39 (7) (2022) e12497.
- [35] Y. Dong, L. Wang, Y. Li, TC-Net: Dual coding network of transformer and CNN for skin lesion segmentation, *PLoS One* 17 (11) (2022) e0277578.
- [36] B. Hafouf, A. Zitouni, A.C. Megherbi, S. Sbaa, An improved and robust encoder-decoder for skin lesion segmentation, *Arab. J. Sci. Eng.* (2022) 1–15.
- [37] D. Dai, C. Dong, S. Xu, Q. Yan, Z. Li, C. Zhang, N. Luo, Ms RED: A novel multi-scale residual encoding and decoding network for skin lesion segmentation, *Med. Image Anal.* 75 (2022) 102293.
- [38] N. Şahin, N. Alpaslan, D. Hanbay, Robust optimization of SegNet hyperparameters for skin lesion segmentation, *Multimedia Tools Appl.* 81 (25) (2022) 36031–36051.
- [39] P.M. Kazaj, M. Koosheshi, A. Shahidi, A.V. Sadr, U-Net-based models for skin lesion segmentation: More attention and augmentation, 2022, [arXiv:2210.16399](#).
- [40] R. Kaur, H. GholumHosseini, R. Sinha, Skin lesion segmentation using an improved framework of encoder-decoder based convolutional neural network, *Int. J. Imaging Syst. Technol.* (2022).
- [41] R. Kaur, H. GholumHosseini, R. Sinha, M. Lindén, Automatic lesion segmentation using atrous convolutional deep neural networks in dermoscopic skin cancer images, *BMC Med. Imaging* 22 (1) (2022) 1–13.
- [42] W. Cao, G. Yuan, Q. Liu, C. Peng, J. Xie, X. Yang, X. Ni, J. Zheng, ICL-Net: Global and local inter-pixel correlations learning network for skin lesion segmentation, *IEEE J. Biomed. Health Inf.* (2022).
- [43] H. Wu, S. Chen, G. Chen, W. Wang, B. Lei, Z. Wen, FAT-Net: Feature adaptive transformers for automated skin lesion segmentation, *Med. Image Anal.* 76 (2022) 102327.
- [44] R. Wang, S. Chen, C. Ji, Y. Li, Cascaded context enhancement network for automatic skin lesion segmentation, *Expert Syst. Appl.* 201 (2022) 117069.
- [45] S. Malik, T. Akram, I. Ashraf, M. Rafiullah, M. Ullah, J. Tanveer, A hybrid preprocessor DE-ABC for efficient skin-lesion segmentation with improved contrast, *Diagnostics* 12 (11) (2022) 2625.
- [46] S. Malik, S.R. Islam, T. Akram, S.R. Naqvi, N.S. Alghamdi, G. Baryannis, A novel hybrid meta-heuristic contrast stretching technique for improved skin lesion segmentation, *Comput. Biol. Med.* 151 (2022) 106222.
- [47] T.-T. Tran, V.-T. Pham, Fully convolutional neural network with attention gate and fuzzy active contour model for skin lesion segmentation, *Multimedia Tools Appl.* 81 (10) (2022) 13979–13999.
- [48] P. Thapar, M. Rakhr, G. Cazzato, M.S. Hossain, A novel hybrid deep learning approach for skin lesion segmentation and classification, *J. Healthc. Eng.* 2022 (2022).
- [49] Q. Liu, J. Wang, M. Zuo, W. Cao, J. Zheng, H. Zhao, J. Xie, NCRNet: Neighborhood context refinement network for skin lesion segmentation, *Comput. Biol. Med.* 146 (2022) 105545.
- [50] Y. Li, C. Xu, J. Han, Z. An, D. Wang, H. Ma, C. Liu, MHAU-net: Skin lesion segmentation based on multi-scale hybrid residual attention network, *Sensors* 22 (22) (2022) 8701.
- [51] M.D. Alahmadi, W. Alghamdi, Semi-supervised skin lesion segmentation with coupling CNN and transformer features, *IEEE Access* (2022).
- [52] M.D. Alahmadi, Multiscale attention U-Net for skin lesion segmentation, *IEEE Access* 10 (2022) 59145–59154.
- [53] Z. Al-Huda, Y. Yao, J. Yao, B. Peng, A. Raza, Weakly supervised skin lesion segmentation based on spot-seeds guided optimal regions, *IET Image Process.* (2022).
- [54] M.M. Stofa, M.A. Zulkifley, M.A.A.M. Zainuri, A.A. Ibrahim, U-net with atrous spatial pyramid pooling for skin lesion segmentation, in: Proceedings of the 6th International Conference on Electrical, Control and Computer Engineering, Springer, 2022, pp. 1025–1033.
- [55] E.K. Aghdam, R. Azad, M. Zarvani, D. Merhof, Attention swin u-net: Cross-contextual attention mechanism for skin lesion segmentation, 2022, [arXiv:2210.16898](#).
- [56] R. Fan, Z. Wang, Q. Zhu, EGFNet: Efficient guided feature fusion network for skin cancer lesion segmentation, in: 2022 the 6th International Conference on Innovation in Artificial Intelligence, ICIAI, 2022, pp. 95–99.
- [57] X. Shu, Y. Yang, R. Xie, J. Liu, X. Chang, B. Wu, ALS: Active learning-based image segmentation model for skin lesion, 2022, *SSRN* 4141765.
- [58] J. Ruan, S. Xiang, M. Xie, T. Liu, Y. Fu, MALUNet: A multi-attention and light-weight unet for skin lesion segmentation, 2022, [arXiv:2211.01784](#).
- [59] Y. Ren, L. Yu, S. Tian, J. Cheng, Z. Guo, Y. Zhang, Serial attention network for skin lesion segmentation, *J. Ambient Intell. Humaniz. Comput.* 13 (2) (2022) 799–810.
- [60] A.H. Khan, D.N. Awang Iskandar, J.F. Al-Asad, H. Mewada, M.A. Sherazi, Ensemble learning of deep learning and traditional machine learning approaches for skin lesion segmentation and classification, *Concurr. Comput.: Pract. Exper.* 34 (13) (2022) e6907.
- [61] S. Barin, G.E. Güraksin, An automatic skin lesion segmentation system with hybrid FCN-ResAlexNet, *Eng. Sci. Technol. Int. J.* (2022) 101174.
- [62] R. Ramadan, S. Aly, DGCU-Net: A new dual gradient-color deep convolutional neural network for efficient skin lesion segmentation, *Biomed. Signal Process. Control* 77 (2022) 103829.

- [63] R. Ramadan, S. Aly, CU-net: a new improved multi-input color U-Net model for skin lesion semantic segmentation, *IEEE Access* 10 (2022) 15539–15564.
- [64] P. Chen, S. Huang, Q. Yue, Skin lesion segmentation using recurrent attentional convolutional networks, *IEEE Access* 10 (2022) 94007–94018.
- [65] Z. Zhang, C. Tian, X. Gao, C. Wang, X. Feng, H.X. Bai, Z. Jiao, Dynamic prototypical feature representation learning framework for semi-supervised skin lesion segmentation, *Neurocomputing* 507 (2022) 369–382.
- [66] G. Zhang, S. Wang, Dense and shuffle attention U-Net for automatic skin lesion segmentation, *Int. J. Imaging Syst. Technol.* 32 (6) (2022) 2066–2079.
- [67] A. Pennisi, D.D. Bloisi, V. Suriani, D. Nardi, A. Facciano, A.R. Giampetrucci, Skin Lesion Area segmentation using attention squeeze U-Net for embedded devices, *J. Digit. Imaging* (2022) 1–14.
- [68] X. Jiang, J. Jiang, B. Wang, J. Yu, J. Wang, SEACU-Net: Attentive ConvLSTM U-Net with squeeze-and-excitation layer for skin lesion segmentation, *Comput. Methods Programs Biomed.* 225 (2022) 107076.
- [69] K. Hu, J. Lu, D. Lee, D. Xiong, Z. Chen, AS-Net: Attention Synergy Network for skin lesion segmentation, *Expert Syst. Appl.* 201 (2022) 117112.
- [70] H. Basak, R. Kundu, R. Sarkar, MFSNet: A multi focus segmentation network for skin lesion segmentation, *Pattern Recognit.* 128 (2022) 108673.
- [71] S. Barzegar, N. Khan, Skin lesion segmentation using a semi-supervised U-NetSC model with an adaptive loss function, in: 2022 44th Annual International Conference of the IEEE Engineering in Medicine & Biology Society, EMBC, IEEE, 2022, pp. 3776–3780.
- [72] Y. Wang, S. Wang, Skin lesion segmentation with attention-based SC-ConvU-Net and feature map distortion, *Signal Image Video Process.* (2022) 1–9.
- [73] X. Liu, W. Fan, D. Zhou, Skin lesion segmentation via intensive atrous spatial transformer, in: International Conference on Wireless Algorithms, Systems, and Applications, Springer, 2022, pp. 15–26.
- [74] Q. Lin, X. Chen, C. Chen, J.M. Garibaldi, Quality quantification in deep convolutional neural networks for skin lesion segmentation using fuzzy uncertainty measurement, in: 2022 IEEE International Conference on Fuzzy Systems (FUZZ-IEEE), IEEE, 2022, pp. 1–8.
- [75] Y. Gulzar, S.A. Khan, Skin lesion segmentation based on vision transformers and convolutional neural networks—A comparative study, *Appl. Sci.* 12 (12) (2022) 5990.
- [76] G.M. Kosgikar, A. Deshpande, K. Anjum, Significant of multi-level pre-processing steps and its proper sequence in SegCaps skin lesion segmentation of dermoscopic images, *Mater. Today Proc.* 51 (2022) 129–141.
- [77] N. Ahmed, X. Tan, L. Ma, A new method proposed to melanoma-skin cancer lesion detection and segmentation based on hybrid convolutional neural network, *Multimedia Tools Appl.* (2022) 1–24.
- [78] C. Akyel, N. Arici, LinkNet-B7: Noise removal and lesion segmentation in images of skin cancer, *Mathematics* 10 (5) (2022) 736.
- [79] A. Alhudhaif, H. Ocal, N. Barisci, İ. Atacak, M. Nour, K. Polat, A novel approach to skin lesion segmentation: Multipath fusion model with fusion loss, *Comput. Math. Methods Med.* 2022 (2022).
- [80] V. Anand, S. Gupta, D. Koundal, K. Singh, Fusion of U-Net and CNN model for segmentation and classification of skin lesion from dermoscopy images, *Expert Syst. Appl.* (2022) 119230.
- [81] Q. Han, H. Wang, M. Hou, T. Weng, Y. Pei, Z. Li, G. Chen, Y. Tian, Z. Qiu, HWA-SegNet: Multi-channel skin lesion image segmentation network with hierarchical analysis and weight adjustment, *Comput. Biol. Med.* (2022) 106343.
- [82] C. Dong, D. Dai, Y. Zhang, C. Zhang, Z. Li, S. Xu, Learning from dermoscopic images in association with clinical metadata for skin lesion segmentation and classification, *Comput. Biol. Med.* (2022) 106321.
- [83] B. Zuo, F. Lee, Q. Chen, An efficient U-shaped network combined with edge attention module and context pyramid fusion for skin lesion segmentation, *Med. Biol. Eng. Comput.* (2022) 1–14.
- [84] Q. Zhou, T. He, Y. Zou, Superpixel-oriented label distribution learning for skin lesion segmentation, *Diagnostics* 12 (4) (2022) 938.
- [85] M. Rehman, M. Ali, M. Obaya, J. Asghar, L. Hussain, M. K. Nour, N. Negm, A. Mustafa Hilal, Machine learning based skin lesion segmentation method with novel borders and hair removal techniques, *PLoS One* 17 (11) (2022) e0275781.
- [86] M. Nour, H. Öcal, A. Alhudhaif, K. Polat, Skin lesion segmentation based on edge attention vnet with balanced focal tversky loss, *Math. Probl. Eng.* 2022 (2022).
- [87] S. Joseph, O.O. Olugbara, Preprocessing effects on performance of skin lesion saliency segmentation, *Diagnostics* 12 (2) (2022) 344.
- [88] Y. Wang, Z. Xu, J. Tian, J. Luo, Z. Shi, Y. Zhang, J. Fan, Z. He, Cross-domain few-shot learning for rare-disease skin lesion segmentation, in: ICASSP 2022–2022 IEEE International Conference on Acoustics, Speech and Signal Processing, ICASSP, IEEE, 2022, pp. 1086–1090.
- [89] C. Lee, S. Yoo, S. Kim, J. Lee, Progressive weighted self-training ensemble for multi-type skin lesion semantic segmentation, *IEEE Access* (2022).
- [90] Z. Zhao, W. Lu, Z. Zeng, K. Xu, B. Veeravalli, C. Guan, Self-supervised assisted active learning for skin lesion segmentation, 2022, arXiv:2205.07021.
- [91] N. Mahmood, S.J. Khan, M. Rashid, K-means clustering-based color segmentation on vitiligo skin lesion, in: 2022 International Conference on Emerging Trends in Smart Technologies, ICETST, IEEE, 2022, pp. 1–5.
- [92] I. Bhakta, S. Phadikar, K. Majumder, A. Sau, S. Chowdhuri, Tsallis's entropy-based segmentation method for accurate pigmented skin lesion identification, *IETE J. Res.* 68 (1) (2022) 743–759.
- [93] M.A. Khan, M. Sharif, T. Akram, R. Damasevičius, R. Maskeliūnas, Skin lesion segmentation and multiclass classification using deep learning features and improved moth flame optimization, *Diagnostics* 11 (5) (2021) 811.
- [94] X. Wang, X. Jiang, H. Ding, Y. Zhao, J. Liu, Knowledge-aware deep framework for collaborative skin lesion segmentation and melanoma recognition, *Pattern Recognit.* 120 (2021) 108075.
- [95] T.-D.-T. Phan, S.-H. Kim, H.-J. Yang, G.-S. Lee, Skin lesion segmentation by u-net with adaptive skip connection and structural awareness, *Appl. Sci.* 11 (10) (2021) 4528.
- [96] C. Jiang, Y. Zhang, J. Wang, W. Chen, Approximated masked global context network for skin lesion segmentation, in: International Conference on Artificial Neural Networks, Springer, 2021, pp. 610–622.
- [97] J. Chauhan, P. Goyal, A multi-path CNN for automated skin lesion segmentation, in: 2021 International Joint Conference on Neural Networks, IJCNN, IEEE, 2021, pp. 1–9.
- [98] J. Wang, L. Wei, L. Wang, Q. Zhou, L. Zhu, J. Qin, Boundary-aware transformers for skin lesion segmentation, in: International Conference on Medical Image Computing and Computer-Assisted Intervention, Springer, 2021, pp. 206–216.
- [99] X. Tong, J. Wei, B. Sun, S. Su, Z. Zuo, P. Wu, ASCU-Net: attention gate, spatial and channel attention u-net for skin lesion segmentation, *Diagnostics* 11 (3) (2021) 501.
- [100] Y. Dong, L. Wang, S. Cheng, Y. Li, Fac-net: Feedback attention network based on context encoder network for skin lesion segmentation, *Sensors* 21 (15) (2021) 5172.
- [101] P. Tang, X. Yan, Q. Liang, D. Zhang, AFLN-DGCL: Adaptive feature learning network with difficulty-guided curriculum learning for skin lesion segmentation, *Appl. Soft Comput.* 110 (2021) 107656.
- [102] S. Saini, Y.S. Jeon, M. Feng, B-SegNet: branched-SegMentor network for skin lesion segmentation, in: Proceedings of the Conference on Health, Inference, and Learning, 2021, pp. 214–221.
- [103] G.M. Kosgikar, A. Deshpande, A. Kauser, SegCaps: An efficient SegCaps network-based skin lesion segmentation in dermoscopic images, *Int. J. Imaging Syst. Technol.* 31 (2) (2021) 874–894.
- [104] K. Abhishek, G. Hamarneh, Matthews correlation coefficient loss for deep convolutional networks: Application to skin lesion segmentation, in: 2021 IEEE 18th International Symposium on Biomedical Imaging, ISBI, IEEE, 2021, pp. 225–229.
- [105] S. Tao, Y. Jiang, S. Cao, C. Wu, Z. Ma, Attention-guided network with densely connected convolution for skin lesion segmentation, *Sensors* 21 (10) (2021) 3462.
- [106] A.A. Adegun, S. Viriri, M.H. Yousaf, A probabilistic-based deep learning model for skin lesion segmentation, *Appl. Sci.* 11 (7) (2021) 3025.
- [107] X. Ding, S. Wang, Efficient Unet with depth-aware gated fusion for automatic skin lesion segmentation, *J. Intell. Fuzzy Systems* 40 (5) (2021) 9963–9975.
- [108] R. Kaur, H. GholumHosseini, R. Sinha, Deep learning in medical applications: Lesion segmentation in skin cancer images using modified and improved encoder-decoder architecture, in: International Symposium on Geometry and Vision, Springer, 2021, pp. 39–52.
- [109] G.J. Chowdary, G.V.D. Yathisha, G. Suganya, M. Premalatha, Automated skin lesion segmentation using multi-scale feature extraction scheme and dual-attention mechanism, in: 2021 3rd International Conference on Advances in Computing, Communication Control and Networking, ICAC3N, IEEE, 2021, pp. 1763–1771.
- [110] J. Xiao, H. Xu, W. Zhao, C. Cheng, H. Gao, A prior-mask-guided few-shot learning for skin lesion segmentation, *Computing* (2021) 1–23.
- [111] Q. Jin, H. Cui, C. Sun, Z. Meng, R. Su, Cascade knowledge diffusion network for skin lesion diagnosis and segmentation, *Appl. Soft Comput.* 99 (2021) 106881.
- [112] G.J. Chowdary, G.V.D. Yathisha, G. Suganya, M. Premalatha, Automated skin lesion segmentation using multi-scale feature extraction scheme and dual-attention mechanism, in: 2021 3rd International Conference on Advances in Computing, Communication Control and Networking, ICAC3N, IEEE, 2021, pp. 1763–1771.
- [113] J. Chen, J. Chen, Z. Zhou, B. Li, A. Yuille, Y. Lu, MT-TransUNet: Mediating multi-task tokens in transformers for skin lesion segmentation and classification, 2021, arXiv:2112.01767.
- [114] A. Wibowo, S.R. Purnama, P.W. Wirawan, H. Rasyidi, Lightweight encoder-decoder model for automatic skin lesion segmentation, *Inform. Med. Unlocked* 25 (2021) 100640.
- [115] L. Wang, L. Zhang, X. Shu, Focal rank loss function with encoder-decoder network for skin lesion segmentation, in: Journal of Physics: Conference Series, Vol. 2010, IOP Publishing, 2021, 012049.
- [116] R. Hussain, H. Basak, RecU-Net++: Improved utilization of receptive fields in U-Net++ for skin lesion segmentation, in: 2021 IEEE 18th India Council International Conference, INDICON, IEEE, 2021, pp. 1–6.
- [117] F. Bagheri, M.J. Tarokh, M. Ziaratban, Skin lesion segmentation from dermoscopic images by using Mask R-CNN, Retina-DeepLab, and graph-based methods, *Biomed. Signal Process. Control* 67 (2021) 102533.

- [118] F. Bagheri, M.J. Tarokh, M. Ziaratban, Skin lesion segmentation based on mask RCNN, Multi Atrous Full-CNN, and a geodesic method, *Int. J. Imaging Syst. Technol.* 31 (3) (2021) 1609–1624.
- [119] Z. Mirikharaji, K. Abhishek, S. Izadi, G. Hamarneh, D-LEMA: Deep learning ensembles from multiple annotations-application to skin lesion segmentation, in: Proceedings of the IEEE/CVF Conference on Computer Vision and Pattern Recognition, 2021, pp. 1837–1846.
- [120] L. Liu, Y.Y. Tsui, M. Mandal, Skin lesion segmentation using deep learning with auxiliary task, *J. Imaging* 7 (4) (2021) 67.
- [121] S. Garg, B. Jindal, Skin lesion segmentation using k-mean and optimized fire fly algorithm, *Multimedia Tools Appl.* 80 (5) (2021) 7397–7410.
- [122] T.-P. Le, Y.-C. Hsu, J.-C. Wang, Modified attention spatial convolution model for skin lesion segmentation, in: 2021 IEEE International Conference on Consumer Electronics-Taiwan, ICCE-TW, IEEE, 2021, pp. 1–2.
- [123] G.S. Araujo, G. Cámar-Chávez, R.B. Oliveira, Convolutional neural networks applied for skin lesion segmentation, in: 2021 XLVII Latin American Computing Conference, CLEI, IEEE, 2021, pp. 1–10.
- [124] K. Gangwar, Study on different skin lesion segmentation techniques and their comparisons, in: 2021 IEEE International Conference on Imaging Systems and Techniques, IST, IEEE, 2021, pp. 1–6.
- [125] M. Yacin Sikkandar, B.A. Alrasheid, N. Prakash, G. Hemalakshmi, A. Mohanarathinam, K. Shankar, Deep learning based an automated skin lesion segmentation and intelligent classification model, *J. Ambient Intell. Humaniz. Comput.* 12 (3) (2021) 3245–3255.
- [126] R. Ali, H.K. Ragb, Skin lesion segmentation and classification using deep learning and handcrafted features, 2021, arXiv:2112.10307.
- [127] Z. Xie, E. Tu, H. Zheng, Y. Gu, J. Yang, Semi-supervised skin lesion segmentation with learning model confidence, in: ICASSP 2021-2021 IEEE International Conference on Acoustics, Speech and Signal Processing, ICASSP, IEEE, 2021, pp. 1135–1139.
- [128] D.A. Reddy, S. Roy, R. Tripathi, S. Kumar, A. De, S. Dutta, Handling uncertainty with fuzzy lesion segmentation improves the classification accuracy of skin diseases using deep convolutional networks, in: 2021 International Conference on Computational Performance Evaluation, ComPE, IEEE, 2021, pp. 451–456.
- [129] S. Qamar, P. Ahmad, L. Shen, Dense encoder-decoder-based architecture for skin lesion segmentation, *Cogn. Comput.* 13 (2) (2021) 583–594.
- [130] D. Jiang, Y. Wang, F. Zhou, H. Ma, W. Zhang, W. Fang, P. Zhao, Z. Tong, Residual refinement for interactive skin lesion segmentation, *J. Biomed. Semant.* 12 (1) (2021) 1–11.
- [131] C.-H. Yang, J.-H. Ren, H.-C. Huang, L.-Y. Chuang, P.-Y. Chang, Deep hybrid convolutional neural network for segmentation of melanoma skin lesion, *Comput. Intell. Neurosci.* 2021 (2021).
- [132] X. Mu, H. Pan, K. Zhang, T. Teng, X. Bian, C. Chen, Channel context and dual-domain attention based U-Net for skin lesion attributes segmentation, in: International Conference of Pioneering Computer Scientists, Engineers and Educators, Springer, 2021, pp. 528–541.
- [133] R. Arora, B. Raman, K. Nayyar, R. Awasthi, Automated skin lesion segmentation using attention-based deep convolutional neural network, *Biomed. Signal Process. Control* 65 (2021) 102358.
- [134] W. Li, A.N.J. Raj, T. Tjahjadi, Z. Zhuang, Digital hair removal by deep learning for skin lesion segmentation, *Pattern Recognit.* 117 (2021) 107994.
- [135] P. Arora, N. Sharma, P. Bhatt, A. Saxena, Skin lesion segmentation using deep convolutional networks, in: Concepts and Real-Time Applications of Deep Learning, Springer, 2021, pp. 111–122.
- [136] L. Singh, R.R. Janghel, S.P. Sahu, SLICACO: An automated novel hybrid approach for dermatoscopic melanocytic skin lesion segmentation, *Int. J. Imaging Syst. Technol.* 31 (4) (2021) 1817–1833.
- [137] D.M. Krishna, S.K. Sahu, G.S. Raju, MLRNet: Skin lesion segmentation using hybrid Gaussian guided filter with CNN, in: 2021 5th International Conference on Electronics, Communication and Aerospace Technology, ICECA, IEEE, 2021, pp. 1337–1343.
- [138] C. Dayananda, W. You, J.Y. Choi, B. Lee, Skin lesion segmentation in dermoscopic images using CNN architecture, in: 2021 International Conference on Information and Communication Technology Convergence, ICTC, IEEE, 2021, pp. 572–575.
- [139] S. Das, D. Das, Skin lesion segmentation and classification: A deep learning and Markovian approach, in: 2021 IEEE Mysore Sub Section International Conference, MysuruCon, IEEE, 2021, pp. 546–551.
- [140] I. Imtiaz, I. Ahmed, G. Jeon, S. Muramatsu, An efficient image processing and machine learning based technique for skin lesion segmentation and classification, in: 2021 Asia-Pacific Signal and Information Processing Association Annual Summit and Conference, APSIPA ASC, IEEE, 2021, pp. 1499–1505.
- [141] H.K. Gajera, M.A. Zaveri, D.R. Nayak, Improving the performance of melanoma detection in dermoscopy images using deep CNN features, in: International Conference on Artificial Intelligence in Medicine, Springer, 2021, pp. 349–354.
- [142] A. Peter Soosai Anandaraj, V. Gomathy, A. Amali Angel Punitha, D. Abitha Kumari, S. Sheeba Rani, S. Sureshkumar, Internet of medical things (IoMT) enabled skin lesion detection and classification using optimal segmentation and restricted Boltzmann machines, in: Cognitive Internet of Medical Things for Smart Healthcare, Springer, 2021, pp. 195–209.
- [143] I. Filali, M. Belkadi, R. Aoudjit, M. Lalami, Graph weighting scheme for skin lesion segmentation in macroscopic images, *Biomed. Signal Process. Control* 68 (2021) 102710.
- [144] M. Osadebey, M. Pedersen, D. Waaler, Evaluation of color spaces for unsupervised and deep learning skin lesion segmentation, in: Proceedings of the IADIS International Conference Computer Graphics, Visualization, Computer Vision and Image Processing, IADIS Press, 2020.
- [145] E. Santos, R. Veras, H. Miguel, K. Aires, M.L. Claro, G.B. Junior, A skin lesion semi-supervised segmentation method, in: 2020 International Conference on Systems, Signals and Image Processing, IWSSIP, IEEE, 2020, pp. 33–38.
- [146] C. Huang, A. Yu, Y. Wang, H. He, Skin lesion segmentation based on mask R-CNN, in: 2020 International Conference on Virtual Reality and Visualization, ICVRV, IEEE, 2020, pp. 63–67.
- [147] Z.N. Khan, Frequency and spatial domain based saliency for pigmented skin lesion segmentation, 2020, arXiv:2010.04022.
- [148] K. Sanjar, O. Bekhzod, J. Kim, J. Kim, A. Paul, J. Kim, Improved U-Net: Fully convolutional network model for skin-lesion segmentation, *Appl. Sci.* 10 (10) (2020) 3658.
- [149] R. Wang, S. Chen, J. Fan, Y. Li, Cascaded context enhancement for automated skin lesion segmentation, 2020, arXiv:2004.08107.
- [150] B. Haftouf, A. Zitouni, A.C. Megherbi, S. Sbaa, A modified U-Net for skin lesion segmentation, in: 2020 1st International Conference on Communications, Control Systems and Signal Processing, CCSSP, IEEE, 2020, pp. 225–228.
- [151] O. Salih, S. Viriri, Skin lesion segmentation using local binary convolution-deconvolution architecture, *Image Anal. Stereol.* 39 (3) (2020) 169–185.
- [152] S. Nathan, P. Kansal, Lesion net-skin lesion segmentation using coordinate convolution and deep residual units, 2020, arXiv:2012.14249.
- [153] G. Ramella, Automatic skin lesion segmentation based on saliency and color, in: VISIGRAPP (4: VISAPP), 2020, pp. 452–459.
- [154] Y. Tang, Z. Fang, S. Yuan, Y. Xing, J.T. Zhou, F. Yang, et al., imscgnet: Iterative multi-scale context-guided segmentation of skin lesion in dermoscopic images, *IEEE Access* 8 (2020) 39700–39712.
- [155] K. Jayapriya, I.J. Jacob, Hybrid fully convolutional networks-based skin lesion segmentation and melanoma detection using deep feature, *Int. J. Imaging Syst. Technol.* 30 (2) (2020) 348–357.
- [156] A.R. Hawas, Y. Guo, C. Du, K. Polat, A.S. Ashour, OCE-NGC: A neutrosophic graph cut algorithm using optimized clustering estimation algorithm for dermoscopic skin lesion segmentation, *Appl. Soft Comput.* 86 (2020) 105931.
- [157] V. Ribeiro, S. Avila, E. Valle, Less is more: Sample selection and label conditioning improve skin lesion segmentation, in: Proceedings of the IEEE/CVF Conference on Computer Vision and Pattern Recognition Workshops, 2020, pp. 738–739.
- [158] Z. Al Nazi, T.A. Abir, Automatic skin lesion segmentation and melanoma detection: Transfer learning approach with u-net and dcnn-svm, in: Proceedings of International Joint Conference on Computational Intelligence, Springer, 2020, pp. 371–381.
- [159] M.P. Pour, H. Seker, Transform domain representation-driven convolutional neural networks for skin lesion segmentation, *Expert Syst. Appl.* 144 (2020) 113129.
- [160] F. Xie, J. Yang, J. Liu, Z. Jiang, Y. Zheng, Y. Wang, Skin lesion segmentation using high-resolution convolutional neural network, *Comput. Methods Programs Biomed.* 186 (2020) 105241.
- [161] R. Rout, P. Parida, Transition region based approach for skin lesion segmentation, *Procedia Comput. Sci.* 171 (2020) 379–388.
- [162] Z. Deng, Y. Xin, X. Qiu, Y. Chen, Weakly and semi-supervised deep level set network for automated skin lesion segmentation, in: Innovation in Medicine and Healthcare, Springer, 2020, pp. 145–155.
- [163] K. Qin, D. Sun, S. Zhang, H. Zhao, Asymmetric encode-decode network with two decoding paths for skin lesion segmentation, in: 2020 5th International Conference on Biomedical Imaging, Signal Processing, 2020, pp. 22–27.
- [164] M.A. Anjum, J. Amin, M. Sharif, H.U. Khan, M.S.A. Malik, S. Kadry, Deep semantic segmentation and multi-class skin lesion classification based on convolutional neural network, *IEEE Access* 8 (2020) 129668–129678.
- [165] K.B. Nampalle, B. Raman, An efficient approach for skin lesion segmentation using dermoscopic images: A deep learning approach, in: International Conference on Computer Vision and Image Processing, Springer, 2020, pp. 430–439.
- [166] K. Abhishek, G. Hamarneh, M.S. Drew, Illumination-based transformations improve skin lesion segmentation in dermoscopic images, in: Proceedings of the IEEE/CVF Conference on Computer Vision and Pattern Recognition Workshops, 2020, pp. 728–729.
- [167] D.N. Thanh, N.N. Hien, V. Surya Prasath, U. Erkan, A. Khamparia, Adaptive thresholding skin lesion segmentation with gabor filters and principal component analysis, in: Intelligent Computing in Engineering, Springer, 2020, pp. 811–820.
- [168] Z. Wei, F. Shi, H. Song, W. Ji, G. Han, Attentive boundary aware network for multi-scale skin lesion segmentation with adversarial training, *Multimedia Tools Appl.* 79 (37) (2020) 27115–27136.
- [169] Y. Jiang, S. Cao, S. Tao, H. Zhang, Skin lesion segmentation based on multi-scale attention convolutional neural network, *IEEE Access* 8 (2020) 122811–122825.

- [170] Y. Qiu, J. Cai, X. Qin, J. Zhang, Inferring skin lesion segmentation with fully connected CRFs based on multiple deep convolutional neural networks, *IEEE Access* 8 (2020) 144246–144258.
- [171] R. Kaymak, C. Kaymak, A. Ucar, Skin lesion segmentation using fully convolutional networks: A comparative experimental study, *Expert Syst. Appl.* 161 (2020) 113742.
- [172] H. Wu, J. Pan, Z. Li, Z. Wen, J. Qin, Automated skin lesion segmentation via an adaptive dual attention module, *IEEE Trans. Med. Imaging* 40 (1) (2020) 357–370.
- [173] M.K. Hasan, L. Dahal, P.N. Samarakoon, F.I. Tushar, R. Martí, DSNet: Automatic dermoscopic skin lesion segmentation, *Comput. Biol. Med.* 120 (2020) 103738.
- [174] R. Azad, M. Asadi-Aghbolaghi, M. Fathy, S. Escalera, Attention deeplabv3+: Multi-level context attention mechanism for skin lesion segmentation, in: European Conference on Computer Vision, Springer, 2020, pp. 251–266.
- [175] K. Zafar, S.O. Gilani, A. Waris, A. Ahmed, M. Jamil, M.N. Khan, A. Sohail Kashif, Skin lesion segmentation from dermoscopic images using convolutional neural network, *Sensors* 20 (6) (2020) 1601.
- [176] Ş. Öztürk, U. Özka, Skin lesion segmentation with improved convolutional neural network, *J. Digit. Imaging* 33 (4) (2020) 958–970.
- [177] Y. Xie, J. Zhang, Y. Xia, C. Shen, A mutual bootstrapping model for automated skin lesion segmentation and classification, *IEEE Trans. Med. Imaging* 39 (7) (2020) 2482–2493.
- [178] A. Mahbod, P. Tschandl, G. Langs, R. Ecker, I. Ellinger, The effects of skin lesion segmentation on the performance of dermatoscopic image classification, *Comput. Methods Programs Biomed.* 197 (2020) 105725.
- [179] P. Shan, Y. Wang, C. Fu, W. Song, J. Chen, Automatic skin lesion segmentation based on FC-DPN, *Comput. Biol. Med.* 123 (2020) 103762.
- [180] B. Lei, Z. Xia, F. Jiang, X. Jiang, Z. Ge, Y. Xu, J. Qin, S. Chen, T. Wang, S. Wang, Skin lesion segmentation via generative adversarial networks with dual discriminators, *Med. Image Anal.* 64 (2020) 101716.
- [181] A.W. Setiawan, Image segmentation metrics in skin lesion: Accuracy, sensitivity, specificity, dice coefficient, jaccard index, and matthews correlation coefficient, in: 2020 International Conference on Computer Engineering, Network, and Intelligent Multimedia, CENIM, IEEE, 2020, pp. 97–102.
- [182] A. Kamalakannan, S.S. Ganesan, G. Rajamanickam, Self-learning AI framework for skin lesion image segmentation and classification, 2020, arXiv:2001.05838.
- [183] Y. Wang, Y. Wei, X. Qian, L. Zhu, Y. Yang, DONet: Dual objective networks for skin lesion segmentation, 2020, arXiv:2008.08278.
- [184] A. Saha, P. Prasad, A. Thabit, Leveraging adaptive color augmentation in convolutional neural networks for deep skin lesion segmentation, in: 2020 IEEE 17th International Symposium on Biomedical Imaging, ISBI, IEEE, 2020, pp. 2014–2017.
- [185] L. Zhu, S. Feng, W. Zhu, X. Chen, ASNet: An adaptive scale network for skin lesion segmentation in dermoscopy images, in: Medical Imaging 2020: Biomedical Applications in Molecular, Structural, and Functional Imaging, Vol. 11317, International Society for Optics and Photonics, 2020, p. 113170W.
- [186] J. Zhang, C. Petitjean, S. Ainouz, Kappa loss for skin lesion segmentation in fully convolutional network, in: 2020 IEEE 17th International Symposium on Biomedical Imaging, ISBI, IEEE, 2020, pp. 2001–2004.
- [187] R. Iranpoor, A.S. Mahboob, S. Shahbandegan, N. Baniasadi, Skin lesion segmentation using convolutional neural networks with improved U-Net architecture, in: 2020 6th Iranian Conference on Signal Processing and Intelligent Systems, ICSPIS, IEEE, 2020, pp. 1–5.
- [188] M. Hajabdollahi, R. Esfandiarpoor, P. Khadivi, S.M.R. Soroushmehr, N. Karimi, S. Samavi, Simplification of neural networks for skin lesion image segmentation using color channel pruning, *Comput. Med. Imaging Graph.* 82 (2020) 101729.
- [189] S. Justin, M. Pattnaik, Skin lesion segmentation by pixel by pixel approach using deep learning, *Int. J. Adv. Signal Image Sci.* 6 (1) (2020) 12–20.
- [190] G.I. Sayed, G. Khoriba, M.H. Haggag, The novel multi-swarm coyote optimization algorithm for automatic skin lesion segmentation, *Evol. Intell.* (2020) 1–33.
- [191] M. Rizzi, C. Guaragnella, Skin lesion segmentation using image bit-plane multilayer approach, *Appl. Sci.* 10 (9) (2020) 3045.
- [192] N. Bansal, S. Sridhar, P.D. Priya, Improved skin lesion detection and segmentation by fusing texture and geometric features, *Int. J. Appl. Eng. Res.* 15 (12) (2020) 1116–1121.
- [193] P. Parida, R. Rout, Transition region based approach for skin lesion segmentation, *Electron. Lett. Comput. Vis. Image Anal.* 19 (1) (2020) 0028–0037.
- [194] V. Pillay, D. Hirasesen, S. Viriri, M.V. Gwetu, Macroscopic skin lesion segmentation using GrabCut, in: International Conference on Computational Collective Intelligence, Springer, 2020, pp. 528–539.
- [195] S. Sivaraj, R. Malmathanraj, P. Palanisamy, et al., Detecting anomalous growth of skin lesion using threshold-based segmentation algorithm and fuzzy K-nearest neighbor classifier, *J. Cancer Res. Ther.* 16 (1) (2020) 40.
- [196] P. Ganesan, B. Sathish, L.L. Joseph, HSL color space based skin lesion segmentation using fuzzy-based techniques, in: Advances in Electrical Control and Signal Systems, Springer, 2020, pp. 903–911.
- [197] Z. Liu, H. Pan, C. Gong, Z. Fan, Y. Wen, T. Jiang, R. Xiong, H. Li, Y. Wang, Multi-class skin lesion segmentation for cutaneous T-cell lymphomas on high-resolution clinical images, in: International Conference on Medical Image Computing and Computer-Assisted Intervention, Springer, 2020, pp. 351–361.
- [198] M. Low, V. Huang, P. Raina, Automating vitiligo skin lesion segmentation using convolutional neural networks, in: 2020 IEEE 17th International Symposium on Biomedical Imaging, ISBI, IEEE, 2020, pp. 1–4.
- [199] L. Agilandeswari, M. Sagar, N. Keerthana, Skin lesion detection using texture based segmentation and classification by convolutional neural networks (CNN), *Art Int. J. Innov. Technol. Explor. Eng.* 9 (2) (2019).
- [200] R. Javed, T. Saba, M. Shafry, M. Rahim, An intelligent saliency segmentation technique and classification of low contrast skin lesion dermoscopic images based on histogram decision, in: 2019 12th International Conference on Developments in ESystems Engineering, DeSE, IEEE, 2019, pp. 164–169.
- [201] M.A. Khan, T. Akram, M. Sharif, T. Saba, K. Javed, I.U. Lali, U.J. Tanik, A. Rehman, Construction of saliency map and hybrid set of features for efficient segmentation and classification of skin lesion, *Microsc. Res. Tech.* 82 (6) (2019) 741–763.
- [202] Y. Tang, F. Yang, S. Yuan, et al., A multi-stage framework with context information fusion structure for skin lesion segmentation, in: 2019 IEEE 16th International Symposium on Biomedical Imaging (ISBI 2019), IEEE, 2019, pp. 1407–1410.
- [203] V.K. Singh, M. Abdel-Nasser, H.A. Rashwan, F. Akram, N. Pandey, A. Lalande, B. Presles, S. Romani, D. Puig, FCA-net: Adversarial learning for skin lesion segmentation based on multi-scale features and factorized channel attention, *IEEE Access* 7 (2019) 130552–130565.
- [204] X. Wang, X. Jiang, H. Ding, J. Liu, Bi-directional dermoscopic feature learning and multi-scale consistent decision fusion for skin lesion segmentation, *IEEE Trans. Image Process.* 29 (2019) 3039–3051.
- [205] L. Huang, Y.-g. Zhao, T.-j. Yang, Skin lesion segmentation using object scale-oriented fully convolutional neural networks, *Signal Image Video Process.* 13 (3) (2019) 431–438.
- [206] R. Seeja, A. Suresh, Deep learning based skin lesion segmentation and classification of melanoma using support vector machine (SVM), *Asian Pac. J. Cancer Prev.* 20 (5) (2019) 1555.
- [207] M.A. Khan, M.I. Sharif, M. Raza, A. Anjum, T. Saba, S.A. Shad, Skin lesion segmentation and classification: A unified framework of deep neural network features fusion and selection, *Expert Syst.* (2019) e12497.
- [208] L. Zhang, G. Yang, X. Ye, Automatic skin lesion segmentation by coupling deep fully convolutional networks and shallow network with textons, *J. Med. Imaging* 6 (2) (2019) 024001.
- [209] S. Baghersalimi, B. Bozorgtabar, P. Schmid-Saugeon, H.K. Ekenel, J.-P. Thiran, DermoNet: densely linked convolutional neural network for efficient skin lesion segmentation, *EURASIP J. Image Video Process.* 2019 (1) (2019) 1–10.
- [210] P. Tang, Q. Liang, X. Yan, S. Xiang, W. Sun, D. Zhang, G. Coppola, Efficient skin lesion segmentation using separable-unet with stochastic weight averaging, *Comput. Methods Programs Biomed.* 178 (2019) 289–301.
- [211] D. Thanh, L. Thanh, S. Dvoenko, V. Prasath, N. San, Adaptive thresholding segmentation method for skin lesion with normalized color channels of NTSC and ycbcr, in: International Conference on Pattern Recognition and Information Processing, PRIP’2019, Minsk, 2019.
- [212] M. Hasan, B. Alyafi, F.I. Tushar, et al., Comparative analysis of automatic skin lesion segmentation with two different implementations, 2019, arXiv: 1904.03075.
- [213] S. Saini, D. Gupta, A.K. Tiwari, Detector-SegMentor network for skin lesion localization and segmentation, in: National Conference on Computer Vision, Pattern Recognition, Image Processing, and Graphics, Springer, 2019, pp. 589–599.
- [214] S. Rawas, A. El-Zaart, HCET-G 2: dermoscopic skin lesion segmentation via hybrid cross entropy thresholding using Gaussian and gamma distributions, in: 2019 Third International Conference on Intelligent Computing in Data Sciences, ICDS, IEEE, 2019, pp. 1–7.
- [215] E. Alfaro, X.B. Fonseca, E.M. Albornoz, C.E. Martínez, S.C. Ramrez, A brief analysis of u-net and mask r-cnn for skin lesion segmentation, in: 2019 IEEE International Work Conference on Bioinspired Intelligence, IWOBI, IEEE, 2019, pp. 000123–000126.
- [216] M.A. Al-Masni, M.A. Al-Antari, H.M. Park, N.H. Park, T.-S. Kim, A deep learning model integrating FrCN and residual convolutional networks for skin lesion segmentation and classification, in: 2019 IEEE Eurasia Conference on Biomedical Engineering, Healthcare and Sustainability, ECBIOS, IEEE, 2019, pp. 95–98.
- [217] A. Soudani, W. Barhoumi, An image-based segmentation recommender using crowdsourcing and transfer learning for skin lesion extraction, *Expert Syst. Appl.* 118 (2019) 400–410.
- [218] M. Goyal, J. Ng, A. Oakley, M.H. Yap, Skin lesion boundary segmentation with fully automated deep extreme cut methods, in: Medical Imaging 2019: Biomedical Applications in Molecular, Structural, and Functional Imaging, Vol. 10953, International Society for Optics and Photonics, 2019, p. 109530Q.
- [219] H. Wang, G. Wang, Z. Sheng, S. Zhang, Automated segmentation of skin lesion based on pyramid attention network, in: International Workshop on Machine Learning in Medical Imaging, Springer, 2019, pp. 435–443.

- [220] D. Ma, H. Wu, J. Sun, C. Yu, L. Liu, A light-weight context-aware self-attention model for skin lesion segmentation, in: Pacific Rim International Conference on Artificial Intelligence, Springer, 2019, pp. 501–505.
- [221] X. Liu, G. Hu, X. Ma, H. Kuang, An enhanced neural network based on deep metric learning for skin lesion segmentation, in: 2019 Chinese Control and Decision Conference, CCDC, IEEE, 2019, pp. 1633–1638.
- [222] G.G. De Angelo, A.G. Pacheco, R.A. Krohling, Skin lesion segmentation using deep learning for images acquired from smartphones, in: 2019 International Joint Conference on Neural Networks, IJCNN, IEEE, 2019, pp. 1–8.
- [223] L. Song, J. Lin, Z.J. Wang, H. Wang, Dense-residual attention network for skin lesion segmentation, in: International Workshop on Machine Learning in Medical Imaging, Springer, 2019, pp. 319–327.
- [224] F. Jiang, F. Zhou, J. Qin, T. Wang, B. Lei, Decision-augmented generative adversarial network for skin lesion segmentation, in: 2019 IEEE 16th International Symposium on Biomedical Imaging, ISBI 2019, IEEE, 2019, pp. 447–450.
- [225] A. Adegun, S. Virir, Deep learning model for skin lesion segmentation: Fully convolutional network, in: International Conference on Image Analysis and Recognition, Springer, 2019, pp. 232–242.
- [226] M.M.K. Sarker, H.A. Rashwan, F. Akram, V.K. Singh, S.F. Banu, F.U. Chowdhury, K.A. Choudhury, S. Chambon, P. Radeva, D. Puig, et al., SLSNet: Skin lesion segmentation using a lightweight generative adversarial network, *Expert Syst. Appl.* (2021) 115433.
- [227] L. Bi, D. Feng, M. Fulham, J. Kim, Improving skin lesion segmentation via stacked adversarial learning, in: 2019 IEEE 16th International Symposium on Biomedical Imaging, ISBI 2019, IEEE, 2019, pp. 1100–1103.
- [228] Q.C. Ninh, T.-T. Tran, T.T. Tran, T.A.X. Tran, V.-T. Pham, Skin lesion segmentation based on modification of SegNet neural networks, in: 2019 6th NAFOSTED Conference on Information and Computer Science, NICS, IEEE, 2019, pp. 575–578.
- [229] V. Ribeiro, S. Avila, E. Valle, Handling inter-annotator agreement for automated skin lesion segmentation, 2019, [arXiv:1906.02415](https://arxiv.org/abs/1906.02415).
- [230] L. Liu, L. Mou, X.X. Zhu, M. Mandal, Skin lesion segmentation based on improved U-Net, in: 2019 IEEE Canadian Conference of Electrical and Computer Engineering, CCECE, IEEE, 2019, pp. 1–4.
- [231] D.N. Thanh, U. Erkan, V.S. Prasath, V. Kumar, N.N. Hien, A skin lesion segmentation method for dermoscopic images based on adaptive thresholding with normalization of color models, in: 2019 6th International Conference on Electrical and Electronics Engineering, ICEEEE, IEEE, 2019, pp. 116–120.
- [232] W. Tu, X. Liu, W. Hu, Z. Pan, Dense-residual network with adversarial learning for skin lesion segmentation, *IEEE Access* 7 (2019) 77037–77051.
- [233] H.M. Ünver, E. Ayan, Skin lesion segmentation in dermoscopic images with combination of YOLO and grabcut algorithm, *Diagnostics* 9 (3) (2019) 72.
- [234] D. Bisla, A. Choromanska, J.A. Stein, D. Polksky, R. Berman, Skin lesion segmentation and classification with deep learning system, 2019, pp. 1–6, [arXiv:1902.06061](https://arxiv.org/abs/1902.06061).
- [235] P. Tschandl, C. Sinz, H. Kittler, Domain-specific classification-pretrained fully convolutional network encoders for skin lesion segmentation, *Comput. Biol. Med.* 104 (2019) 111–116.
- [236] Z. Wei, H. Song, L. Chen, Q. Li, G. Han, Attention-based DenseUnet network with adversarial training for skin lesion segmentation, *IEEE Access* 7 (2019) 136616–136629.
- [237] P.-f. Shan, Y.-d. Wang, C. Fu, Improving skin lesion segmentation with deep convolutional generative adversarial networks, in: International Conference on Frontier Computing, Springer, 2019, pp. 138–147.
- [238] O. Salih, S. Virir, Skin lesion segmentation techniques based on Markov random field, in: International Conference on Mining Intelligence and Knowledge Exploration, Springer, 2019, pp. 210–220.
- [239] Z. Cui, L. Wu, R. Wang, W.-S. Zheng, Ensemble transductive learning for skin lesion segmentation, in: Chinese Conference on Pattern Recognition and Computer Vision, PRCV, Springer, 2019, pp. 572–581.
- [240] A.H. Shahin, K. Amer, M.A. Elattar, Deep convolutional encoder-decoders with aggregated multi-resolution skip connections for skin lesion segmentation, in: 2019 IEEE 16th International Symposium on Biomedical Imaging, ISBI 2019, IEEE, 2019, pp. 451–454.
- [241] A.-R. Ali, J. Li, T. Trappenberg, Supervised versus unsupervised deep learning based methods for skin lesion segmentation in dermoscopy images, in: Canadian Conference on Artificial Intelligence, Springer, 2019, pp. 373–379.
- [242] J. Wu, E.Z. Chen, R. Rong, X. Li, D. Xu, H. Jiang, Skin lesion segmentation with C-UNet, in: 2019 41st Annual International Conference of the IEEE Engineering in Medicine and Biology Society, EMBC, IEEE, 2019, pp. 2785–2788.
- [243] R. Ali, R.C. Hardie, M.S. De Silva, T.M. Kebede, Skin lesion segmentation and classification for ISIC 2018 by combining deep CNN and handcrafted features, 2019, [arXiv:1908.05730](https://arxiv.org/abs/1908.05730).
- [244] J. Lameski, A. Jovanov, E. Zdravevski, P. Lameski, S. Gievaska, Skin lesion segmentation with deep learning, in: IEEE EUROCON 2019-18th International Conference on Smart Technologies, IEEE, 2019, pp. 1–5.
- [245] S.N. Hasan, M. Gezer, R.A. Azeez, S. Gülsen, Skin lesion segmentation by using deep learning techniques, in: 2019 Medical Technologies Congress, TIPTEKNO, IEEE, 2019, pp. 1–4.
- [246] L. Canalini, F. Pollastri, F. Bolelli, M. Cancilla, S. Allegretti, C. Grana, Skin lesion segmentation ensemble with diverse training strategies, in: International Conference on Computer Analysis of Images and Patterns, Springer, 2019, pp. 89–101.
- [247] M.H. Aljanabi, F.A. Jumaa, A.O. Aftan, M.S.S. Alkafaji, N. Alani, Z.H. Al-Tameemi, D.H. Al-Mamoori, Various types of skin tumors lesion medical imaging (STLM) of healthy and unhealthy moles a review and computational of: Segmentation, classification, methods and algorithms, in: IOP Conference Series: Materials Science and Engineering, Vol. 518, IOP Publishing, 2019, p. 052014.
- [248] W.S. Ooi, B.E. Khoo, C.P. Lim, An interactive evolutionary multi-objective approach to skin lesion segmentation, in: 10th International Conference on Robotics, Vision, Signal Processing and Power Applications, Springer, Singapore, 2019, pp. 641–647.
- [249] O. Bingöl, S. Paçacı, U. Güvenç, Entropy-based skin lesion segmentation using stochastic fractal search algorithm, in: The International Conference on Artificial Intelligence and Applied Mathematics in Engineering, Springer, 2019, pp. 801–811.
- [250] P. Brahmbhatt, S.N. Rajan, Skin lesion segmentation using SegNet with binary cross-entropy, in: International Conference on Artificial Intelligence and Speech Technology, AIST2019, Vol. 14, 2019, p. 15th.
- [251] H.N. Abdullah, H.K. Abduljaleel, Deep CNN based skin lesion image denoising and segmentation using active contour method, *Eng. Technol. J.* 37 (11A) (2019) 464–469.
- [252] T. Yang, Y. Chen, J. Lu, Z. Fan, Sampling with level set for pigmented skin lesion segmentation, *Signal Image Video Process.* 13 (4) (2019) 813–821.
- [253] Y. Filali, S. Abdellouahed, A. Aarab, An improved segmentation approach for skin lesion classification, *Stat. Optim. Inf. Comput.* 7 (2) (2019) 456–467.
- [254] I. Filali, M. Belkadi, Multi-scale contrast based skin lesion segmentation in digital images, *Optik* 185 (2019) 794–811.
- [255] S. Sengupta, N. Mittal, M. Modi, Segmentation of skin lesion images using fudge factor based techniques, in: Advances in Interdisciplinary Engineering, Springer, 2019, pp. 837–846.
- [256] I. Bhakta, S. Phadikar, K. Majumder, A. Sau, S. Chowdhuri, Tsalli's entropy-based segmentation method for accurate Pigmented skin lesion identification, *IETE J. Res.* (2019) 1–17.
- [257] M. Dash, N.D. Londhe, S. Ghosh, A. Semwal, R.S. Sonawane, PsLSNet: Automated psoriasis skin lesion segmentation using modified U-Net-based fully convolutional network, *Biomed. Signal Process. Control* 52 (2019) 226–237.
- [258] F. Riaz, S. Naeem, R. Nawaz, M. Coimbra, Active contours based segmentation and lesion periphery analysis for characterization of skin lesions in dermoscopy images, *IEEE J. Biomed. Health Inf.* 23 (2) (2018) 489–500.
- [259] J. Burdick, O. Marques, J. Weintal, B. Furht, Rethinking skin lesion segmentation in a convolutional classifier, *J. Digit. Imaging* 31 (4) (2018) 435–440.
- [260] X. He, Z. Yu, T. Wang, B. Lei, Y. Shi, Dense deconvolution net: Multi path fusion and dense deconvolution for high resolution skin lesion segmentation, *Technol. Health Care* 26 (S1) (2018) 307–316.
- [261] S.S. Kolekar, P.G. Magdum, Skin lesion semantic segmentation using convolutional encoder decoder architecture, in: 2018 Fourth International Conference on Computing Communication Control and Automation, ICCUBEA, IEEE, 2018, pp. 1–3.
- [262] O.O. Olugbara, T.B. Taiwo, D. Heukelman, Segmentation of melanoma skin lesion using perceptual color difference saliency with morphological analysis, *Math. Probl. Eng.* 2018 (2018).
- [263] T. Akram, M.A. Khan, M. Sharif, M. Yasmin, Skin lesion segmentation and recognition using multichannel saliency estimation and M-SVM on selected serially fused features, *J. Ambient Intell. Humaniz. Comput.* (2018) 1–20.
- [264] M.A. Khan, T. Akram, M. Sharif, A. Shahzad, K. Aurangzeb, M. Alhussein, S.I. Haider, A. Altamrah, An implementation of normal distribution based segmentation and entropy controlled features selection for skin lesion detection and classification, *BMC Cancer* 18 (1) (2018) 1–20.
- [265] H. Li, X. He, F. Zhou, Z. Yu, D. Ni, S. Chen, T. Wang, B. Lei, Dense deconvolutional network for skin lesion segmentation, *IEEE J. Biomed. Health Inf.* 23 (2) (2018) 527–537.
- [266] M. Aljanabi, Y.E. Özok, J. Rahebi, A.S. Abdullah, Skin lesion segmentation method for dermoscopy images using artificial bee colony algorithm, *Symmetry* 10 (8) (2018) 347.
- [267] H. Li, X. He, Z. Yu, F. Zhou, J.-Z. Cheng, L. Huang, T. Wang, B. Lei, Skin lesion segmentation via dense connected deconvolutional network, in: 2018 24th International Conference on Pattern Recognition, ICPR, IEEE, 2018, pp. 671–675.
- [268] S. Vesal, S.M. Patil, N. Ravikumar, A.K. Maier, A multi-task framework for skin lesion detection and segmentation, in: OR 2.0 Context-Aware Operating Theaters, Computer Assisted Robotic Endoscopy, Clinical Image-Based Procedures, and Skin Image Analysis, Springer, 2018, pp. 285–293.
- [269] X. Li, L. Yu, H. Chen, C.-W. Fu, P.-A. Heng, Semi-supervised skin lesion segmentation via transformation consistent self-ensembling model, 2018, [arXiv:1808.03887](https://arxiv.org/abs/1808.03887).

- [270] S. Vesal, N. Ravikumar, A. Maier, Skinnet: A deep learning framework for skin lesion segmentation, in: 2018 IEEE Nuclear Science Symposium and Medical Imaging Conference Proceedings, NSS/MIC, IEEE, 2018, pp. 1–3.
- [271] Z. Mirikhraji, S. Izadi, J. Kawahara, G. Hamarneh, Deep auto-context fully convolutional neural network for skin lesion segmentation, in: 2018 IEEE 15th International Symposium on Biomedical Imaging, ISBI 2018, IEEE, 2018, pp. 877–880.
- [272] G. Venkatesh, Y. Naresh, S. Little, N.E. O'Connor, A deep residual architecture for skin lesion segmentation, in: OR 2.0 Context-Aware Operating Theaters, Computer Assisted Robotic Endoscopy, Clinical Image-Based Procedures, and Skin Image Analysis, Springer, 2018, pp. 277–284.
- [273] Y. Yuan, Automatic skin lesion segmentation with fully convolutional-deconvolutional networks, 2017, arXiv:1703.05165.
- [274] S.M. Jaisakthi, P. Mirunalini, C. Aravindan, Automated skin lesion segmentation of dermoscopic images using GrabCut and k-means algorithms, IET Comput. Vis. 12 (8) (2018) 1088–1095.
- [275] G. Zeng, G. Zheng, Multi-scale fully convolutional DenseNets for automated skin lesion segmentation in dermoscopy images, in: International Conference Image Analysis and Recognition, Springer, 2018, pp. 513–521.
- [276] S. Chen, Z. Wang, J. Shi, B. Liu, N. Yu, A multi-task framework with feature passing module for skin lesion classification and segmentation, in: 2018 IEEE 15th International Symposium on Biomedical Imaging, ISBI 2018, IEEE, 2018, pp. 1126–1129.
- [277] N.-Q. Nguyen, ISIC 2017 skin lesion segmentation using deep encoder-decoder network, 2018, arXiv:1807.09083.
- [278] M. Ammar, S.G. Khawaja, A. Atif, M.U. Akram, M. Sakeena, Learning based segmentation of skin lesion from dermoscopic images, in: 2018 IEEE 20th International Conference on E-Health Networking, Applications and Services, Healthcom, IEEE, 2018, pp. 1–6.
- [279] A. Youssef, D.D. Bloisi, M. Muscio, A. Pennisi, D. Nardi, A. Facchiano, Deep convolutional pixel-wise labeling for skin lesion image segmentation, in: 2018 IEEE International Symposium on Medical Measurements and Applications, MeMeA, IEEE, 2018, pp. 1–6.
- [280] S. Ross-Howe, H.R. Tizhoosh, The effects of image pre-and post-processing, wavelet decomposition, and local binary patterns on U-Nets for skin lesion segmentation, in: 2018 International Joint Conference on Neural Networks, IJCNN, IEEE, 2018, pp. 1–8.
- [281] D. Patiño, J. Avendaño, J.W. Branch, Automatic skin lesion segmentation on dermoscopic images by the means of superpixel merging, in: International Conference on Medical Image Computing and Computer-Assisted Intervention, Springer, 2018, pp. 728–736.
- [282] F. Navarro, M. Escudero-Vinolo, J. Bescós, Accurate segmentation and registration of skin lesion images to evaluate lesion change, IEEE J. Biomed. Health Inf. 23 (2) (2018) 501–508.
- [283] H. Jiang, R. Rong, J. Wu, X. Li, X. Dong, E.Z. Chen, Skin lesion segmentation with improved C-UNet networks, BioRxiv (2018) 382549.
- [284] F. Guth, T.E. deCampos, Skin lesion segmentation using U-Net and good training strategies, 2018, arXiv:1811.11314.
- [285] H. Xu, T.H. Hwang, Automatic skin lesion segmentation using deep fully convolutional networks, 2018, arXiv:1807.06466.
- [286] Y. Wang, S. Sun, J. Yu, et al., Skin lesion segmentation using atrous convolution via DeepLab V3, 2018, arXiv:1807.08891.
- [287] L. Bi, D. Feng, J. Kim, Improving automatic skin lesion segmentation using adversarial learning based data augmentation, 2018, arXiv:1807.08392.
- [288] C. Qian, T. Liu, H. Jiang, Z. Wang, P. Wang, M. Guan, B. Sun, A detection and segmentation architecture for skin lesion segmentation on dermoscopy images, 2018, arXiv:1809.03917.
- [289] A. Bissoto, F. Perez, V. Ribeiro, M. Fornaciali, S. Avila, E. Valle, Deep-learning ensembles for skin-lesion segmentation, analysis, classification: RECOD titans at ISIC challenge 2018, 2018, arXiv:1808.08480.
- [290] S. Louhichi, M. Gzara, H.B. Abdallah, Skin lesion segmentation using multiple density clustering algorithm MDCUT and region growing, in: 2018 IEEE/ACIS 17th International Conference on Computer and Information Science, ICIS, IEEE, 2018, pp. 74–79.
- [291] K. Hu, S. Liu, Y. Zhang, C. Cao, F. Xiao, W. Huang, X. Gao, A skin lesion segmentation method based on saliency and adaptive thresholding in wavelet domain, in: International Symposium on Artificial Intelligence and Robotics, Springer, 2018, pp. 445–453.
- [292] M. Nasir, M. Attique Khan, M. Sharif, I.U. Lali, T. Saba, T. Iqbal, An improved strategy for skin lesion detection and classification using uniform segmentation and feature selection based approach, Microsc. Res. Tech. 81 (6) (2018) 528–543.
- [293] A.P. Chakkavarthy, A. Chandrasekar, An automatic segmentation of skin lesion from dermoscopy images using watershed segmentation, in: 2018 International Conference on Recent Trends in Electrical, Control and Communication, RTECC, IEEE, 2018, pp. 15–18.
- [294] W. Luo, M. Yang, Fast skin lesion segmentation via fully convolutional network with residual architecture and CRF, in: 2018 24th International Conference on Pattern Recognition, ICPR, IEEE, 2018, pp. 1438–1443.
- [295] I. Ahmed, Q.N.u. Rehman, G. Masood, A. Adnan, A. Ahmad, S. Rho, Segmentation of affected skin lesion with blind deconvolution and 1st ast b colour space, in: Proceedings of the 33rd Annual ACM Symposium on Applied Computing, 2018, pp. 634–639.
- [296] O. Salih, S. Viriri, Skin lesion segmentation using enhanced unified Markov random field, in: International Conference on Mining Intelligence and Knowledge Exploration, Springer, 2018, pp. 331–340.
- [297] N.C. Lynn, Z.M. Kyu, Segmentation and classification of skin cancer melanoma from skin lesion images, in: 2017 18th International Conference on Parallel and Distributed Computing, Applications and Technologies, PDCAT, IEEE, 2017, pp. 117–122.
- [298] M.P. Pour, H. Seker, L. Shao, Automated lesion segmentation and dermoscopic feature segmentation for skin cancer analysis, in: 2017 39th Annual International Conference of the IEEE Engineering in Medicine and Biology Society, EMBC, IEEE, 2017, pp. 640–643.
- [299] B. Bozorgtabar, Z. Ge, R. Chakravorty, M. Abedini, S. Demyanov, R. Garnavi, Investigating deep side layers for skin lesion segmentation, in: 2017 IEEE 14th International Symposium on Biomedical Imaging, ISBI 2017, IEEE, 2017, pp. 256–260.
- [300] X. He, Z. Yu, T. Wang, B. Lei, Skin lesion segmentation via deep RefineNet, in: Deep Learning in Medical Image Analysis and Multimodal Learning for Clinical Decision Support, Springer, 2017, pp. 303–311.
- [301] B. Bozorgtabar, S. Sedai, P.K. Roy, R. Garnavi, Skin lesion segmentation using deep convolution networks guided by local unsupervised learning, IBM J. Res. Dev. 61 (4/5) (2017) 1–6.
- [302] L. Bi, J. Kim, E. Ahn, D. Feng, M. Fulham, Semi-automatic skin lesion segmentation via fully convolutional networks, in: 2017 IEEE 14th International Symposium on Biomedical Imaging, ISBI 2017, IEEE, 2017, pp. 561–564.
- [303] D. Ramachandran, G.W. Taylor, Skin lesion segmentation using deep hypercolumn descriptors, J. Comput. Vis. Imaging Syst. 3 (1) (2017).
- [304] D. Alvarez, M. Iglesias, k-means clustering and ensemble of regressions: an algorithm for the ISIC 2017 skin lesion segmentation challenge, 2017, arXiv: 1702.07333.
- [305] J. Qi, M. Le, C. Li, P. Zhou, Global and local information based deep network for skin lesion segmentation, 2017, arXiv:1703.05467.
- [306] S. Jaisakthi, A. Chandrabose, P. Mirunalini, Automatic skin lesion segmentation using semi-supervised learning technique, 2017, arXiv:1703.04301.
- [307] R. Mishra, O. Daescu, Deep learning for skin lesion segmentation, in: 2017 IEEE International Conference on Bioinformatics and Biomedicine, BIBM, IEEE, 2017, pp. 1189–1194.
- [308] B.S. Lin, K. Michael, S. Kalra, H.R. Tizhoosh, Skin lesion segmentation: U-Nets versus clustering, in: 2017 IEEE Symposium Series on Computational Intelligence, SSC, IEEE, 2017, pp. 1–7.
- [309] A. Pardo, E. Real, G. Fernandez-Barreras, F. Madruga, J. López-Higuera, O. Conde, Automated skin lesion segmentation with kernel density estimation, in: European Conference on Biomedical Optics, Optical Society of America, 2017, p. 104110P.
- [310] E. Nasr-Esfahani, S. Rafiei, M.H. Jafari, N. Karimi, J.S. Wrobel, S. Soroushmehr, S. Samavi, K. Najarian, Dense fully convolutional network for skin lesion segmentation, 2017, arXiv:1712.10207.
- [311] C.E. Martínez, E.M. Albornoz, Pigmented skin lesion segmentation based on sparse texture representations, in: 12th International Symposium on Medical Information Processing and Analysis, Vol. 10160, International Society for Optics and Photonics, 2017, p. 101600N.
- [312] A. Gupta, A. Issac, M.K. Dutta, H.-H. Hsu, Adaptive thresholding for skin lesion segmentation using statistical parameters, in: 2017 31st International Conference on Advanced Information Networking and Applications Workshops, WAINA, IEEE, 2017, pp. 616–620.
- [313] A. Agarwal, A. Issac, M.K. Dutta, K. Riha, V. Uher, Automated skin lesion segmentation using K-means clustering from digital dermoscopic images, in: 2017 40th International Conference on Telecommunications and Signal Processing, TSP, IEEE, 2017, pp. 743–748.
- [314] Y.M. George, M. Aldeen, R. Garnavi, Automatic psoriasis lesion segmentation in two-dimensional skin images using multiscale superpixel clustering, J. Med. Imaging 4 (4) (2017) 044004.
- [315] B. Bozorgtabar, M. Abedini, R. Garnavi, Sparse coding based skin lesion segmentation using dynamic rule-based refinement, in: International Workshop on Machine Learning in Medical Imaging, Springer, 2016, pp. 254–261.
- [316] T. Majtner, K. Lidayova, S. Yildirim-Yayiglan, J.Y. Hardeberg, Improving skin lesion segmentation in dermoscopic images by thin artefacts removal methods, in: 2016 6th European Workshop on Visual Information Processing, EUVIP, IEEE, 2016, pp. 1–6.
- [317] M. Hassan, M. Hossny, S. Nahavandi, A. Yazdabadi, Skin lesion segmentation using gray level co-occurrence matrix, in: 2016 IEEE International Conference on Systems, Man, and Cybernetics, SMC, IEEE, 2016, pp. 000820–000825.
- [318] R. Kasmi, K. Mokrani, R. Rader, J. Cole, W. Stoecker, Biologically inspired skin lesion segmentation using a geodesic active contour technique, Skin Res. Technol. 22 (2) (2016) 208–222.
- [319] S. Khalid, U. Jamil, K. Saleem, M.U. Akram, W. Manzoor, W. Ahmed, A. Sohail, Segmentation of skin lesion using Cohen-Daubechies-Feauveau biorthogonal wavelet, SpringerPlus 5 (1) (2016) 1–17.

- [320] S. Joseph, J.R. Panicker, Skin lesion analysis system for melanoma detection with an effective hair segmentation method, in: 2016 International Conference on Information Science, ICIS, IEEE, 2016, pp. 91–96.
- [321] L. Bi, J. Kim, E. Ahn, D. Feng, M. Fulham, Automated skin lesion segmentation via image-wise supervised learning and multi-scale superpixel based cellular automata, in: 2016 IEEE 13th International Symposium on Biomedical Imaging, ISBI, IEEE, 2016, pp. 1059–1062.
- [322] A. Pennisi, D.D. Bloisi, D. Nardi, A.R. Giampetrucci, C. Mondino, A. Facchiano, Skin lesion image segmentation using Delaunay Triangulation for melanoma detection, *Comput. Med. Imaging Graph.* 52 (2016) 89–103.
- [323] C. Sagar, L.M. Saini, Color channel based segmentation of skin lesion from clinical images for the detection of melanoma, in: 2016 IEEE 1st International Conference on Power Electronics, Intelligent Control and Energy Systems, ICPEICES, IEEE, 2016, pp. 1–5.
- [324] A. Ortega-Martinez, J.P. Padilla-Martinez, W. Franco, Statistical image segmentation for the detection of skin lesion borders in UV fluorescence excitation, in: Imaging, Manipulation, and Analysis of Biomolecules, Cells, and Tissues IX, Vol. 9711, International Society for Optics and Photonics, 2016, p. 97111B.
- [325] G.M. Azehouen-Pazou, K.M. Assogba, H. Adegbidi, A novel approach of black skin lesion images segmentation based on MLP neural network, in: 2016 International Conference on Bio-Engineering for Smart Technologies, BioSMART, IEEE, 2016, pp. 1–4.
- [326] N.F.M. Azmi, H.M. Sarkan, Y. Yahya, S. Chuprat, Abcd rules segmentation on malignant tumor and benign skin lesion images, in: 2016 3rd International Conference on Computer and Information Sciences, ICCOINS, IEEE, 2016, pp. 66–70.
- [327] F. Torkashvand, M. Fartash, Automatic segmentation of skin lesion using Markov random field, *Can. J. Basic Appl. Sci.* 3 (3) (2015) 93–107.
- [328] F. Rashid Sheykhamad, N. Razmjoo, M. Ramezani, A novel method for skin lesion segmentation, *Int. J. Informat. Secur. Syst. Manag.* 4 (2) (2015) 458–466.
- [329] J. Pereira, A. Mendes, C. Nogueira, D. Baptista, R. Fonseca-Pinto, An adaptive approach for skin lesion segmentation in dermoscopy images using a multiscale local normalization, in: Dynamics, Games and Science, Springer, 2015, pp. 537–545.
- [330] O. Trabelsi, L. Tlig, M. Sayadi, F. Fnaiech, Skin lesion segmentation using the DS evidence theory based on the FCM using feature parameters, in: 2015 IEEE 12th International Multi-Conference on Systems, Signals & Devices, SSD15, IEEE, 2015, pp. 1–5.
- [331] J. Yasmin, M. Sathik, An improved iterative segmentation algorithm using canny edge detector for skin lesion border detection., *Int. Arab J. Inf. Technol.* 12 (4) (2015).
- [332] S.S. Khattak, G. Saman, I. Khan, A. Salam, Maximum entropy based image segmentation of human skin lesion, *World Acad. Sci. Eng. Technol. Int. J. Comp. Elect. Autom. Cont. Info. Eng.* 9 (5) (2015) 1094–1098.
- [333] A.A. Abbas, X. Guo, W.-H. Tan, H. Jalab, Combined spline and B-spline for an improved automatic skin lesion segmentation in dermoscopic images using optimal color channel, *J. Med. Syst.* 38 (8) (2014) 1–8.
- [334] A.A.A. Al-abayechia, X. Guoa, W.-H. Tana, H.A. Jalabc, Automatic skin lesion segmentation with optimal colour channel from dermoscopic images, *Sci. Asia* 40 (1) (2014) 1–7.
- [335] O. Lézoray, M. Revenu, M. Desvignes, Graph-based skin lesion segmentation of multispectral dermoscopic images, in: 2014 IEEE International Conference on Image Processing, ICIP, IEEE, 2014, pp. 897–901.
- [336] Y.K. Ch'ng, H. Nisar, V.V. Yap, J.J. Tang, A two level k-means segmentation technique for eczema skin lesion segmentation using class specific criteria, in: 2014 IEEE Conference on Biomedical Engineering and Sciences, IECBES, IEEE, 2014, pp. 985–990.
- [337] K. Jyothilakshmi, J. Jeeva, Detection of malignant skin diseases based on the lesion segmentation, in: Proc. International Conference on Communications and Signal Processing, ICCSP, 2014, pp. 382–386.
- [338] A. Masood, A.A. Al-Jumaily, Integrating soft and hard threshold selection algorithms for accurate segmentation of skin lesion, in: 2nd Middle East Conference on Biomedical Engineering, IEEE, 2014, pp. 83–86.
- [339] A. Amelio, C. Pizzuti, Skin lesion image segmentation using a color genetic algorithm, in: Proceedings of the 15th Annual Conference Companion on Genetic and Evolutionary Computation, 2013, pp. 1471–1478.
- [340] H. Nisar, Y.K. Ch'ng, T.Y. Chew, V.V. Yap, K.H. Yeap, J.J. Tang, A color space study for skin lesion segmentation, in: 2013 IEEE International Conference on Circuits and Systems, ICCAS, IEEE, 2013, pp. 172–176.
- [341] Y. Wu, F. Xie, Z. Jiang, R. Meng, Automatic skin lesion segmentation based on supervised learning, in: 2013 Seventh International Conference on Image and Graphics, IEEE, 2013, pp. 164–169.
- [342] A.A. Abbas, W.-H. Tan, An improved automatic segmentation skin lesion from dermoscopic images using optimal RGB channel, in: Conference on Computer Science & Computational Mathematics, ICCSCM 2013, Vol. 39, 2013.
- [343] S. Khakabi, P. Wighton, T.K. Lee, M.S. Atkins, Multi-level feature extraction for skin lesion segmentation in dermoscopic images, in: Medical Imaging 2012: Computer-Aided Diagnosis, Vol. 8315, International Society for Optics and Photonics, 2012, p. 83150E.
- [344] A. Madooei, M.S. Drew, M. Sadeghi, M.S. Atkins, Automated pre-processing method for dermoscopic images and its application to pigmented skin lesion segmentation, in: Color and Imaging Conference, Vol. 2012, Society for Imaging Science and Technology, 2012, pp. 158–163.
- [345] M. Ivanovici, D. Stoica, Color diffusion model for active contours-an application to skin lesion segmentation, in: 2012 Annual International Conference of the IEEE Engineering in Medicine and Biology Society, IEEE, 2012, pp. 5347–5350.
- [346] Y. He, F. Xie, Automatic skin lesion segmentation based on texture analysis and supervised learning, in: Asian Conference on Computer Vision, Springer, 2012, pp. 330–341.
- [347] G. Schaefer, M.I. Rajab, M.E. Celebi, H. Iyatomi, Colour and contrast enhancement for improved skin lesion segmentation, *Comput. Med. Imaging Graph.* 35 (2) (2011) 99–104.
- [348] H. Zhou, G. Schaefer, M.E. Celebi, F. Lin, T. Liu, Gradient vector flow with mean shift for skin lesion segmentation, *Comput. Med. Imaging Graph.* 35 (2) (2011) 121–127.
- [349] A. Wong, J. Scharcanski, P. Fieguth, Automatic skin lesion segmentation via iterative stochastic region merging, *IEEE Trans. Inf. Technol. Biomed.* 15 (6) (2011) 929–936.
- [350] X. Li, B. Aldridge, R. Fisher, J. Rees, Estimating the ground truth from multiple individual segmentations incorporating prior pattern analysis with application to skin lesion segmentation, in: 2011 IEEE International Symposium on Biomedical Imaging: From Nano to Macro, IEEE, 2011, pp. 1438–1441.
- [351] K.M. Hosny, M.A. Kassem, Refined residual deep convolutional network for skin lesion classification, *J. Digit. Imaging* 35 (2) (2022) 258–280.
- [352] F. Afza, M. Sharif, M. Mittal, M.A. Khan, D.J. Hemanth, A hierarchical three-step superpixels and deep learning framework for skin lesion classification, *Methods* 202 (2022) 88–102.
- [353] X. He, Y. Wang, S. Zhao, C. Yao, Deep metric attention learning for skin lesion classification in dermoscopy images, *Complex Intell. Syst.* 8 (2) (2022) 1487–1504.
- [354] L.H. Ngo, M. Luong, N.M. Sirakov, E. Viennet, T. Le-Tien, Skin lesion image classification using sparse representation in quaternion wavelet domain, *Signal Image Video Process.* (2022) 1–9.
- [355] S. Shen, M. Xu, F. Zhang, P. Shao, H. Liu, L. Xu, C. Zhang, P. Liu, Z. Zhang, P. Yao, et al., A low-cost high-performance data augmentation for deep learning-based skin lesion classification, *BME Front.* 2022 (2022).
- [356] L.G. Batista, P.H. Bugatti, P.T. Saito, Classification of skin lesion through active learning strategies, *Comput. Methods Programs Biomed.* 226 (2022) 107122.
- [357] K. Nakai, X.-H. Han, DPE-BoTNet: Dual position encoding bottleneck transformer network for skin lesion classification, in: 2022 IEEE 19th International Symposium on Biomedical Imaging, ISBI, IEEE, 2022, pp. 1–5.
- [358] Z. Wei, Q. Li, H. Song, Dual attention based network for skin lesion classification with auxiliary learning, *Biomed. Signal Process. Control* 74 (2022) 103549.
- [359] Y. Wan, Y. Cheng, M. Shao, MSLANet: multi-scale long attention network for skin lesion classification, *Appl. Intell.* (2022) 1–19.
- [360] X. Deng, Q. Yin, P. Guo, Efficient structural pseudoinverse learning-based hierarchical representation learning for skin lesion classification, *Complex Intell. Syst.* 8 (2) (2022) 1445–1457.
- [361] K. Nakai, Y.-W. Chen, X.-H. Han, Enhanced deep bottleneck transformer model for skin lesion classification, *Biomol. Signal Process. Control* 78 (2022) 103997.
- [362] P. Shan, C. Fu, L. Dai, T. Jia, M. Tie, J. Liu, Automatic skin lesion classification using a new densely connected convolutional network with an SF module, *Med. Biol. Eng. Comput.* (2022) 1–16.
- [363] G. Yue, P. Wei, T. Zhou, Q. Jiang, W. Yan, T. Wang, Towards multi-center skin lesion classification using deep neural network with adaptively weighted balance loss, *IEEE Trans. Med. Imaging* (2022).
- [364] F. Afza, M. Sharif, M.A. Khan, U. Tariq, H.-S. Yong, J. Cha, Multiclass skin lesion classification using hybrid deep features selection and extreme learning machine, *Sensors* 22 (3) (2022) 799.
- [365] L. Hoang, S.-H. Lee, E.-J. Lee, K.-R. Kwon, Multiclass skin lesion classification using a novel lightweight deep learning framework for smart healthcare, *Appl. Sci.* 12 (5) (2022) 2677.
- [366] D. Popescu, M. El-Khatib, L. Ichim, Skin lesion classification using collective intelligence of multiple neural networks, *Sensors* 22 (12) (2022) 4399.
- [367] T.H. Aldhyani, A. Verma, M.H. Al-Adhaileh, D. Koundal, Multi-class skin lesion classification using a lightweight dynamic kernel deep-learning-based convolutional neural network, *Diagnostics* 12 (9) (2022) 2048.
- [368] A.C. Foahom Gouabou, R. Igouraissi, J.-L. Damoiseaux, A. Moudafi, D. Merad, End-to-end decoupled training: A robust deep learning method for long-tailed classification of dermoscopic images for skin lesion classification, *Electronics* 11 (20) (2022) 3275.
- [369] V.D. Nguyen, N.D. Bui, H.K. Do, Skin lesion classification on imbalanced data using deep learning with soft attention, *Sensors* 22 (19) (2022) 7530.
- [370] S.S. Samsudin, H. Arof, S.W. Harun, A.W. Abdul Wahab, M.Y.I. Idris, Skin lesion classification using multi-resolution empirical mode decomposition and local binary pattern, *PLoS One* 17 (9) (2022) e0274896.
- [371] B. Shetty, R. Fernandes, A.P. Rodrigues, R. Chengoden, S. Bhattacharya, K. Lakshmanan, Skin lesion classification of dermoscopic images using machine learning and convolutional neural network, *Sci. Rep.* 12 (1) (2022) 1–11.

- [372] O. Alptekin, Z. Isik, Analysis of data augmentation on skin lesion classification by using deep learning models, in: 2022 International Symposium on Multidisciplinary Studies and Innovative Technologies, ISMSIT, IEEE, 2022, pp. 629–634.
- [373] V. Anand, S. Gupta, D. Koundal, K. Singh, Fusion of U-Net and CNN model for segmentation and classification of skin lesion from dermoscopy images, *Expert Syst. Appl.* 213 (2023) 119230.
- [374] F. Bozkurt, Skin lesion classification on dermatoscopic images using effective data augmentation and pre-trained deep learning approach, *Multimedia Tools Appl.* (2022) 1–19.
- [375] V.A.O. Nancy, M.S. Arya, N. Nitin, Impact of data augmentation on skin lesion classification using deep learning, in: 2022 5th International Conference on Information and Computer Technologies, ICICT, IEEE, 2022, pp. 67–72.
- [376] N. Mohanty, M. Pradhan, A.V. Reddy, S. Kumar, A. Alkhayyat, Integrated design of optimized weighted deep feature fusion strategies for skin lesion image classification, *Cancers* 14 (22) (2022) 5716.
- [377] M.M.K. Sarker, C.F. Moreno-García, J. Ren, E. Elyan, TransSLC: Skin lesion classification in dermatoscopic images using transformers, in: Annual Conference on Medical Image Understanding and Analysis, Springer, 2022, pp. 651–660.
- [378] E. Somfai, B. Baffy, K. Fenech, R. Hosszú, D. Korózs, M. Pólik, M. Sárdy, A. Lőrincz, Handling dataset dependence with model ensembles for skin lesion classification from dermoscopic and clinical images, *Int. J. Imaging Syst. Technol.* (2022).
- [379] S. Qian, K. Ren, W. Zhang, H. Ning, Skin lesion classification using CNNs with grouping of multi-scale attention and class-specific loss weighting, *Comput. Methods Programs Biomed.* 226 (2022) 107166.
- [380] S. Ayas, Multiclass skin lesion classification in dermoscopic images using swin transformer model, *Neural Comput. Appl.* (2022) 1–10.
- [381] E. Chabi Adjobo, A.T. Sanda Mahama, P. Gouton, J. Tossa, Towards accurate skin lesion classification across all skin categories using a PCNN fusion-based data augmentation approach, *Computers* 11 (3) (2022) 44.
- [382] Y. Wang, Y. Wang, J. Cai, T.K. Lee, C. Miao, Z.J. Wang, SSD-KD: A self-supervised diverse knowledge distillation method for lightweight skin lesion classification using dermoscopic images, *Med. Image Anal.* (2022) 102693.
- [383] D. Zhuang, K. Chen, J.M. Chang, CS-AF: A cost-sensitive multi-classifier active fusion framework for skin lesion classification, *Neurocomputing* 491 (2022) 206–216.
- [384] N. Nigar, M. Umar, M.K. Shahzad, S. Islam, D. Abalo, A deep learning approach based on explainable artificial intelligence for skin lesion classification, *IEEE Access* 10 (2022) 113715–113725.
- [385] B.W.-Y. Hsu, V.S. Tseng, Hierarchy-aware contrastive learning with late fusion for skin lesion classification, *Comput. Methods Programs Biomed.* 216 (2022) 106666.
- [386] M. Rasel, U.H. Obaidellah, S.A. Kareem, Convolutional neural network-based skin lesion classification with variable nonlinear activation functions, *IEEE Access* 10 (2022) 83398–83414.
- [387] C. Serrano, M. Lazo, A. Serrano, T. Toledo-Pastrana, R. Barros-Tornay, B. Acha, Clinically inspired skin lesion classification through the detection of dermoscopic criteria for basal cell carcinoma, *J. Imaging* 8 (7) (2022) 197.
- [388] V.H. Sahin, I. Ozte, G. Yolcu Ozte, Human monkeypox classification from skin lesion images with deep pre-trained network using mobile application, *J. Med. Syst.* 46 (11) (2022) 1–10.
- [389] A. Pundhir, S. Dadhich, A. Agarwal, B. Raman, Towards improved skin lesion classification using metadata supervision, in: 2022 26th International Conference on Pattern Recognition, ICPR, IEEE, 2022, pp. 4313–4320.
- [390] Y. Wang, Y. Feng, L. Zhang, J.T. Zhou, Y. Liu, R.S.M. Goh, L. Zhen, Adversarial multimodal fusion with attention mechanism for skin lesion classification using clinical and dermoscopic images, *Med. Image Anal.* 81 (2022) 102535.
- [391] P. Tang, X. Yan, Y. Nan, S. Xiang, S. Krammer, T. Lasser, FusionM4Net: A multi-stage multi-modal learning algorithm for multi-label skin lesion classification, *Med. Image Anal.* 76 (2022) 102307.
- [392] A. Yilmaz, G. Gencoglan, R. Varol, A.A. Demircali, M. Keshavarz, H. Uvet, MobileSkin: Classification of skin lesion images acquired using mobile phone-attached hand-held dermoscopes, *J. Clin. Med.* 11 (17) (2022) 5102.
- [393] J.A. Camacho-Gutiérrez, S. Solorza-Calderón, J. Álvarez-Borrego, Multi-class skin lesion classification using prism-and segmentation-based fractal signatures, *Expert Syst. Appl.* 197 (2022) 116671.
- [394] L. Piatek, T. Mroczek, Analysis and classification of melanocytic skin lesion images, *Procedia Comput. Sci.* 207 (2022) 1911–1918.
- [395] I. Lihacova, A. Bondarenko, Y. Chizhov, D. Uteshev, D. Bliznuk, N. Kiss, A. Lihachev, Multi-class CNN for classification of multispectral and autofluorescence skin lesion clinical images, *J. Clin. Med.* 11 (10) (2022) 2833.
- [396] S. Ding, Z. Wu, Y. Zheng, Z. Liu, X. Yang, X. Yang, G. Yuan, J. Xie, Deep attention branch networks for skin lesion classification, *Comput. Methods Programs Biomed.* 212 (2021) 106447.
- [397] R. Nersisson, T.J. Iyer, A.N. Joseph Raj, V. Rajangam, A dermoscopic skin lesion classification technique using YOLO-CNN and traditional feature model, *Arab. J. Sci. Eng.* 46 (10) (2021) 9797–9808.
- [398] B.K. Balabantary, R. Chakravarty, A.K. Panda, R. Nayak, Melanoma classification through transfer learning by the analysis of skin lesion images, in: Proceedings of the International Conference on Computing and Communication Systems, Springer, 2021, pp. 403–413.
- [399] M.A. Khan, Y.-D. Zhang, M. Sharif, T. Akram, Pixels to classes: intelligent learning framework for multiclass skin lesion localization and classification, *Comput. Electr. Eng.* 90 (2021) 106956.
- [400] A. Mahbod, G. Schaefer, C. Wang, R. Ecker, G. Dorffner, I. Ellinger, Investigating and exploiting image resolution for transfer learning-based skin lesion classification, in: 2020 25th International Conference on Pattern Recognition, ICPR, IEEE, 2021, pp. 4047–4053.
- [401] H. Zanddizari, N. Nguyen, B. Zeinali, J.M. Chang, A new preprocessing approach to improve the performance of CNN-based skin lesion classification, *Med. Biol. Eng. Comput.* 59 (5) (2021) 1123–1131.
- [402] J. Bian, S. Zhang, S. Wang, J. Zhang, J. Guo, Skin lesion classification by multi-view filtered transfer learning, *IEEE Access* 9 (2021) 66052–66061.
- [403] X. Wang, W. Huang, Z. Lu, S. Huang, Multi-level attentive skin lesion learning for melanoma classification, in: 2021 43rd Annual International Conference of the IEEE Engineering in Medicine & Biology Society, EMBC, IEEE, 2021, pp. 3924–3927.
- [404] R. Carvalho, J. Pedrosa, T. Nedelcu, Multimodal multi-tasking for skin lesion classification using deep neural networks, in: International Symposium on Visual Computing, Springer, 2021, pp. 27–38.
- [405] D. Wang, N. Pang, Y. Wang, H. Zhao, Unlabeled skin lesion classification by self-supervised topology clustering network, *Biomed. Signal Process. Control* 66 (2021) 102428.
- [406] R. Ali, H.K. Ragb, Skin lesion segmentation and classification using deep learning and handcrafted features, 2021, arXiv:2112.10307.
- [407] Y.-P. Liu, Z. Wang, Z. Li, J. Li, T. Li, P. Chen, R. Liang, Multiscale ensemble of convolutional neural networks for skin lesion classification, *IET Image Process.* 15 (10) (2021) 2309–2318.
- [408] N. Bayasi, G. Hamarneh, R. Garbi, Culprit-prune-net: Efficient continual sequential multi-domain learning with application to skin lesion classification, in: International Conference on Medical Image Computing and Computer-Assisted Intervention, Springer, 2021, pp. 165–175.
- [409] P. Yao, S. Shen, M. Xu, P. Liu, F. Zhang, J. Xing, P. Shao, B. Kaffenberger, R.X. Xu, Single model deep learning on imbalanced small datasets for skin lesion classification, *IEEE Trans. Med. Imaging* 41 (5) (2021) 1242–1254.
- [410] K. Melbin, Y. Raj, Integration of modified ABCD features and support vector machine for skin lesion types classification, *Multimedia Tools Appl.* 80 (6) (2021) 8909–8929.
- [411] S. Jain, U. Singhania, B. Tripathy, E.A. Nasr, M.K. Aboudaif, A.K. Kamrani, Deep learning-based transfer learning for classification of skin cancer, *Sensors* 21 (23) (2021) 8142.
- [412] N. Bansal, S. Sridhar, Skin lesion classification using ensemble transfer learning, in: International Conference on Image Processing and Capsule Networks, Springer, 2021, pp. 557–566.
- [413] P.K. Samanta, N.K. Rout, Skin lesion classification using deep convolutional neural network and transfer learning approach, in: Advances in Smart Communication Technology and Information Processing, Springer, 2021, pp. 327–335.
- [414] Z. Rahman, M.S. Hossain, M.R. Islam, M.M. Hasan, R.A. Hridhee, An approach for multiclass skin lesion classification based on ensemble learning, *Inform. Med. Unlocked* 25 (2021) 100659.
- [415] C. Reimers, N. Penzel, P. Bodesheim, J. Runge, J. Denzler, Conditional dependence tests reveal the usage of ABCD rule features and bias variables in automatic skin lesion classification, in: Proceedings of the IEEE/CVF Conference on Computer Vision and Pattern Recognition, 2021, pp. 1810–1819.
- [416] K. Thurnhofer-Hemsi, E. López-Rubio, E. Domínguez, D.A. Elizondo, Skin lesion classification by ensembles of deep convolutional networks and regularly spaced shifting, *IEEE Access* 9 (2021) 112193–112205.
- [417] C.-S. Hu, A. Lawson, J.-S. Chen, Y.-M. Chung, C. Smyth, S.-M. Yang, Toporesnet: A hybrid deep learning architecture and its application to skin lesion classification, *Mathematics* 9 (22) (2021) 2924.
- [418] C. Calderón, K. Sanchez, S. Castillo, H. Arguello, BILSK: A bilinear convolutional neural network approach for skin lesion classification, *Comput. Methods Programs Biomed.* Update 1 (2021) 100036.
- [419] M. Arshad, M.A. Khan, U. Tariq, A. Armghan, F. Alenezi, M. Younus Javed, S.M. Aslam, S. Kadry, A computer-aided diagnosis system using deep learning for multiclass skin lesion classification, *Comput. Intell. Neurosci.* 2021 (2021).
- [420] O. Sevil, A deep convolutional neural network-based pigmented skin lesion classification application and experts evaluation, *Neural Comput. Appl.* 33 (18) (2021) 12039–12050.
- [421] Q. Sun, C. Huang, M. Chen, H. Xu, Y. Yang, Skin lesion classification using additional patient information, *BioMed Res. Int.* 2021 (2021).
- [422] F. Santos, F. Silva, P. Georgieva, Transfer learning for skin lesion classification using convolutional neural networks, in: 2021 International Conference on Innovations in Intelligent SysTems and Applications, INISTA, IEEE, 2021, pp. 1–6.

- [423] M. Cullell-Dalmau, S. Noé, M. Otero-Viñas, I. Meić, C. Manzo, Convolutional neural network for skin lesion classification: understanding the fundamentals through hands-on learning, *Front. Med.* 8 (2021) 644327.
- [424] T. Bdair, N. Navab, S. Albarqouni, Semi-supervised federated peer learning for skin lesion classification, 2021, arXiv e-prints arXiv-2103.
- [425] Y. Tian, L. Zhang, L. Shen, G. Yin, L. Chen, Mixed re-sampled class-imbalanced semi-supervised learning for skin lesion classification, *Intell. Autom. Soft Comput.* 28 (1) (2021) 195–211.
- [426] F. Shahabi, A. Rouhi, R. Rastegari, The performance of deep and conventional machine learning techniques for skin lesion classification, in: 2021 IEEE 18th International Conference on Smart Communities: Improving Quality of Life using ICT, IoT and AI, HONET, IEEE, 2021, pp. 50–55.
- [427] T. Bdair, N. Navab, S. Albarqouni, Fedperl: Semi-supervised peer learning for skin lesion classification, in: International Conference on Medical Image Computing and Computer-Assisted Intervention, Springer, 2021, pp. 336–346.
- [428] J. Xiao, H. Xu, D. Fang, C. Cheng, H. Gao, Boosting and rectifying few-shot learning prototype network for skin lesion classification based on the internet of medical things, *Wirel. Netw.* (2021) 1–15.
- [429] S. Moldovanu, F.A. Damian Michis, K.C. Biswas, A. Culea-Florescu, L. Moraru, Skin lesion classification based on surface fractal dimensions and statistical color cluster features using an ensemble of machine learning techniques, *Cancers* 13 (21) (2021) 5256.
- [430] B. Samia, M. Boudjelal, O. Lézoray, Skin lesion classification using convolutional neural networks based on multi-features extraction, in: 19th International Conference on Computer Analysis of Images and Patterns, CAIP 2021, 2021.
- [431] P.M. Pereira, L.A. Thomaz, L.M. Tavora, P.A. Assuncao, R. Fonseca-Pinto, R.P. Paiva, S.M. Faria, Skin lesion classification using bag-of-3D-features, in: 2021 Telecoms Conference, Conftele, IEEE, 2021, pp. 1–6.
- [432] B. Krohling, P.B. Castro, A.G. Pacheco, R.A. Krohling, A smartphone based application for skin cancer classification using deep learning with clinical images and lesion information, 2021, arXiv:2104.14353.
- [433] S. Mukherjee, D. Ganguly, Transfer learning in skin lesion classification, in: Proceedings of International Conference on Frontiers in Computing and Systems, Springer, 2021, pp. 343–349.
- [434] J. Wu, W. Hu, Y. Wen, W. Tu, X. Liu, Skin lesion classification using densely connected convolutional networks with attention residual learning, *Sensors* 20 (24) (2020) 7080.
- [435] L. Wei, K. Ding, H. Hu, Automatic skin cancer detection in dermoscopy images based on ensemble lightweight deep learning network, *IEEE Access* 8 (2020) 99633–99647.
- [436] E. Yilmaz, M. Trocan, Benign and malignant skin lesion classification comparison for three deep-learning architectures, in: Asian Conference on Intelligent Information and Database Systems, Springer, 2020, pp. 514–524.
- [437] D.D.A. Rodrigues, R.F. Ivo, S.C. Satapathy, S. Wang, J. Hemanth, P.P. Reboucas Filho, A new approach for classification skin lesion based on transfer learning, deep learning, and IoT system, *Pattern Recognit. Lett.* 136 (2020) 8–15.
- [438] A. Kwasigroch, M. Grochowski, A. Mikołajczyk, Neural architecture search for skin lesion classification, *IEEE Access* 8 (2020) 9061–9071.
- [439] C. Dhivya, K. Sangeetha, M. Balamurugan, S. Amaran, T. Vetriselvi, P. Johnpaul, Skin lesion classification using decision trees and random forest algorithms, *J. Ambient Intell. Humaniz. Comput.* (2020) 1–13.
- [440] A. Kwasigroch, M. Grochowski, A. Mikołajczyk, Self-supervised learning to increase the performance of skin lesion classification, *Electronics* 9 (11) (2020) 1930.
- [441] F. Afza, M.A. Khan, M. Sharif, T. Saba, A. Rehman, M.Y. Javed, Skin lesion classification: An optimized framework of optimal color features selection, in: 2020 2nd International Conference on Computer and Information Sciences, ICCIS, IEEE, 2020, pp. 1–6.
- [442] T. Akram, H.M.J. Lodhi, S.R. Naqvi, S. Naeem, M. Alhaisoni, M. Ali, S.A. Haider, N.N. Qadri, A multilevel features selection framework for skin lesion classification, *Human-Centric Comput. Inf. Sci.* 10 (1) (2020) 1–26.
- [443] S. Yildirim-Yaylgan, B. Arifaj, M. Rahimpour, J.Y. Hardeberg, L. Ahmed, Pre-trained CNN based deep features with hand-crafted features and patient data for skin lesion classification, in: International Conference on Intelligent Technologies and Applications, Springer, 2020, pp. 151–162.
- [444] L. Rieger, C. Singh, W. Murdoch, B. Yu, Interpretations are useful: penalizing explanations to align neural networks with prior knowledge, in: International Conference on Machine Learning, PMLR, 2020, pp. 8116–8126.
- [445] L. Liu, L. Mou, X.X. Zhu, M. Mandal, Automatic skin lesion classification based on mid-level feature learning, *Comput. Med. Imaging Graph.* 84 (2020) 101765.
- [446] J. Wu, W. Hu, Y. Wang, Y. Wen, A multi-input CNNs with attention for skin lesion classification, in: 2020 IEEE International Conference on Smart Cloud, SmartCloud, IEEE, 2020, pp. 78–83.
- [447] I. Mporas, I. Perikos, M. Paraskevas, Color models for skin lesion classification from dermatoscopic images, in: Advances in Integrations of Intelligent Methods, Springer, 2020, pp. 85–98.
- [448] J. Sun, T. Chakraborti, J.A. Noble, A comparative study of explainer modules applied to automated skin lesion classification, in: XI-ML@ KI, 2020.
- [449] A.C. Salian, S. Vaze, P. Singh, G.N. Shaikh, S. Chapaneri, D. Jayaswal, Skin lesion classification using deep learning architectures, in: 2020 3rd International Conference on Communication System, Computing and IT Applications, CSCITA, IEEE, 2020, pp. 168–173.
- [450] S.S. Chaturvedi, K. Gupta, P.S. Prasad, Skin lesion analyser: An efficient seven-way multi-class skin cancer classification using mobilenet, in: International Conference on Advanced Machine Learning Technologies and Applications, Springer, 2020, pp. 165–176.
- [451] V. Miglani, M. Bhatia, Skin lesion classification: A transfer learning approach using efficienets, in: International Conference on Advanced Machine Learning Technologies and Applications, Springer, 2020, pp. 315–324.
- [452] A. Mahbod, G. Schaefer, C. Wang, G. Dorffner, R. Ecker, I. Ellinger, Transfer learning using a multi-scale and multi-network ensemble for skin lesion classification, *Comput. Methods Programs Biomed.* 193 (2020) 105475.
- [453] Z. Rahman, A.M. Ami, A transfer learning based approach for skin lesion classification from imbalanced data, in: 2020 11th International Conference on Electrical and Computer Engineering, ICECE, IEEE, 2020, pp. 65–68.
- [454] Z. Qin, Z. Liu, P. Zhu, Y. Xue, A GAN-based image synthesis method for skin lesion classification, *Comput. Methods Programs Biomed.* 195 (2020) 105568.
- [455] S.R. Guha, S. Rafizul Haque, Performance comparison of machine learning-based classification of skin diseases from skin lesion images, in: International Conference on Communication, Computing and Electronics Systems, Springer, 2020, pp. 15–25.
- [456] B. Harangi, A. Baran, A. Hajdu, Assisted deep learning framework for multi-class skin lesion classification considering a binary classification support, *Biomed. Signal Process. Control* 62 (2020) 102041.
- [457] S.R. Hassan, S. Afroge, M.B. Mizan, Skin lesion classification using densely connected convolutional network, in: 2020 IEEE Region 10 Symposium, TENSYMP, IEEE, 2020, pp. 750–753.
- [458] A. Jibhakate, P. Parnerkar, S. Mondal, V. Bharambe, S. Mantri, Skin lesion classification using deep learning and image processing, in: 2020 3rd International Conference on Intelligent Sustainable Systems, ICISS, IEEE, 2020, pp. 333–340.
- [459] J.-A. Almaraz-Damian, V. Ponomaryov, S. Sadovnychiy, H. Castillejos-Fernandez, Melanoma and nevus skin lesion classification using handcraft and deep learning feature fusion via mutual information measures, *Entropy* 22 (4) (2020) 484.
- [460] D. Zhuang, K. Chen, J.M. Chang, CS-AF: A cost-sensitive multi-classifier active fusion framework for skin lesion classification, 2020, arXiv:2004.12064.
- [461] E.O. Molina-Molina, S. Solorza-Calderón, J. Álvarez-Borrego, Classification of dermoscopy skin lesion color-images using fractal-deep learning features, *Appl. Sci.* 10 (17) (2020) 5954.
- [462] S.A.A. Ahmed, B. Yanıkoglu, Ö. Göksu, E. Aptoula, Skin lesion classification with deep CNN ensembles, in: 2020 28th Signal Processing and Communications Applications Conference, SIU, IEEE, 2020, pp. 1–4.
- [463] S. Muckatira, Properties of winning tickets on skin lesion classification, 2020, arXiv:2008.12141.
- [464] F. Nunnari, C. Bhuvaneshwara, A.O. Ezema, D. Sonntag, A study on the fusion of pixels and patient metadata in CNN-based classification of skin lesion images, in: International Cross-Domain Conference for Machine Learning and Knowledge Extraction, Springer, 2020, pp. 191–208.
- [465] S. Bagchi, A. Banerjee, D.R. Bathula, Learning a meta-ensemble technique for skin lesion classification and novel class detection, in: Proceedings of the IEEE/CVF Conference on Computer Vision and Pattern Recognition Workshops, 2020, pp. 746–747.
- [466] N. Gessert, M. Nielsen, M. Shaikh, R. Werner, A. Schlaefer, Skin lesion classification using ensembles of multi-resolution EfficientNets with meta data, *MethodsX* 7 (2020) 100864.
- [467] G.S. Ghalejoogh, H.M. Kordy, F. Ebrahimi, A hierarchical structure based on stacking approach for skin lesion classification, *Expert Syst. Appl.* 145 (2020) 113127.
- [468] L. Bi, D.D. Feng, M. Fulham, J. Kim, Multi-label classification of multi-modality skin lesion via hyper-connected convolutional neural network, *Pattern Recognit.* 107 (2020) 107502.
- [469] P.M. Pereira, R. Fonseca-Pinto, R.P. Paiva, P.A. Assuncao, L.M. Tavora, L.A. Thomaz, S.M. Faria, Skin lesion classification enhancement using border-line features—The melanoma vs nevus problem, *Biomed. Signal Process. Control* 57 (2020) 101765.
- [470] F.A. Damian, S. Moldovanu, N. Dey, A.S. Ashour, L. Moraru, Feature selection of non-dermoscopic skin lesion images for nevus and melanoma classification, *Computation* 8 (2) (2020) 41.
- [471] K. Thomsen, A.L. Christensen, L. Iversen, H.B. Lomholt, O. Winther, Deep learning for diagnostic binary classification of multiple-lesion skin diseases, *Front. Med.* 7 (2020) 604.
- [472] E. Goceri, A.A. Karakas, Comparative evaluations of cnn based networks for skin lesion classification, in: 14th International Conference on Computer Graphics, Visualization, Computer Vision and Image Processing, CGVCVIP, Zagreb, Croatia, 2020, pp. 1–6.
- [473] J. Yan, F. Liu, W. Wang, Scalable skin lesion multi-classification recognition system, *Comput. Mater. Continua* 62 (2) (2020) 801–816.

- [474] Y. Filali, H. El Khoukhi, M.A. Sabri, A. Yahyaouy, A. Aarab, Texture classification of skin lesion using convolutional neural network, in: 2019 International Conference on Wireless Technologies, Embedded and Intelligent Systems, WITS, IEEE, 2019, pp. 1–5.
- [475] Y. Wang, H. Pan, B. Yang, X. Bian, Q. Cui, Mutual learning model for skin lesion classification, in: International Conference of Pioneering Computer Scientists, Engineers and Educators, Springer, 2019, pp. 214–222.
- [476] M.A. Khan, M.Y. Javed, M. Sharif, T. Saba, A. Rehman, Multi-model deep neural network based features extraction and optimal selection approach for skin lesion classification, in: 2019 International Conference on Computer and Information Sciences, ICCIS, IEEE, 2019, pp. 1–7.
- [477] E. Veltmeijer, S. Karaoglu, T. Gevers, et al., Integrating clinically-relevant features into skin lesion classification, in: BNAIC/BENELEARN, 2019.
- [478] P. Tschandl, G. Argenziano, M. Razmara, J. Yap, Diagnostic accuracy of content-based dermatoscopic image retrieval with deep classification features, *Br. J. Dermatol.* 181 (1) (2019) 155–165.
- [479] C. Xue, Q. Dou, X. Shi, H. Chen, P.-A. Heng, Robust learning at noisy labeled medical images: Applied to skin lesion classification, in: 2019 IEEE 16th International Symposium on Biomedical Imaging, ISBI 2019, IEEE, 2019, pp. 1280–1283.
- [480] W. Zheng, C. Gou, L. Yan, A relation hashing network embedded with prior features for skin lesion classification, in: International Workshop on Machine Learning in Medical Imaging, Springer, 2019, pp. 115–123.
- [481] A. Mahbod, G. Schaefer, C. Wang, R. Ecker, I. Ellinger, Skin lesion classification using hybrid deep neural networks, in: ICASSP 2019–2019 IEEE International Conference on Acoustics, Speech and Signal Processing, ICASSP, IEEE, 2019, pp. 1229–1233.
- [482] A. Mahbod, G. Schaefer, I. Ellinger, R. Ecker, A. Pitiot, C. Wang, Fusing fine-tuned deep features for skin lesion classification, *Comput. Med. Imaging Graph.* 71 (2019) 19–29.
- [483] R. Kulhalli, C. Savadikar, B. Garware, A hierarchical approach to skin lesion classification, in: Proceedings of the ACM India Joint International Conference on Data Science and Management of Data, 2019, pp. 245–250.
- [484] S. Serte, H. Demirel, Wavelet-based deep learning for skin lesion classification, *IET Image Process.* 14 (4) (2019) 720–726.
- [485] S. Serte, H. Demirel, Gabor wavelet-based deep learning for skin lesion classification, *Comput. Biol. Med.* 113 (2019) 103423.
- [486] M.A. Albahar, Skin lesion classification using convolutional neural network with novel regularizer, *IEEE Access* 7 (2019) 38306–38313.
- [487] M. Sadeghi, P. Chilana, J. Yap, P. Tschandl, M.S. Atkins, Using content-based image retrieval of dermatoscopic images for interpretation and education: A pilot study, *Skin Res. Technol.* 26 (4) (2020) 503–512.
- [488] N. Gessert, T. Sentker, F. Madesta, R. Schmitz, H. Kniep, I. Baltruschat, R. Werner, A. Schlaefer, Skin lesion classification using cnns with patch-based attention and diagnosis-guided loss weighting, *IEEE Trans. Biomed. Eng.* 67 (2) (2019) 495–503.
- [489] M.A.A. Milton, Automated skin lesion classification using ensemble of deep neural networks in ISIC 2018: Skin lesion analysis towards melanoma detection challenge, 2019, [arXiv:1901.10802](https://arxiv.org/abs/1901.10802).
- [490] H. Rashid, M.A. Tanveer, H.A. Khan, Skin lesion classification using GAN based data augmentation, in: 2019 41st Annual International Conference of the IEEE Engineering in Medicine and Biology Society, EMBC, IEEE, 2019, pp. 916–919.
- [491] C. Yoon, G. Hamarneh, R. Garbi, Generalizable feature learning in the presence of data bias and domain class imbalance with application to skin lesion classification, in: International Conference on Medical Image Computing and Computer-Assisted Intervention, Springer, 2019, pp. 365–373.
- [492] Y.-M. Chung, C.-S. Hu, A. Lawson, C. Smyth, Toporesnet: A hybrid deep learning architecture and its application to skin lesion classification, 2019, [arXiv:1905.08607](https://arxiv.org/abs/1905.08607).
- [493] P. Van Molle, T. Verbelen, C. De Boom, B. Vankeirsbilck, J. De Vylder, B. Diricx, T. Kimpe, P. Simoens, B. Dhoedt, Quantifying uncertainty of deep neural networks in skin lesion classification, in: Uncertainty for Safe Utilization of Machine Learning in Medical Imaging and Clinical Image-Based Procedures, Springer, 2019, pp. 52–61.
- [494] S.H. Kassani, P.H. Kassani, M.J. Wesolowski, K.A. Schneider, R. Deters, Depth-wise separable convolutional neural network for skin lesion classification, in: 2019 IEEE International Symposium on Signal Processing and Information Technology, ISSPIT, IEEE, 2019, pp. 1–6.
- [495] A.E. Aldwgeri, N.F. Abubacker, Ensemble of deep convolutional neural network for skin lesion classification in dermatoscopy images, in: International Visual Informatics Conference, Springer, 2019, pp. 214–226.
- [496] A. Eddine Guissous, Skin lesion classification using deep neural network, 2019, arXiv e-prints [arXiv:1911](https://arxiv.org/abs/1911).
- [497] A.E. Guissous, Skin lesion classification using deep neural network, 2019, arXiv:1911.07817.
- [498] R.B. Fisher, J. Rees, A. Bertrand, Classification of ten skin lesion classes: Hierarchical knn versus deep net, in: Annual Conference on Medical Image Understanding and Analysis, Springer, 2019, pp. 86–98.
- [499] M. Monisha, A. Suresh, B.T. Bapu, M. Rashmi, Classification of malignant melanoma and benign skin lesion by using back propagation neural network and ABCD rule, *Cluster Comput.* 22 (5) (2019) 12897–12907.
- [500] J. Zhang, Y. Xie, Q. Wu, Y. Xia, Skin lesion classification in dermoscopy images using synergic deep learning, in: International Conference on Medical Image Computing and Computer-Assisted Intervention, Springer, 2018, pp. 12–20.
- [501] M. ur Rehman, S.H. Khan, S.D. Rizvi, Z. Abbas, A. Zafar, Classification of skin lesion by interference of segmentation and convolutional neural network, in: 2018 2nd International Conference on Engineering Innovation, ICEI, IEEE, 2018, pp. 81–85.
- [502] M.A. Wahba, A.S. Ashour, Y. Guo, S.A. Napoleon, M.M. Abd Elnaby, A novel cumulative level difference mean based GLDM and modified ABCD features ranked using eigenvector centrality approach for four skin lesion types classification, *Comput. Methods Programs Biomed.* 165 (2018) 163–174.
- [503] T.-C. Pham, C.-M. Luong, M. Visani, V.-D. Hoang, Deep CNN and data augmentation for skin lesion classification, in: Asian Conference on Intelligent Information and Database Systems, Springer, 2018, pp. 573–582.
- [504] K. Thandiackal, O. Goksel, A structure-aware convolutional neural network for skin lesion classification, in: OR 2.0 Context-Aware Operating Theaters, Computer Assisted Robotic Endoscopy, Clinical Image-Based Procedures, and Skin Image Analysis, Springer, 2018, pp. 312–319.
- [505] B. Harangi, Skin lesion classification with ensembles of deep convolutional neural networks, *J. Biomed. Inform.* 86 (2018) 25–32.
- [506] Y. Filali, A. Ennouri, M.A. Sabri, A. Aarab, A study of lesion skin segmentation, features selection and classification approaches, in: 2018 International Conference on Intelligent Systems and Computer Vision, ISCV, IEEE, 2018, pp. 1–7.
- [507] M. Sadeghi, P.K. Chilana, M.S. Atkins, How users perceive content-based image retrieval for identifying skin images, in: Understanding and Interpreting Machine Learning in Medical Image Computing Applications, Springer, 2018, pp. 141–148.
- [508] Y. Xie, J. Zhang, Y. Xia, A multi-level deep ensemble model for skin lesion classification in dermoscopy images, 2018, [arXiv:1807.08488](https://arxiv.org/abs/1807.08488).
- [509] X. Li, J. Wu, H. Jiang, E.Z. Chen, X. Dong, R. Rong, Skin lesion classification via combining deep learning features and clinical criteria representations, *BioRxiv* (2018) 382010.
- [510] Y.C. Lee, S.-H. Jung, H.-H. Won, WonDerM: Skin lesion classification with fine-tuned neural networks, 2018, [arXiv:1808.03426](https://arxiv.org/abs/1808.03426).
- [511] S. Kitada, H. Iyatomi, Skin lesion classification with ensemble of squeeze-and-excitation networks and semi-supervised learning, 2018, [arXiv:1809.02568](https://arxiv.org/abs/1809.02568).
- [512] A. Namozov, D. Ergashev, Y. Im Cho, Adaptive activation functions for skin lesion classification using deep neural networks, in: 2018 Joint 10th International Conference on Soft Computing and Intelligent Systems (SCIS) and 19th International Symposium on Advanced Intelligent Systems, ISIS, IEEE, 2018, pp. 232–235.
- [513] Y. Pan, Y. Xia, Residual network based aggregation model for skin lesion classification, 2018, [arXiv:1807.09150](https://arxiv.org/abs/1807.09150).
- [514] F.P. dos Santos, M.A. Ponti, Robust feature spaces from pre-trained deep network layers for skin lesion classification, in: 2018 31st SIBGRAPI Conference on Graphics, Patterns and Images, SIBGRAPI, IEEE, 2018, pp. 189–196.
- [515] H. Liao, J. Luo, A deep multi-task learning approach to skin lesion classification, 2018, [arXiv:1812.03527](https://arxiv.org/abs/1812.03527).
- [516] W. Songpan, Improved skin lesion image classification using clustering with local-GLCM normalization, in: 2018 2nd European Conference on Electrical Engineering and Computer Science, EECS, IEEE, 2018, pp. 206–210.
- [517] J. Yap, W. Yolland, P. Tschandl, Multimodal skin lesion classification using deep learning, *Exp. Dermatol.* 27 (11) (2018) 1261–1267.
- [518] P. Van Molle, M. De Strooper, T. Verbelen, B. Vankeirsbilck, P. Simoens, B. Dhoedt, Visualizing convolutional neural networks to improve decision support for skin lesion classification, in: Understanding and Interpreting Machine Learning in Medical Image Computing Applications, Springer, 2018, pp. 115–123.
- [519] F. Navarro, S. Conjeti, F. Tombari, N. Navab, Webly supervised learning for skin lesion classification, in: International Conference on Medical Image Computing and Computer-Assisted Intervention, Springer, 2018, pp. 398–406.
- [520] M.A. Wahba, A.S. Ashour, S.A. Napoleon, M.M. Abd Elnaby, Y. Guo, Combined empirical mode decomposition and texture features for skin lesion classification using quadratic support vector machine, *Health Inf. Sci. Syst.* 5 (1) (2017) 1–13.
- [521] T. Satheesha, D. Satyanarayana, M.G. Prasad, K.D. Dhruve, Melanoma is skin deep: a 3D reconstruction technique for computerized dermatoscopic skin lesion classification, *IEEE J. Transl. Eng. Health Med.* 5 (2017) 1–17.
- [522] A.R. Lopez, X. Giro-i Nieto, J. Burdick, O. Marques, Skin lesion classification from dermatoscopic images using deep learning techniques, in: 2017 13th IASTED International Conference on Biomedical Engineering, BioMed, IEEE, 2017, pp. 49–54.
- [523] D.H. Murphree, C. Ngufor, Transfer learning for melanoma detection: Participation in ISIC 2017 skin lesion classification challenge, 2017, [arXiv:1703.05235](https://arxiv.org/abs/1703.05235).
- [524] P. Mirunalini, A. Chandrabose, V. Gokul, S. Jaisakthi, Deep learning for skin lesion classification, 2017, [arXiv:1703.04364](https://arxiv.org/abs/1703.04364).
- [525] X. Jia, L. Shen, Skin lesion classification using class activation map, 2017, [arXiv:1703.01053](https://arxiv.org/abs/1703.01053).

- [526] T. DeVries, D. Ramachandram, Skin lesion classification using deep multi-scale convolutional neural networks, 2017, [arXiv:1703.01402](https://arxiv.org/abs/1703.01402).
- [527] N. Danpakdee, W. Songpan, Classification model for skin lesion image, in: International Conference on Information Science and Applications, Springer, 2017, pp. 553–561.
- [528] S.A. Mahdiraji, Y. Baleghi, S.M. Sakhaii, Skin lesion images classification using new color pigmented boundary descriptors, in: 2017 3rd International Conference on Pattern Recognition and Image Analysis, IPRIA, IEEE, 2017, pp. 102–107.
- [529] L. Haofu, J. Luo, A deep multi-task learning approach to skin lesion classification, in: Workshops at the Thirty-First AAAI Conference on Artificial Intelligence, 2017.
- [530] Y. Filali, A. Ennouri, M.A. Sabri, A. Aarab, Multiscale approach for skin lesion analysis and classification, in: 2017 International Conference on Advanced Technologies for Signal and Image Processing, ATSiP, IEEE, 2017, pp. 1–6.
- [531] A.A.A. Al-abayechi, H.A. Jalab, R.W. Ibrahim, A classification of skin lesion using fractional poisson for texture feature extraction, in: Proceedings of the Second International Conference on Internet of Things, Data and Cloud Computing, 2017, pp. 1–7.
- [532] T. Majtner, S. Yildirim-Yayilgan, J.Y. Hardeberg, Combining deep learning and hand-crafted features for skin lesion classification, in: 2016 Sixth International Conference on Image Processing Theory, Tools and Applications, IPTA, IEEE, 2016, pp. 1–6.
- [533] R. Chakravorty, S. Liang, M. Abedini, R. Garnavi, Dermatologist-like feature extraction from skin lesion for improved asymmetry classification in PH 2 database, in: 2016 38th Annual International Conference of the IEEE Engineering in Medicine and Biology Society, EMBC, IEEE, 2016, pp. 3855–3858.
- [534] H. Liao, Y. Li, J. Luo, Skin disease classification versus skin lesion characterization: Achieving robust diagnosis using multi-label deep neural networks, in: 2016 23rd International Conference on Pattern Recognition, ICPR, IEEE, 2016, pp. 355–360.
- [535] V. Pomponiu, H. Nejati, N.-M. Cheung, Deepmole: Deep neural networks for skin mole lesion classification, in: 2016 IEEE International Conference on Image Processing, ICIP, IEEE, 2016, pp. 2623–2627.
- [536] M.A. Farooq, M.A.M. Azhar, R.H. Raza, Automatic lesion detection system (ALDS) for skin cancer classification using SVM and neural classifiers, in: 2016 IEEE 16th International Conference on Bioinformatics and Bioengineering, BIBE, IEEE, 2016, pp. 301–308.
- [537] C. Di Leo, V. Bevilacqua, L. Ballerini, R. Fisher, B. Aldridge, J. Rees, Hierarchical classification of ten skin lesion classes, in: Proc. SICSA Dundee Medical Image Analysis Workshop, 2015.
- [538] M.K.A. Mahmoud, A. Al-Jumaily, A hybrid system for skin lesion detection: Based on gabor wavelet and support vector machine, in: Information Technology: Proceedings of the 2014 International Symposium on Information Technology, ISIT 2014, Dalian, China, 2014, p. 39.
- [539] N.M. Sirakov, Y.-L. Ou, M. Mete, Skin lesion feature vectors classification in models of a Riemannian manifold, *Ann. Math. Artif. Intell.* 75 (1) (2015) 217–229.
- [540] M.E. Celebi, A. Zornberg, Automated quantification of clinically significant colors in dermoscopy images and its application to skin lesion classification, *IEEE Syst. J.* 8 (3) (2014) 980–984.
- [541] U. Jamil, S. Khalid, Comparative study of classification techniques used in skin lesion detection systems, in: 17th IEEE International Multi Topic Conference 2014, IEEE, 2014, pp. 266–271.
- [542] G. Surówka, M. Ogorzałek, On optimal wavelet bases for classification of skin lesion images through ensemble learning, in: 2014 International Joint Conference on Neural Networks, IJCNN, IEEE, 2014, pp. 165–170.
- [543] Z. She, P. Excell, Lesion classification using 3D skin surface tilt orientation, *Skin Res. Technol.* 19 (1) (2013) e305–e311.
- [544] L. Rosado, M. Ferreira, A prototype for a mobile-based system of skin lesion analysis using supervised classification, in: 2013 2nd Experiment@ International Conference, Exp. At'13, IEEE, 2013, pp. 156–157.
- [545] P.G. Cavalcanti, J. Scharcanski, Macroscopic pigmented skin lesion segmentation and its influence on lesion classification and diagnosis, in: Color Medical Image Analysis, Springer, 2013, pp. 15–39.
- [546] M. Mete, Y.-L. Ou, N.M. Sirakov, Skin lesion feature vector space with a metric to model geometric structures of malignancy for classification, in: International Workshop on Combinatorial Image Analysis, Springer, 2012, pp. 285–297.
- [547] R. Amelard, A. Wong, D.A. Clausi, Extracting morphological high-level intuitive features (HLIF) for enhancing skin lesion classification, in: 2012 Annual International Conference of the IEEE Engineering in Medicine and Biology Society, IEEE, 2012, pp. 4458–4461.
- [548] L. Ballerini, R.B. Fisher, B. Aldridge, J. Rees, Non-melanoma skin lesion classification using colour image data in a hierarchical K-NN classifier, in: 2012 9th IEEE International Symposium on Biomedical Imaging, ISBI, IEEE, 2012, pp. 358–361.
- [549] Z. She, P.S. Excell, Skin pattern analysis for lesion classification using local isotropy, *Skin Res. Technol.* 17 (2) (2011) 206–212.
- [550] K. Ramlakhan, Y. Shang, A mobile automated skin lesion classification system, in: 2011 IEEE 23rd International Conference on Tools with Artificial Intelligence, IEEE, 2011, pp. 138–141.
- [551] M.A. Al-Masni, M.A. Al-Antari, M.-T. Choi, S.-M. Han, T.-S. Kim, Skin lesion segmentation in dermoscopy images via deep full resolution convolutional networks, *Comput. Methods Programs Biomed.* 162 (2018) 221–231.
- [552] F.I. Tushar, B. Alyafi, M.K. Hasan, L. Dahal, Brain tissue segmentation using neuronet with different pre-processing techniques, in: 2019 Joint 8th International Conference on Informatics, Electronics & Vision (ICIEV) and 2019 3rd International Conference on Imaging, Vision & Pattern Recognition (ICIVPR), IEEE, 2019, pp. 223–227.
- [553] Q. Abbas, M.E. Celebi, I.F. García, Hair removal methods: A comparative study for dermoscopy images, *Biomed. Signal Process. Control* 6 (4) (2011) 395–404.
- [554] S. Fawzy, H.E.-D. Moustafa, M.M. Ata, E.H. AbdelHay, High performed skin lesion segmentation based on modified active contour, in: 2022 International Telecommunications Conference, ITC-Egypt, IEEE, 2022, pp. 1–5.
- [555] J. Ramya, H. Vijaylakshmi, H.M. Saifuddin, Segmentation of skin lesion images using discrete wavelet transform, *Biomed. Signal Process. Control* 69 (2021) 102839.
- [556] A. Mikołajczyk, M. Grochowski, Data augmentation for improving deep learning in image classification problem, in: 2018 International Interdisciplinary PhD Workshop, IIPhDW, IEEE, 2018, pp. 117–122.
- [557] H. Zunair, A.B. Hamza, Melanoma detection using adversarial training and deep transfer learning, *Phys. Med. Biol.* 65 (13) (2020) 135005.
- [558] P. Marosán, K. Szalai, D. Csabai, G. Csány, A. Horváth, M. Gyöngy, Automated seeding for ultrasound skin lesion segmentation, *Ultrasonics* 110 (2021) 106268.
- [559] A. Veeramuthu, A. Anne Frank Joe, B. Sathish, L. Leo Joseph, P. Ganeshan, V. Elamaran, Comparative study of skin lesion segmentation and feature extraction in different color spaces, in: Proceedings of International Conference on Communication, Circuits, and Systems, Springer, 2021, pp. 303–312.
- [560] Y. LeCun, Y. Bengio, G. Hinton, Deep learning, *Nature* 521 (7553) (2015) 436–444.
- [561] A. Krizhevsky, I. Sutskever, G.E. Hinton, Imagenet classification with deep convolutional neural networks, in: Advances in Neural Information Processing Systems, 2012, pp. 1097–1105.
- [562] Ö. Yıldırım, P. Plawiak, R.-S. Tan, U.R. Acharya, Arrhythmia detection using deep convolutional neural network with long duration ECG signals, *Comput. Biol. Med.* 102 (2018) 411–420.
- [563] A.Y. Hannun, P. Rajpurkar, M. Haghpanahi, G.H. Tison, C. Bourn, M.P. Turakhia, A.Y. Ng, Cardiologist-level arrhythmia detection and classification in ambulatory electrocardiograms using a deep neural network, *Nat. Med.* 25 (1) (2019) 65.
- [564] U.R. Acharya, S.L. Oh, Y. Hagiwara, J.H. Tan, M. Adam, A. Gertych, R. San Tan, A deep convolutional neural network model to classify heartbeats, *Comput. Biol. Med.* 89 (2017) 389–396.
- [565] A. Esteva, B. Kuprel, R.A. Novoa, J. Ko, S.M. Swetter, H.M. Blau, S. Thrun, Dermatologist-level classification of skin cancer with deep neural networks, *Nature* 542 (7639) (2017) 115–118.
- [566] N.C. Codella, Q.-B. Nguyen, S. Pankanti, D.A. Gutman, B. Helba, A.C. Halpern, J.R. Smith, Deep learning ensembles for melanoma recognition in dermoscopy images, *IBM J. Res. Dev.* 61 (4/5) (2017) 1–5.
- [567] Y. Celik, M. Talo, O. Yıldırım, M. Karabatak, U.R. Acharya, Automated invasive ductal carcinoma detection based using deep transfer learning with whole-slide images, *Pattern Recognit. Lett.* (2020).
- [568] A. Cruz-Roa, A. Basavanhally, F. González, H. Gilmore, M. Feldman, S. Ganesan, N. Shih, J. Tomaszewski, A. Madabhushi, Automatic detection of invasive ductal carcinoma in whole slide images with convolutional neural networks, in: Medical Imaging 2014: Digital Pathology, Vol. 9041, International Society for Optics and Photonics, 2014, p. 904103.
- [569] M.K. Hasan, T.A. Aleef, S. Roy, Automatic mass classification in breast using transfer learning of deep convolutional neural network and support vector machine, in: 2020 IEEE Region 10 Symposium, TENSYMP, IEEE, 2020, pp. 110–113.
- [570] M. Talo, O. Yıldırım, U.B. Baloglu, G. Aydin, U.R. Acharya, Convolutional neural networks for multi-class brain disease detection using MRI images, *Comput. Med. Imaging Graph.* 78 (2019) 101673.
- [571] P. Rajpurkar, J. Irvin, K. Zhu, B. Yang, H. Mehta, T. Duan, D. Ding, A. Bagul, C. Langlotz, K. Shpanskaya, et al., Chexnet: Radiologist-level pneumonia detection on chest x-rays with deep learning, 2017, [arXiv:1711.05225](https://arxiv.org/abs/1711.05225).
- [572] J.H. Tan, H. Fujita, S. Sivaprasad, S.V. Bhadary, A.K. Rao, K.C. Chua, U.R. Acharya, Automated segmentation of exudates, haemorrhages, microaneurysms using single convolutional neural network, *Inform. Sci.* 420 (2017) 66–76.
- [573] M.K. Hasan, M.A. Alam, M.T.E. Elahi, S. Roy, R. Martí, DRNet: Segmentation and localization of optic disc and fovea from diabetic retinopathy image, *Artif. Intell. Med.* 111 (2021) 102001.
- [574] M.K. Hasan, L. Calvet, N. Rabbani, A. Bartoli, Detection, segmentation, and 3D pose estimation of surgical tools using convolutional neural networks and algebraic geometry, *Med. Image Anal.* 70 (2021) 101994.

- [575] G. Gaál, B. Maga, A. Lukács, Attention u-net based adversarial architectures for chest x-ray lung segmentation, 2020, arXiv:2003.10304.
- [576] Z. Chen, S. Wang, The NL-SC net for skin lesion segmentation, in: Chinese Conference on Pattern Recognition and Computer Vision, PRCV, Springer, 2021, pp. 313–324.
- [577] O. Ronneberger, P. Fischer, T. Brox, U-net: Convolutional networks for biomedical image segmentation, in: International Conference on Medical Image Computing and Computer-Assisted Intervention, Springer, 2015, pp. 234–241.
- [578] J. Long, E. Shelhamer, T. Darrell, Fully convolutional networks for semantic segmentation, in: Proceedings of the IEEE Conference on Computer Vision and Pattern Recognition, 2015, pp. 3431–3440.
- [579] A. Odena, V. Dumoulin, C. Olah, Deconvolution and checkerboard artifacts, *Distill* 1 (10) (2016) e3.
- [580] Z. Mirikharaji, C. Barata, K. Abhishek, A. Bissoto, S. Avila, E. Valle, M.E. Celebi, G. Hamarneh, A survey on deep learning for skin lesion segmentation, 2022, arXiv:2206.00356.
- [581] T. Chowdhury, A.R. Bajwa, T. Chakraborti, J. Rittscher, U. Pal, Exploring the correlation between deep learned and clinical features in melanoma detection, in: Annual Conference on Medical Image Understanding and Analysis, Springer, 2021, pp. 3–17.
- [582] C. Barata, M.E. Celebi, J.S. Marques, Explainable skin lesion diagnosis using taxonomies, *Pattern Recognit.* 110 (2021) 107413.
- [583] C. Barata, M.E. Celebi, J.S. Marques, Melanoma detection algorithm based on feature fusion, in: 2015 37th Annual International Conference of the IEEE Engineering in Medicine and Biology Society, EMBC, IEEE, 2015, pp. 2653–2656.
- [584] M. Rastgoo, R. Garcia, O. Morel, F. Marzani, Automatic differentiation of melanoma from dysplastic nevi, *Comput. Med. Imaging Graph.* 43 (2015) 44–52.
- [585] G. Schaefer, B. Krawczyk, M.E. Celebi, H. Iyatomi, An ensemble classification approach for melanoma diagnosis, *Memet. Comput.* 6 (4) (2014) 233–240.
- [586] Z. Abbas, M.-u. Rehman, S. Najam, S.D. Rizvi, An efficient gray-level co-occurrence matrix (GLCM) based approach towards classification of skin lesion, in: 2019 Amity International Conference on Artificial Intelligence, AICAI, IEEE, 2019, pp. 317–320.
- [587] I. Giotis, N. Molders, S. Land, M. Biehl, M.F. Jonkman, N. Petkov, MED-NODE: A computer-assisted melanoma diagnosis system using non-dermoscopic images, *Expert Syst. Appl.* 42 (19) (2015) 6578–6585.
- [588] R. Garnavi, M. Aldeen, J. Bailey, Computer-aided diagnosis of melanoma using border-and wavelet-based texture analysis, *IEEE Trans. Inf. Technol. Biomed.* 16 (6) (2012) 1239–1252.
- [589] I. Maglogiannis, K.K. Delibasis, Enhancing classification accuracy utilizing globules and dots features in digital dermoscopy, *Comput. Methods Programs Biomed.* 118 (2) (2015) 124–133.
- [590] Q. Abbas, M.E. Celebi, C. Serrano, I.F. Garcia, G. Ma, Pattern classification of dermoscopy images: A perceptually uniform model, *Pattern Recognit.* 46 (1) (2013) 86–97.
- [591] M. Sadeghi, T.K. Lee, D. McLean, H. Lui, M.S. Atkins, Global pattern analysis and classification of dermoscopic images using textons, in: Medical Imaging 2012: Image Processing, Vol. 8314, International Society for Optics and Photonics, 2012, p. 83144X.
- [592] M.K. Hasan, M.T. Jawad, A. Dutta, M.A. Awal, M.A. Islam, M. Masud, J.F. Al-Amri, Associating measles vaccine uptake classification and its underlying factors using an ensemble of machine learning models, *IEEE Access* 9 (2021) 119613–119628.
- [593] H. Iyatomi, K.-A. Norton, M.E. Celebi, G. Schaefer, M. Tanaka, K. Ogawa, Classification of melanocytic skin lesions from non-melanocytic lesions, in: 2010 Annual International Conference of the IEEE Engineering in Medicine and Biology, IEEE, 2010, pp. 5407–5410.
- [594] P.P. Patil, S.A. Patil, V. Udupi, Detection and classification of skin lesion in dermoscopy images, *Int. J. Appl. Eng. Res.* 9 (24) (2014) 27719–27731.
- [595] I.A. Ozkan, M. KOKLU, Skin lesion classification using machine learning algorithms, *Int. J. Intell. Syst. Appl. Eng.* 5 (4) (2017) 285–289.
- [596] R.C. Hardie, R. Ali, M.S. De Silva, T.M. Kebede, Skin lesion segmentation and classification for ISIC 2018 using traditional classifiers with hand-crafted features, 2018, arXiv:1807.07001.
- [597] P. Jayapal, R. Manikandan, M. Ramanan, R.S. Sundar, T.U. Suriya, Skin lesion classification using hybrid spatial features and radial basis network, *Skin* 3 (3) (2014).
- [598] F. Nunari, M.A. Kadir, D. Sonntag, On the overlap between grad-cam saliency maps and explainable visual features in skin cancer images, in: International Cross-Domain Conference for Machine Learning and Knowledge Extraction, Springer, 2021, pp. 241–253.
- [599] C. Barata, C. Santiago, Improving the explainability of skin cancer diagnosis using CBIR, in: International Conference on Medical Image Computing and Computer-Assisted Intervention, Springer, 2021, pp. 550–559.
- [600] J. Yang, F. Xie, H. Fan, Z. Jiang, J. Liu, Classification for dermoscopy images using convolutional neural networks based on region average pooling, *IEEE Access* 6 (2018) 65130–65138.
- [601] W. Li, J. Zhuang, R. Wang, J. Zhang, W.-S. Zheng, Fusing metadata and dermoscopy images for skin disease diagnosis, in: 2020 IEEE 17th International Symposium on Biomedical Imaging, ISBI, IEEE, 2020, pp. 1996–2000.
- [602] J. Zhang, Y. Xie, Y. Xia, C. Shen, Attention residual learning for skin lesion classification, *IEEE Trans. Med. Imaging* 38 (9) (2019) 2092–2103.
- [603] Q. Ha, B. Liu, F. Liu, Identifying melanoma images using efficient ensemble: Winning solution to the siim-isic melanoma classification challenge, 2020, arXiv:2010.05351.
- [604] A.G. Pacheco, A.-R. Ali, T. Trappenberg, Skin cancer detection based on deep learning and entropy to detect outlier samples, 2019, arXiv:1909.04525.
- [605] A.H. Shahin, A. Kamal, M.A. Elattar, Deep ensemble learning for skin lesion classification from dermoscopic images, in: 2018 9th Cairo International Biomedical Engineering Conference, CIBEC, IEEE, 2018, pp. 150–153.
- [606] I. Kandel, M. Castelli, The effect of batch size on the generalizability of the convolutional neural networks on a histopathology dataset, *ICT Express* 6 (4) (2020) 312–315.
- [607] J. Burdick, O. Marques, A. Romero-Lopez, X. Giró Nieto, J. Weinthal, The impact of segmentation on the accuracy and sensitivity of a melanoma classifier based on skin lesion images, in: SIIM 2017 Scientific Program: Pittsburgh, PA, June 1-June 3, 2017, David L. Lawrence Convention Center, 2017, pp. 1–6.
- [608] F. Bagheri, M.J. Tarokh, M. Ziaratban, Two-stage skin lesion segmentation from dermoscopic images by using deep neural networks, *Jorjani Biomed.* 8 (2) (2020) 58–72.
- [609] S. Wang, Y. Yin, D. Wang, Y. Wang, Y. Jin, Interpretability-based multimodal convolutional neural networks for skin lesion diagnosis, *IEEE Trans. Cybern.* (2021).
- [610] Y. Yan, J. Kawahara, G. Hamarneh, Melanoma recognition via visual attention, in: International Conference on Information Processing in Medical Imaging, Springer, 2019, pp. 793–804.
- [611] R.T. Sousa, L.V. de Moraes, Araguaia medical vision lab at ISIC 2017 skin lesion classification challenge, 2017, arXiv:1703.00856.
- [612] K. Young, G. Booth, B. Simpson, R. Dutton, S. Shrapnel, Deep neural network or dermatologist? in: Interpretability of Machine Intelligence in Medical Image Computing and Multimodal Learning for Clinical Decision Support, Springer, 2019, pp. 48–55.
- [613] S. Jeniva, C. Santhi, An efficient skin lesion segmentation analysis using statistical texture distinctiveness, *Int. J. Adv. Res. Trends Eng. Technol.* 3777 (2015) 111–116.
- [614] M. Yuvaraju, D. Divya, A. Poornima, Segmentation of skin lesion from digital images using morphological filter, *Int. Res. J. Eng. Technol.* 3 (5) (2016) 3223–3229.
- [615] A.A. Adeyinka, S. Viriri, Skin lesion images segmentation: A survey of the state-of-the-art, in: International Conference on Mining Intelligence and Knowledge Exploration, Springer, 2018, pp. 321–330.
- [616] S.H. SALIH, S. AL-RAHEYM, Comparison of skin lesion image between segmentation algorithms, *J. Theor. Appl. Inf. Technol.* 96 (18) (2018).
- [617] R. Javed, M.S.M. Rahim, T. Saba, M. Rashid, Region-based active contour JSEG fusion technique for skin lesion segmentation from dermoscopic images, *Biomed. Res.* 30 (6) (2019) 1–10.
- [618] S.S. Devi, N.H. Singh, R.H. Laskar, Fuzzy C-means clustering with histogram based cluster selection for skin lesion segmentation using non-dermoscopic images, *Int. J. Interact. Multimedia Artif. Intell.* 6 (1) (2020).
- [619] S. Jabbari, Y. Baleghi, Segmentation of skin lesion images using a combination of texture and color information, *J. Soft Comput. Inf. Technol.* 8 (4) (2020) 87–97.
- [620] A. Dutta, M.K. Hasan, M. Ahmad, Skin lesion classification using convolutional neural network for melanoma recognition, in: Proceedings of International Joint Conference on Advances in Computational Intelligence, Springer, 2021, pp. 55–66.
- [621] P.M. Pereira, L.M. Tavora, R. Fonseca-Pinto, R.P. Paiva, P.A.A. Assunção, S.M. de Faria, Image segmentation using gradient-based histogram thresholding for skin lesion delineation, in: Biomaging, 2019, pp. 84–91.
- [622] A. Huang, S.-Y. Kwan, W.-Y. Chang, M.-Y. Liu, M.-H. Chi, G.-S. Chen, A robust hair segmentation and removal approach for clinical images of skin lesions, in: 2013 35th Annual International Conference of the IEEE Engineering in Medicine and Biology Society, EMBC, IEEE, 2013, pp. 3315–3318.
- [623] C.K. Rekha, K. Manjunathachari, B. Prakash, Log-Gaussian fuzzy C-means clustering algorithm for skin lesion segmentation, *J. Sci. Technol.* 3 (6) (2018) 18–27.
- [624] M.H. Hamd, L.M. Mohamad, Skin cancer prognosis based on color matching and segmentation of pigmented skin lesion, *Eng. Technol.* J. 31 (2013).
- [625] G. Yang, Q. Ye, J. Xia, Unbox the black-box for the medical explainable AI via multi-modal and multi-centre data fusion: A mini-review, two showcases and beyond, *Inf. Fusion* 77 (2022) 29–52.
- [626] A.B. Arrieta, N. Díaz-Rodríguez, J. Del Ser, A. Bennetot, S. Tabik, A. Barbado, S. García, S. Gil-López, D. Molina, R. Benjamins, et al., Explainable artificial intelligence (XAI): Concepts, taxonomies, opportunities and challenges toward responsible AI, *Inf. Fusion* 58 (2020) 82–115.
- [627] M.K. Hasan, M.A. Alam, L. Dahal, S. Roy, S.R. Wahid, M.T.E. Elahi, R. Martí, B. Khanal, Challenges of deep learning methods for COVID-19 detection using public datasets, *Inform. Med. Unlocked* 30 (2022) 100945.

- [628] K. Hauser, A. Kurz, S. Haggenmüller, R.C. Maron, C. von Kalle, J.S. Utikal, F. Meier, S. Hobelsberger, F.F. Gellrich, M. Sergon, et al., Explainable artificial intelligence in skin cancer recognition: A systematic review, *Eur. J. Cancer* 167 (2022) 54–69.
- [629] S. Haggenmüller, R.C. Maron, A. Hekler, J.S. Utikal, C. Barata, R.L. Barnhill, H. Beltraminelli, C. Berking, B. Betz-Stablein, A. Blum, et al., Skin cancer classification via convolutional neural networks: systematic review of studies involving human experts, *Eur. J. Cancer* 156 (2021) 202–216.
- [630] T.J. Brinker, A. Hekler, A.H. Enk, J. Klode, A. Hauschild, C. Berking, B. Schilling, S. Haferkamp, D. Schadendorf, T. Holland-Letz, et al., Deep learning outperformed 136 of 157 dermatologists in a head-to-head dermoscopic melanoma image classification task, *Eur. J. Cancer* 113 (2019) 47–54.
- [631] M. Micocci, S. Borsci, V. Thakerar, S. Walne, Y. Manshadi, F. Edridge, D. Mullarkey, P. Buckle, G.B. Hanna, Do GPs trust artificial intelligence insights and what could this mean for patient care? A case study on GPs skin cancer diagnosis in the UK, 2021.
- [632] K. Lekadir, R. Osuala, C. Gallin, N. Lazrak, K. Kushibar, G. Tsakou, S. Aussó, L.C. Alberich, K. Marias, M. Tsiknakis, et al., FUTURE-AI: Guiding principles and consensus recommendations for trustworthy artificial intelligence in medical imaging, 2021, arXiv preprint [arXiv:2109.09658](https://arxiv.org/abs/2109.09658).